Sci

JET PROPULSION

A publication of the

AMERICAN ROCKET SOCIETY

Research and Development

VOLUME 28 JUNE 1958 SCIENCE & TECHNOLOGY NUMBER 6


on guard . . .
the NIKE HERCULES
To guard our cities and other vital areas the Army's new Nike is more powerful than ever before.
Designated Nike Hercules, the ground-to-air missile maneuvers with pin-point accuracy at extremely high altitudes to intercept today's most advanced aircraft.
The range and other details of the Nike Hercules are secret. But to propel the lethal new Nike at supersonic speed to its target, Army Ordnance and Douglas Aircraft Co. chose an entirely new power plant for the missile proper— a solid propellant rocket system developed by Thiokol Chemical Corporation, one of the leaders in solid propellant engines.
U.S. ARMY
Thiokol®
CHEMICAL CORPORATION
TRENTON, N. J. • ELKTON, MD. • HUNTSVILLE, ALA.
MOSS POINT, MISS. • MARSHALL, TEXAS • BRIGHAM CITY, UTAH
® Registered trademark of the Thiokol Chemical Corporation for its liquid polymers, rocket propellants, plasticizers and other chemical products.

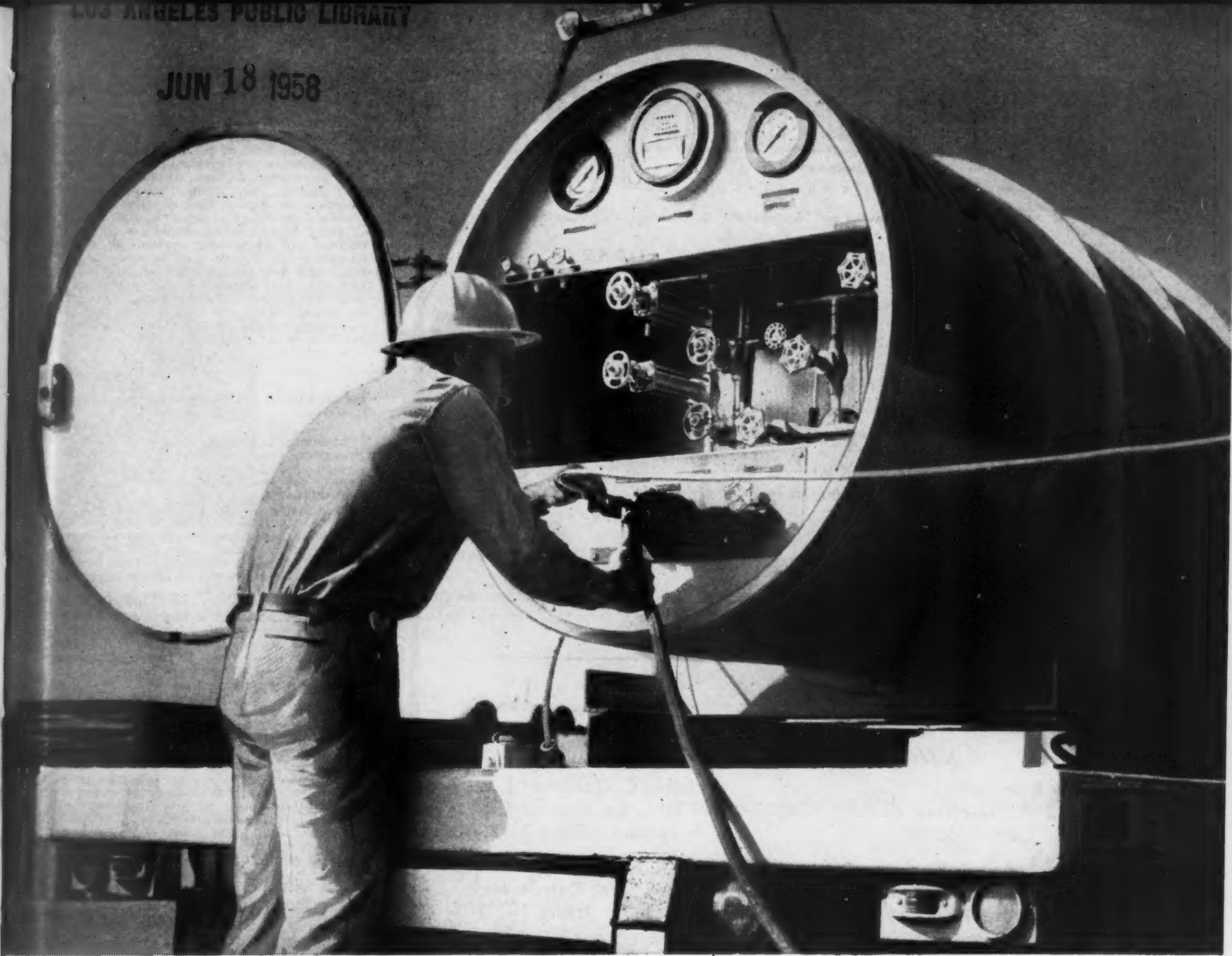

TAMED: *the elemental fury of fluorine!*

Still thinking of elemental fluorine as "too hard to handle"? Not any more! As a result of General Chemical research, this "optimum" oxidizer can now be stored, transported and handled directly *as a liquid* in tank-truck tonnages. If you are interested in working with fluorine as an oxidizer for rocket fuels, or for any other application, this development could be of major importance to you.

Benefits of liquid fluorine. Now that fluorine is available in liquid form and in bulk quantities, you can handle and store it more easily, more safely and more economically than ever before. An important *plus* value—the shipping containers can also be used as storage tanks.

Halogen fluorides also available. The halogen fluorides, too, are commercially available from General Chemical. Chlorine trifluoride is available in ton cylinders and cylinders of 150 lbs. net. Bromine trifluoride, bromine pentafluoride and iodine pentafluoride are offered in various-sized cylinders to suit demand.

Write for free technical bulletins. A comprehensive new technical bulletin, "Fluorine," will be sent you on request. Also Technical Bulletin TA-8532-2, covering Chlorine Trifluoride and other Halogen Fluorides. Write for your free copies today.

Allied Chemical

First in Fluorine Chemistry

GENERAL CHEMICAL DIVISION

40 Rector Street, New York 6, N. Y.

JET PROPULSION

A publication of the

AMERICAN ROCKET SOCIETY

Research and Development

Scope of JET PROPULSION

This Journal is a publication of the American Rocket Society devoted to the advancement of the field of jet propulsion through the dissemination of original papers disclosing new knowledge or new developments. As used herein, the term "jet propulsion" embraces all engines that develop thrust by rearward discharge of a jet through a nozzle or duct; and thus it includes air-consuming engines and underwater systems as well as rockets. JET PROPULSION is open to contributions dealing not only with propulsion but with other aspects of jet-propelled flight, such as flight mechanics, guidance, telemetering, and research instrumentation. Increasing emphasis will be given to the scientific problems of extraterrestrial flight.

Information for Authors

Manuscripts must be as brief as the proper presentation of the ideas will allow. Exclusion of dispensable material and conciseness of expression will influence the Editors' acceptance of a manuscript. In terms of standard-size double-spaced typed pages, a typical maximum length is 22 pages of text (including equations), 1 page of references, 1 page of abstract, and 12 illustrations. Fewer illustrations permit more text, and vice versa. Greater length will be acceptable only in exceptional cases.

Short manuscripts, not more than one quarter of the maximum length stated for full articles, may qualify for publication as Technical Notes or Technical Comments. They may be devoted to new developments requiring prompt disclosure or to comments on previously published papers. Such manuscripts are usually published within two months of the date of receipt.

Sponsored manuscripts are published occasionally as an ARS service to the industry. A manuscript that does not qualify for publication according to the above-stated requirements as to subject scope or length, but which nevertheless deserves widespread distribution among jet propulsion engineers, may be printed as an extra part of the Journal or as a special supplement, if the author or his sponsor will reimburse the Society for actual publication costs. Estimates are available on request. Acknowledgment of such financial sponsorship appears as a footnote on the first page of the article. Publication is prompt since such papers are not in the ordinary backlog.

Manuscripts must be double spaced on one side of paper only with wide margins to allow for instructions to printer. Include a 100 to 200 word abstract. State the authors' positions and affiliations in a footnote on the first page. Equations and symbols may be handwritten or typewritten; clarity for the printer is essential. Greek letters and unusual symbols should be identified in the margin. If handwritten, distinguish between capital and lower case letters, and indicate subscripts and superscripts. References are to be grouped at the end of the manuscript and are to be given as follows: for journal articles: authors first, then title, journal, volume, year, page numbers; for books: authors first, then title, publisher, city, edition, and page or chapter numbers. Line drawings must be clear and sharp to make clear engravings. Use black ink on white paper or tracing cloth. Lettering should be large enough to be legible after reduction. Photographs should be glossy prints, not matte or semi-matte. Each illustration must have a legend; legends should be listed in order on a separate sheet.

Manuscripts must be accomplished by written assurance as to security clearance in the event the subject matter lies in a classified area or if the paper originates under government sponsorship. Full responsibility rests with the author.

Submit manuscripts in duplicate (original plus first carbon, with two sets of illustrations) to the Editor, Martin Summerfield, Professor of Aeronautical Engineering, Princeton University, Princeton, N. J. Preprints of papers presented at ARS national meetings are automatically considered for publication.

JET PROPULSION is published monthly by the American Rocket Society, Inc., and the American Interplanetary Society at 20th & Northampton Sts., Easton, Pa., U. S. A. Editorial offices: 500 Fifth Ave., New York 36, N. Y. Price: $12.50 per year, $2.00 per single copy. Second-class mail privileges authorized at Easton, Pa. Notice of change of address should be sent to the Secretary, ARS, at least 30 days prior to publication. Opinions expressed herein are the authors' and do not necessarily reflect the views of the Editors or of the Society.

Recent Advances in Rocket Reliability Concepts

M. LIPOW

Aerojet-General Corp., Azusa, Calif.

The author received a B.S. degree in mathematics from the California Institute of Technology in 1949. Since that time he has been with Aerojet-General Corp., Azusa, Calif., a subsidiary of the General Tire & Rubber Co. His work at Aerojet-General has included the practical side as well as theoretical research in solid propellant rocket development; in particular, problems of heat transfer and combustion instability. More recently, within the last three years, Mr. Lipow has been a member of the reliability control staff. In this capacity he has contributed to reliability programs planning and to resolution of many of the statistical problems of reliability. Mr. Lipow has contributed several papers on reliability topics to the scientific literature.

Introduction

IT IS of great importance to achieve high rocket reliability in the shortest time possible. Present or anticipated uses of rocket propulsion systems involve the most critical aspects of our national defense. Aside from the tactical or strategic purpose, the economic aspects of rockets are of major importance. Rocket propulsion systems are, and will be for a long time to come, enormously expensive to develop and use for their intended purposes.

The advent of the reliability concept is due to the concerted effort to find methods which will with maximum assurance of satisfactory accomplishment shorten the time from design through development and production to the most efficient tactical use of rocket propulsion systems at least possible cost. What is the reliability concept? What new principles has the reliability concept helped to formulate? What are some of the techniques used to implement these principles?

The Nature of Reliability

The currently accepted definition of the word "reliability" in the present context is: "The (mathematical) probability of a device performing its purpose adequately for the period of time intended under the conditions encountered" (1).[1] This definition is useful because it implies a purpose of *measuring* certain meaningful *events*. In other words, by making use of the theory of probability we can assign in a unique and consistent manner a number to the event: "The rocket engine will deliver a stated level of performance, within specified limits, for a given period of time, while being subjected to certain environmental conditions." A knowledge of the probability of such an event would be necessary in order to make a realistic replacement policy or, for example, to decide how many rockets to use in a given application. There can be no serious objection to a "probablistic" definition of the world "reliability."

A point which has become more clearly recognized in negotiating legally binding contracts for rocket development as well as in specifying the objectives of a rocket development program is that "events" are *always conditional*. In other words the conditions (usage environments) under which an event is to be measured must be known and stated. In many instances, however, the conditions are not important; that is to say the conditional probability of the stated "event" is unaltered, whether given conditions are taken into account or not. The "event" and the conditions are then independent in the probability sense and also in a very real sense. For example, the tendency for a rocket to malfunction in some manner might be quite "insensitive" to a given set of vibrational conditions imposed on it. (This would indicate an ideal situation, since it is one of the goals of rocket development to design "environmental factor insensitivity" into the rocket (2).)

A second concept of perhaps more recent recognition is that "reliability" can be identified as a performance parameter of a given system (3); thus there can be experimental error in its measurement. In many instances this recognition has taken the form of a measure of precision, or confidence in the estimate of reliability as part of contractual requirements.

I wish to emphasize here the point that, by paying due attention to the mathematical structure of probability, problems in stating, and therefore in achieving realistic objectives in a rocket development program, can be minimized to a significant extent.

General Considerations of Rocket Reliability

Since the beginnings of modern rocket technology, high performance-to-weight ratio application of rocket engines has generally called for liquid fueled systems. It has long been realized that solid propellant rockets being inherently simpler in design would offer increased chances of reliable operation. Some advantages of solid propellant rockets with respect to reliability are discussed in (4).

If we look at solid propellant rockets more critically from a reliability standpoint, it is a major problem that an individual rocket engine cannot be test-fired prior to its intended use, since this type of inspection destroys the product. On the other hand, a liquid propellant rocket engine can be test-fired not only at the factory site, but also prior to launching (if it is part of a missile system) to check for errors in assembly, defective components or other malperformance which might result in an unsuccessful accomplishment of its intended mission.

This leads to the necessity of measuring "life" of a liquid fuel rocket engine under conditions of repetitive performance. On the other hand, in so far as the actual firing operation is concerned, this approach has little value for a solid propellant rocket. Viewed in the most general sense, however, the possibility of application of the "life" concept to both solid and liquid fueled rockets is really only a matter of emphasizing the types and severity of environment applied. For example, the Aerojet-General solid propellant 15KS-1000 JATO,[2] approved for use on commercial aircraft, must operate satisfactorily after undergoing up to 500 hours of vibration while attached to the aircraft (5). It has been established with a high degree of assurance that the 500 hour limitation allows for a large margin of safety; i.e., the probability is very high that the rocket engine would not fail to operate as intended until a point of time far beyond the 500 hour vibration limit.

In general then, paying due attention to the conditions of use, it is important to measure the life of a given rocket en-

Received March 31, 1958.

[1] Numbers in parentheses indicate References at end of paper.

[2] Rated at 1000 lb of thrust for 15 sec.

gine design, whether solid or liquid propellant, since only then can the optimum check-out, maintenance and supply procedures be determined.

In the next section, the "life" or time-to-failure concept of reliability will be presented. The discussion of problems peculiar to measurement of reliability of solid propellant rockets, i.e., "destructive testing," are deferred to the references, particularly (20).

Time-to-Failure Concept

It is important to realize that the definition of reliability given previously provides the logical basis for measuring "life" or "time-to-failure." Since we want to measure an event, namely, ". . . the device performs its purpose adequately for the period of time intended under the conditions encountered," we are, literally by definition, immediately led to the mathematical existence of a probability distribution of a random variable: time-to-failure. We expect that the *actual* time-to-failure of a rocket engine is characterized by a probability distribution, if only for the reason that such models have been used successfully to describe and predict physical phenomena of a similar nature on numerous occasions in the past. This is the rational justification for the given definition. Accepting this hypothesis for the present, we will now describe some of the proposed models used for measuring time-to-failure in more detail.

Chance, Wearout and Initial Failure

The concept of chance failure appears to have first been formulated by Davis (6). The model for this type of failure is meant to correspond to the observation that many devices, particularly electronic components, appear to fail, as it were, by "accident," perhaps to occurrence of unusually severe, unpredictable or unavoidable environmental conditions. The theoretical chance failure distribution can be derived by assuming that the conditional probability of failure within a time interval $(t, t + dt)$, given that the device has performed successfully up to time t (called the "hazard" function), is proportional to dt. This yields the exponential distribution

$$R(t) \equiv \mathrm{P}(\tau > t) = e^{-\mu t} \quad [1]$$

where the left-hand side is the probability that the time-to-failure (τ) is greater than time t. Thus if t were the "period of time intended" then the reliability would be given by the right-hand side of Equation [1]. The quantity μ is the proportionality constant mentioned above; its reciprocal turns out to be the mean or average time-to-failure. Many articles have been published which give efficient methods for planning and conducting experiments based upon this model of failure (7, 8, 9, 10).

If the exponential failure model applies in a given instance, the optimum replacement policy is to wait until a device fails before replacing it. In other words no matter how much operating time has been accumulated, the expected time-to-failure is the same. For systems with large numbers of components and a high degree of complexity, and where replacement is made when a component fails, the over-all system failure characteristic can usually be described by the exponential distribution, regardless of the nature of failure distributions of the individual components and subsystems (10). However as we proceed to systems of lower orders of complexity, it is generally found that the exponential model is not a complete enough description.

Davis (6) also discussed the concept of wearout failure, as that type in which the device is completely reliable for an operating period less than the time required for "material depletion," and will be certain to fail when required to operate for a longer period. This type of failure appears to be associated with a normal or Gaussian distribution of time-to-failure. It was shown by Davis that if the hazard function is assumed to be a linear function of time, then the derived probability distribution is approximately normal.

In many instances, a combination of both an exponential and a normal distribution will more accurately describe failure rate characteristics, as shown in (6). Gunn (11) proposed the distribution

$$R(t) = e^{-\mu t}\left[1 - \Phi\left(\frac{t-m}{\sigma}\right)\right] \quad [2]$$

where Φ is the (cumulative) normal distribution function with mean m and a standard deviation, σ. By generalizing the concept of chance failure, Lipow (12) derived a similar distribution

$$R(t) = e^{-\mu t}\left[1 - P(N, \lambda t)\right] \quad [3]$$

where $P(N, \lambda t)$ is the gamma distribution function.[3]

In other instances it has also been useful to assume in the model that a certain percentage of equipments are defective before they are operated. In other words, there is a positive probability P_i of failure at time zero. Thus, for time following the start of operation, the probability of survival of the equipment would be given by the expression $(1 - P_i)$ $R(t)$. Initial type failures, so called, may occur after the start of operation. They appear to be characterized by an "abnormally" high failure rate for a short period after start, compared to a lower incidence of failures of equipment surviving this initial period. This type of characteristic is made of practical use by "burning-in" certain high-quality type electron tubes before delivery to the customer. The possible existence of an "infant" mortality rate as described is also one of the reasons why it is necessary to test-fire a liquid fuel rocket engine prior to its mission. As indicated before, it is necessary to find out for a given system just how much pre-mission operation is feasible.

The important problem of determining the optimum replacement policy for various types of equipment failure distributions has been investigated by Weiss (14).

Performance Type Failures

The types of failure that have been discussed in the last section are sometimes considered as "catastrophic" in the sense that blow-up, breakage, burn-out, etc., exemplify failure. It is also important to consider performance-type failure, defined as that type in which a device is still "working," but not near enough to its design output parameter values to give satisfactory performance. This is essentially a "tolerance" problem. In any event, according to the given definition of reliability, a device must neither fail catastrophically nor have performance outputs out-of-specification during its intended operating period, in order to be reliable.

Meltzer (15) has constructed a reliability model, applied to electronic circuits, in which both catastrophic and performance-type failures are included. In this model the design equations relating the output performance parameters, e.g., mid-band gain, frequency, etc., to the component characteristics, e.g., resistances, capacitances, etc., are used to determine a probability distribution of the output parameters.[4] Independently, it is assumed that the circuit has a survival probability $R(t)$. The reliability of the circuit is then obtained by multiplying the probability that all the output parameters stay within specifications by $R(t)$. This model may be looked upon as providing a "higher-order" system analysis.

Acheson (16) illustrates, perhaps more clearly than anyone else, the value of such a system analysis. He points out with

[3] $\mathrm{P}(N, \lambda t)$ is tabulated in (13), Table II, where $c \equiv N$, $a \equiv \lambda t$.

[4] It is assumed that the variances and covariances of the component characteristic parameters are known. Using the design equations, the means, variances and covariances of output performance parameters are then calculated. These quantities are sufficient to completely specify a multivariate normal probability distribution of the output performance parameters.

many examples that the interactions, i.e., enhancing or degrading effects due to joint variations in component characteristics, are frequently of far larger importance to reliability than effects due to component variation considered separately, especially in electronic circuitry. Just as important are the interactions which influence the occurrence of "catastrophic" failure. For example, the heat generated by an electron tube can result in increased burn-out rate of other tubes in close proximity. It is evident that to describe or predict the reliability of a complex system in a satisfactory manner both types of failure must be considered. To my knowledge, a satisfactory model of failure, taking into account the joint effects of performance variation and interaction, catastrophic failure interaction, and influences of external environment has not yet been formulated.

Achievement of Reliability

While we have been led astray somewhat from the pure field of rocket propulsion in the preceding discussion, I think that many of the clues leading to the achievement of more reliable rockets are afforded by the active search for reliability in electronic systems. Perhaps the key word is "interactions." Interactions are far more *apparent* with electronic circuitry than with, say, "mechanical" devices. However, the rocket engineer is certainly aware of the existence of interactions in the system he is designing and developing. For example, there is certainly an interaction between the performance of an igniter, the configuration or shape of the solid propellant grain and the type of propellant composition. Insufficient appreciation of this fact has impeded many rocket development programs in the past. Another example of interaction, which has been a difficult problem in the development of a certain type of gas generator employing a fuel-rich mixture ratio, is the influence of injector design and chamber shape on the formation of carbon deposits on the injector face and in the chamber nozzle.

The particular point to be made here is that even if interactions are apparent, it is too often the case that rocket development is planned and carried out in "piecemeal" fashion. The rocket development engineer must conduct his program in such a manner as to find out, at the earliest possible moment, possible interaction effects conducive to system and component failure.

Principles of Developing Reliable Rockets

The clearest statement, in my opinion, of the principles of developing reliable rocket engines is made by Geckler (17). While the principles are specifically related to development of solid propellant rockets, they are sufficiently broad to include liquid propellant rockets, and, indeed, any complex equipment of an advanced technological nature. In particular, however, it is cogently recognized in (17) that due to (a) the impossibility of 100 per cent direct inspection of a solid propellant rocket and (b) the economic impracticability of relying on statistical laws of large numbers, especially where larger and more expensive rockets are concerned, emphasis must be placed on building reliability into the rocket design. The four principles stated to achieve this objective are the principles of *Redundant Design*, *Peripheral Testing*, *Adequate Representation* and *Continuous Development*.

The Principle of Redundant Design

In all too numerous instances, unique reliance is placed upon the proper working of every part of a rocket propulsion system; if any part fails, the system as a whole may fail to operate as intended. One direct method of overcoming this difficulty is to provide parallel function of parts, components, subsystems, etc., all the way up to the entire system level. In other words, the idea is: "If one doesn't work the other will." There are obvious difficulties in applying this practice to rocket propulsion devices and guided missiles. For one, duplication of subsystems or components would in general increase weight, one of the most severe limitations to efficient performance. Secondly, duplication is actually not a guarantee of reliability since, of two parallel components, one may fail for the same reason the other fails, for example, because of externally applied excessive vibration or heat. In other types of parallelism, an additional system is needed to "switch-over" from a failed component to its nonfailed counterpart. The additional system may, however, add a significant amount of weight and in itself may be of insufficient reliability, and so on. However, applying principles of parallel function can well be of benefit when the associated limitations are of lesser importance. Today's modern passenger aircraft provide one of the best examples of the value of redundant or parallel functioning in complex equipment.

The principle of redundant design is not limited to duplication of function, however. It extends to the well-known concept of "safety" factors, especially important and applicable in rocket propulsion systems. This is where careful planning for design interaction comes in. In a case cited in (17), it is mentioned that because of early establishment of a "tight design" in a particular rocket motor, a costly amount of redesign and time-consuming testing was needed to incorporate a relatively simple and inexpensive component (for purposes of insulation) into the rocket. Although this particular rocket engine had a low frequency of failure to begin with, the additional redundancy reduced this failure rate considerably.

In a certain liquid fuel application, additional reliability in initiating combustion has been assured by addition of a special circuit into the electrical sequence ignition system. When the firing switch is pressed once, the ignition sequence is automatically repeated more than once. The success of this method depended upon the ease with which the circuit could be added, as well as the fact that repeated firing of a spark-plug in the absence of fuel burns off residual carbon deposits which could prevent the occurrence of a hot spark. Of course, in this case a short delay in ignition is allowable.

The two examples illustrate the virtues of careful planning for redundancy early in the design and development stages. In a more general sense, then, the rocket engineer must be acutely aware of the possibilities of utilizing enhancing interactions. He must guard equally against the almost certain occurrence of degrading ones. The second principle enunciated in (17) supplies the method of verifying the effectiveness of designed-in safety factors, as well as the method of searching out unsuspected new factors detrimental to high reliability.

The Principle of Peripheral Testing

Geckler states in (17), "In using the term 'peripheral testing' we intend to emphasize the desirability of conducting tests at or beyond the limits of all applicable specifications during rocket development. This means not only testing under conditions known to be more severe than specified, but also testing under a wider variety of conditions. Moreover, it means testing components and propellant purposely produced at or beyond the limits of processing and material specifications.

"A natural outcome of the principle broached here would be the occurrence of a fairly large number of malfunctions during the testing program. Not only is this unobjectionable, but, on the contrary, it is to be desired. In fact, an appreciable portion of the testing program should be devoted to provoking malfunctions in various ways in order to bring to light the weak points in the design. As an example, one would consider deliberately increasing the chamber pressure during an otherwise normal firing to the point where the chamber ruptures. The purpose of such a test would not ordinarily be to check the design calculations, since this can best be done in other ways. Instead, it would be to discover

whether unpredictable events occur as a result of variations in the conditions of operation."

It should be evident, that in accordance with this principle, the methods of statistical design of experiments can be used to the utmost in the testing phase of a rocket development program. Now, the phrase "statistical design of experiments" may connote to a rocket development engineer (especially one who is *familiar* with statistics) an exotic method of analyzing data obtained in an experiment in which there are several variables, and under closely controlled laboratory-type conditions. He would be correct, certainly, from one point of view. However, let the statistician worry about the exotic methods of analysis! The rocket engineer has to worry about the variables and the controlled conditions. He should not have to worry about them alone, however.

Rather, the most important idea the engineer should be aware of in this respect is "confounding." This is another way of stating that if an experiment is not planned properly, not only may fictitious interactions be introduced, but actual interactions may be masked. All too often, perhaps, the engineer thinks in terms of "main effects"; i.e., the *separate* influences of the variables on the outcome of the experiment. It should also be well known that experiments cannot be conducted efficiently by the one-factor-at-a-time approach, since it is too costly in amount of experimentation, and, more important, there is no possibility whatsoever of discovering interactions. A good example of confounding in a proposed qualification test program for solid propellant rockets, and its resolution, is given in (2).

The preceding paragraph points to the necessity of combining engineering analysis with the tools of the expert statistician. Every engineer should read (18) in this respect.

The Principle of Adequate Representation

Geckler states of the principle of adequate representation (17), "By this we mean the effort to make every aspect of the rockets truly representative of the product to be mass-produced at a later date. Not only the specific design factors need to be the same, but also tooling, methods of fabrication, and methods of inspection."

It is evident, as is pointed out in (17), that this principle cannot be employed to a very great extent early in the development stage of a rocket engine. The intent of the principle is to stress that every opportunity should be utilized to introduce the final techniques at the earliest possible stage of the testing program.

In the final stage of testing that precedes initial delivery of rocket engines to the customer, this principle cannot be ignored, however, "In such a case it is imperative that the product be representative of the process to be employed for the delivered item. This "... by no means implies a freezing of the production design, specifications or process. It is in the very nature of things to suppose that improvements will be discovered and incorporated into the manufacturing process periodically." The next principle assures, in fact, that this will happen.

The Principle of Continuous Development

Geckler states of the principle of continuous development, "By this is meant the recognition that development work can never be considered complete; after any item has been fixed as a result of testing and the program is advanced to the next phase, the development program should go back to the original problems and examine alternative solutions."

However, " . . . there would be no economy if development were continued at a high level merely to demonstrate that alternative solutions were possible. The real intent of continuous development is to establish a mechanism for avoiding crises and their attendant expense by providing a backlog or surplus of information in the areas where there is reason to believe that trouble may be most likely to develop. After a production line has been operated for some time, there is naturally less reason for continuous development as insurance. At this stage it is more profitable to reorient the development program toward product and process improvement."

The full value of the four principles " . . . depends upon their being used together and the nature of their interconnections recognized. It would be pointless, for example, to undertake peripheral testing if there were no continuous development to correct the defects as they are discovered, or if there were not sufficient redundancy in the design to make corrections possible. Likewise, many of the advantages of redundant design would be lost if development did not make use of the flexibility inherent in redundancy to correct the defects disclosed by peripheral testing. In addition, continuous development would too often be aimless exploration unless given a goal by the results of peripheral testing, and an opportunity by redundant design. Lastly, adequate representation insures that all the development work bears directly upon the final product."

In connection with the fourth, and to a great extent with the third, principle enunciated in (17), I would like to call attention to a remarkable paper by G. E. P. Box, an eminent statistician (19). Unfortunately, I cannot give any details here; but the method of "evolutionary operation" proposed seems to me to offer exciting possibilities especially with respect to improvement of solid propellant production processes, with a direct bearing on reliability of most solid propellant rockets being produced today.

Summary and Acknowledgment

In most part this is a summary of topics that have not been discussed rather than those which have. I have attempted to confine the discussion to reliability concepts and the most important general methods, rather than to enter into some of the extremely valuable statistical methods that have been formulated to measure and achieve high reliability. The reader will find many of these topics in the references, however. With no apology necessary, I have quoted at considerable length from (17). Due to the security classified nature of other parts of this particular paper, it probably has not been disseminated as widely as it deserves to be. Other topics, just as important to achievement of high rocket reliability, such as project and quality control organization and failure reporting systems, are subjects of many of the reliability and quality control symposia, some of whose proceedings are listed below.

I would like to acknowledge the many constructive suggestions and helpful discussions of D. E. Hartvigsen and N. R. Garner. Of course, I have the sole responsibility for the opinions directly expressed in the article.

References

1 The systems reliability analysis task group of RETMA, "A General Guide for Reporting of Electronic Systems Reliability Measurement."

2 Hartvigsen, D. E., and Lloyd, D. K., "The Application of Statistical Test Designs to Qualification Testing of Rockets and Guided Missiles," Western Regional Conference Proceedings, ASQC, Sept. 9–10, 1957.

3 Riordan, J. J., "The Techniques and Relationships of Quality Control and Reliability," Proceedings, Fourth National Symposium on Reliability and Quality Control in Electronics, Jan. 6–8, 1958.

4 Geckler, R. D., and Davis, R. E., "Modern Developments in Solid Propellant Rocket Engineering," *Aeronautical Engineering Review*, Aug. 1957.

5 JATO Instruction Manual for the Model 15KS-1000-A1 Aircraft Rocket Engine, Aerojet-General Report 997, Sept. 1955.

6 Davis, D. J., "An Analysis of Some Failure Data," *Journal of the American Statistical Association*, vol. 47, 1952, pp. 113–150.

7 Zelen, M., "Multi-Factor Experiments for Evaluating Reliability," Nov. 1957 (to be published in the open literature).
8 Epstein, B., and Sobel, M., "Life Testing," *Journal of the American Statistical Association*, 1953, pp. 486–502.
9 Sobel, M., "Statistical Techniques for Reducing the Experiment Time in Reliability Studies," *Bell System Technical Journal*, vol. XXXV, no. 1, 1956, pp. 179–202.
10 Parsons, J. H., Wong, K. L., and Yeiser, A. S., "Statistics of Electronic System Failures," IRE Convention Record, Part 6, 1955, pp. 69–73.
11 Gunn, W. A., "The Reliability of Complex Systems," Western Regional Conference Proceedings ASQC, Aug. 20–21, 1956.
12 Lipow, M., "A Unified Model for Catastrophic Failure," Western Regional Conference Proceedings ASQC, Sept. 9–10, 1957.
13 Molina, E. C., "Poisson's Exponential Binomial Limit," Van Nostrand, New York, 1942.
14 Weiss, G. H., "On the Theory of Replacement of Machinery with Random Failure Time," Ballistic Research Laboratories, Aberdeen Proving Ground, Report 982, March 1956.
15 Meltzer, S. A., "Statistical Analysis of Equipment Reliability," Radio Corporation of America EM 4194, June 1955.
16 Acheson, M. A., "The Whole Is Not the Sum of Its Parts," Fourth National Symposium on Reliability and Quality Control in Electronics, Jan. 6–8, 1958.
17 Geckler, R. D., "The Principles of Developing Solid-Propellant Rockets," Aerojet-General TM 220, June 1953 (unclassified excerpts from reference; main document classified).
18 Del Priore, F. R., and Day, B. B., "The Engineer and Statistician Can Meet," NAVORD Report 4028, 1953.
19 Box, G. E. P., "Evolutionary Operation," Proceedings of the Symposium on Design of Industrial Experiments, Institute of Statistics, University of North Carolina, Nov. 5–9, 1956.

Additional References

20 Breakwell, J. V., "Economically Optimum Acceptance Tests," *Journal of the American Statistical Association*, vol. 51, June 1956, p. 243.
21 Howard, W. J., "A Simple Failure Model for Complex Mechanisms," The Rand Corp., Report RM-1058 March 1953.
22 Lawrence, H. R., and Amster, W. H., "Reliability Achievement and Demonstration in a Development Program," Space Technology Laboratories, Ramo-Wooldridge Corp. (to be published).

Exhaust Nozzle Contour for Optimum Thrust

G. V. R. RAO[1]

Marquardt Aircraft Co., Van Nuys, Calif.

A method for designing the wall contour of an exhaust nozzle to yield optimum thrust is established. The nozzle length, ambient pressure and flow conditions in the immediate vicinity of the throat appear as governing conditions under which the thrust on the nozzle is maximized. Isentropic flow is assumed and the variational integral of this maximizing problem is formulated by considering a suitably chosen control surface. The solution of the variational problem yields certain flow properties on the control surface, and the nozzle contour is constructed by the method of characteristics to give this flow. An example is carried out and typical nozzle contours are given.

Nomenclature

A	=	cross-sectional area of nozzle
F_i, f_i, G_i	=	various functions defined in the text, with $i = 1, 2, 3$
h	=	Lagrangian multiplier, which is a function of y
L	=	length of the nozzle
M	=	Mach number
p	=	local pressure
p_a	=	ambient pressure
W	=	flow velocity (scalar)
x	=	coordinate in the axial direction
y	=	coordinate in the radial direction
α	=	Mach angle
γ	=	ratio of specific heats
δ	=	variation
θ	=	angle between flow direction and nozzle axis
λ_2, λ_3	=	Lagrangian multiplier constants
ρ	=	density
ϕ	=	angle between control surface and nozzle axis

Subscripts

c	=	chamber conditions
C, E, F	=	values taken at respective points
M, θ	=	denote partial differentiation
t	=	conditions at throat

Presented at the ARS Semi-Annual Meeting, San Francisco, Calif., June 10–13, 1957.
[1] Research Scientist. Now with Rocketdyne, Canoga Park, Calif.

Introduction

THE diverging portion of an exhaust nozzle is an important feature for all engines which depend upon the thrust produced by the exhaust gases. Maximum possible thrust on a nozzle can be obtained by complete expansion of the exhaust gases to the ambient pressure through a nozzle designed to give a parallel uniform jet at the exit. One may apply the method suggested by Foelsch (1)[2] for the design of such nozzles. For jet engines operating at high altitudes and especially for rocket motors, one is required to design nozzles for very low ambient pressures. Even the shortest nozzle designed by the aforementioned method would be excessively long and heavy. Logically, one would seek a nozzle of limited length, since length is a fair indication of nozzle weight. The problem then is the choice of a nozzle having a specified length and yielding maximum thrust. Semi-empirical investigations of this problem were carried out by Dillaway (2) and Fraser and Rowe (3). A mathematically rigorous formulation and some numerical examples are due to Guderley and Hantsch (4). Their principal idea is the introduction of a characteristic surface as control surface for the momentum, the mass flow and the length of the nozzle. By this choice, the partial differential equations governing the gas flow reduce to one ordinary differential equation, and a one-dimensional variational problem is obtained.

The present paper proceeds in a similar fashion but does not specify in advance that the control surface is a characteristic surface. The form of the control surface and the velocity distribution along it are determined in such a manner that the thrust assumes a maximum, while the mass flow has a constant value. Obviously, this formulation fails to include an expression for the flow differential equations, and thus one might be in doubt if the velocity distribution along the control surface thus obtained can occur within an actual flow. However, one finds that the control surface becomes automatically a characteristic surface. For this reason, the characteristic conditions need not be included in the present formulation.

[2] Numbers in parentheses indicate References at end of paper.

This results in a great reduction of the computational work. Moreover, the approach shown here may possess a mathematical interest of its own.

Initial Expansion in the Nozzle

Let $ATBE$, as shown in Fig. 1(a), represent the intersection of the nozzle contour with the meridional plane. Contour AT is the contraction upstream of the throat and TBE is the diverging portion of the nozzle. The initial expansion occurs along TB and the wall contour B to E turns the flow back to a direction nearer the axial. Guderley and Hantsch considered this initial expansion to occur through a sharp corner. Since it is advisable to avoid sharp corners in exhaust nozzle contours, one can prescribe a suitable contour TBB' in the throat region. However, the location of point B along this prescribed curve is left open in considering various nozzle shapes. The location of point B, in fact, is a part of the solution of the problem. After the point B is determined the contour BB' does not effect the construction of the optimum nozzle contour.

Sauer (5) gives a method of analyzing transonic flow in the throat region in terms of the radius of curvature of the nozzle wall at the throat. Using this method, a line TT' (Fig. 1(a)) can be defined along which the Mach number is constant. The flow directions at various locations along the line can be computed. In the few examples carried out by the author, the Mach number along TT' was larger than unity and no difficulty was encountered in applying the method of characteristics to determine the flow downstream of the line TT'.

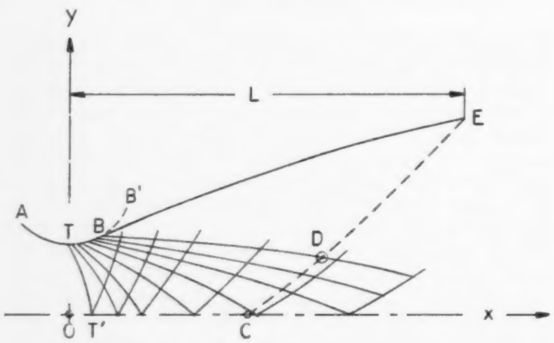

Fig. 1(a) Characteristics net and control surface

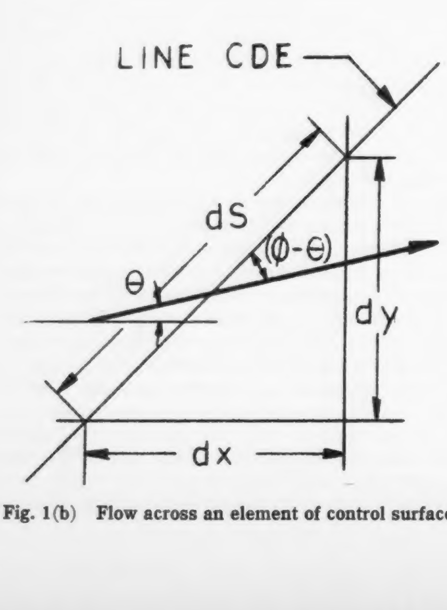

Fig. 1(b) Flow across an element of control surface

The origin of the coordinate system lies at the throat section, the x-axis coincides with the nozzle axis, and y represents the radial distance from the nozzle axis. To construct the flow field a number of points between T and B' are chosen and the values of x, y and θ for the given contour are determined at these points. Using these initial conditions along TT' and TBB', the method of characteristics (6) can be applied to construct a characteristics net and evaluate flow properties at the net points. Such a net of characteristics is schematically shown in Fig. 1(a) and is denoted as the "kernel" since the variations in the nozzle shape between B and E do not alter the flow properties in the region upstream of right characteristic through B. Location of point B on the prescribed contour is implied in the determination of the last right characteristic up to which the "kernel" of Fig. 1(a) is to be utilized in the construction of the nozzle shape.

Formulation of the Problem

For computing thrust on the nozzle and mass flow through the nozzle, let us consider a control surface passing through the exit of the nozzle. In Fig. 1(a), let CE describe the intersection of the control surface with the meridional plane. Let ϕ, a function of y, denote the inclination of line CE to the nozzle axis. The location of the point C on the axis and the function $\phi(y)$ would then completely define the control surface. Along CE consider an elemental length ds (Fig. 1(b)) at a distance y from the nozzle axis. The elemental area generated by rotation about the axis is $dA = 2\pi y ds$. Also, $ds = dy/\sin\phi$.

Let ρ, W and θ denote respectively the density, velocity and flow direction considered uniform over the element ds. The mass flow crossing the elemental area is given by

$$\rho W \frac{\sin(\phi - \theta)}{\sin\phi} 2\pi y dy$$

and the momentum flux in the x direction

$$\rho W^2 \frac{\sin(\phi - \theta)\cos\theta}{\sin\phi} 2\pi y dy$$

By integrating along CE one obtains the mass flow crossing the control surface

$$\text{mass flow} = \int_C^E \rho W \frac{\sin(\phi - \theta)}{\sin\phi} 2\pi y dy \quad\text{[1]}$$

Similarly, thrust on the nozzle can be obtained by integrating pressure differential and momentum flux across CE

$$\text{thrust} = \int_C^E \left[(p - p_a) + \rho W^2 \frac{\sin(\phi - \theta)\cos\theta}{\sin\phi}\right] 2\pi y dy \quad\text{[2]}$$

In the present problem the conditions at the inlet to the nozzle are assumed to be given and hence maximizing the above expression is sufficient.

The axial distance between C and E is given by

$$x_E - x_C = \int_C^E \cot\phi \, dy$$

Hence the length of the diverging portion of the nozzle is

$$\text{length} = x_C + \int_C^E \cot\phi \, dy \quad\text{[3]}$$

Varying the nozzle contour would involve corresponding variations in the control surface. One can leave point C fixed and vary ϕ to obtain the variations in the control surface. The location of the point C depends upon the length chosen for the nozzle. Point C can be treated as fixed in the present problem, since the variations of nozzle contour are subject

to constant length. Hence the following condition must be satisfied

$$\int_C^E \cot \phi \, dy = \text{const} \qquad [4]$$

Continuity of mass flow requires that the mass flow as given by Equation [1] must be equal to mass flow through the throat section, which is invariant with changes in the nozzle contour. Hence it is required to maximize thrust on the nozzle subjected to the restrictions given by Equations [1, 4]. Using the Lagrangian multiplier method this problem can be reduced to maximizing the integral

$$I = \int_C^E (f_1 + \lambda_2 f_2 + \lambda_3 f_3) dy \qquad [5]$$

where

$$f_1 = \left[(p - p_a) + \rho W^2 \frac{\sin(\phi - \theta)\cos\theta}{\sin\phi} \right] y$$

$$f_2 = \rho W \frac{\sin(\phi - \theta)}{\sin\phi} y$$

$$f_3 = \cot\phi$$

and λ_2, λ_3 are Lagrangian multiplier constants.

Solution of the Problem

The solution of the problem lies in setting the first variation of I (Equation [5]) equal to zero and thereby obtaining the required control surface and flow conditions along it. Let us first enumerate all the permissible variations of the quantities appearing in the integral. In the following discussion, δ denotes variation of a function, and partial derivatives are indicated by the respective subscripts.

As explained in the introduction, the initial expansion immediately behind the throat region is assumed to occur along a prescribed contour TBB' (Fig. 1(a)). Let B indicate the point up to which such an expansion takes place, and let the right characteristic from B intersect the control surface at D. Any variation in nozzle contour downstream of point B would not affect the flow between C and D.

For convenience the control surface between C and D is assumed to coincide with a left characteristic in the "kernel" of the characteristics net. This leads to δC, δM and $\delta\theta$ all zero in this region. $\phi = (\alpha + \theta)$ is a known quantity along CD, yielding $\delta\phi = 0$. The location of point D, i.e., the extent to which the assumed initial expansion occurs, is not known. Hence δD is not zero.

Between D and E, we have δD, δM, $\delta\theta$ and $\delta\phi$ all nonzero. Since only the length of the nozzle is prescribed, δy_E is nonzero. M and θ are continuous in the interior of the flow, and ϕ is also required to be continuous along CDE. Hence the integrand in Equation [5] is continuous. The variation of point D therefore does not enter into the first variation of the integral I, and one obtains

$$\delta I = 0 = \int_{y_D}^{y_E} \{(f_{1M} + \lambda_2 f_{2M} + \lambda_3 f_{3M})\delta M + (f_{1\theta} + \lambda_2 f_{2\theta} + \lambda_3 f_{3\theta})\delta\theta + (f_{1\phi} + \lambda_2 f_{2\phi} + \lambda_3 f_{3\phi})\delta\phi\} dy + \delta y_E (f_1 + \lambda_2 f_2 + \lambda_3 f_3)_{\text{at } E} \qquad [6]$$

Since the variations in M, θ, ϕ and y_E are arbitrary, the above leads to

$$f_{1M} + \lambda_2 f_{2M} + \lambda_3 f_{3M} = 0 \qquad [7]$$

$$f_{1\theta} + \lambda_2 f_{2\theta} + \lambda_3 f_{3\theta} = 0 \qquad [8]$$

$$f_{1\phi} + \lambda_2 f_{2\phi} + \lambda_3 f_{3\phi} = 0 \qquad [9]$$

along DE, and

$$f_1 + \lambda_2 f_2 + \lambda_3 f_3 = 0 \quad \text{at } E \qquad [10]$$

Since f_{3M} and $f_{3\theta}$ are zero, one obtains from Equations [7, 8]

$$f_{1M} f_{2\theta} = f_{1\theta} f_{2M}$$

It should be noted that y drops out of the above equation, leading to

$$\phi = \theta + \alpha \quad \text{along } DE \qquad [11]$$

This above relation shows that the control surface coincides with the last left characteristic in the nozzle flow, and the conditions along this line are obtained by introducing this relation into Equations [8, 9]. Hence

$$\frac{W \cos(\theta - \alpha)}{\cos\alpha} = -\lambda_2 \qquad [12]$$

and

$$y \rho W^2 \sin^2\theta \tan\alpha = -\lambda_3 \qquad [13]$$

along DE are the necessary conditions for the integral [5] to be a maximum. Substituting Equations [11, 12, 13] into Equation [10], the following condition results

$$\sin 2\theta = \frac{p - p_a}{\frac{1}{2}\rho W^2} \cot\alpha \quad \text{at } E \qquad [14]$$

This condition relating M and θ at the end point of the nozzle is the same as given in (4).

From Equations [12, 13] one can obtain the following relation dM/dy and $d\theta/dy$

$$\frac{d\theta}{dy} - \frac{\sqrt{M^2 - 1}}{M\left(1 + \frac{\gamma - 1}{2} M^2\right)} \frac{dM}{dy} + \frac{\sin\alpha \sin\theta}{y \sin(\theta + \alpha)} = 0 \qquad [15]$$

This relation is the compatibility condition between the Mach number and the flow direction along a left characteristic. It is crucial to this approach that such a condition is implicit in the solution of Equations [12, 13], since according to Equation [11] the control surface has the direction of the left characteristic. If the condition of compatibility were not fulfilled, the control surface would become a limiting line, i.e., the flow pattern would be physically impossible. Equations [12, 13], in connection with [11], give the form of the control surface and the velocity distribution in a form which does not require the solution of partial differential equations. In this regard, the present paper goes beyond Guderley's solution. In retrospect, one recognizes from the present approach, that the additional Lagrangian multiplier h introduced in Guderley's paper will assume the value zero.

Method of Constructing Optimum Nozzle Contour

To illustrate the application of the solution given in the previous section toward obtaining a nozzle contour, a numerical example is carried out in detail in this section. A constant value of $\gamma = 1.23$ and zero ambient pressure are used in the example. The method is simple enough to make the appropriate changes for other conditions.

The first step is to choose a suitable curve for the nozzle wall contour in the throat region. A circular arc of radius $1.5y_t$ (y_t is the radius of throat section) is chosen for the nozzle contour upstream of the throat section. The asssumed nozzle wall contour in the throat region is shown in Fig. 2. Calculations according to (4) indicate a Mach number 1.103 on the wall at the throat section. In Fig. (2), TT' represents the line along which $M = 1.103$. The initial expansion im-

mediately behind the throat is assumed to occur along a circular arc of 0.45 y_t radius. Since flow across TT' is sufficiently supersonic, it is assumed unaffected by downstream conditions. A characteristic net is computed (see the section on initial expansion in the nozzle) for these initial conditions, a portion of which is shown in Fig. 2. The five right characteristic lines shown in the figure start from initial points on the nozzle wall in the throat region, where the wall slopes are 28, 30, 32, 34 and 35 deg, respectively.

Instead of choosing a particular nozzle length, M_E, the Mach number on the nozzle wall at the exit, will be prescribed. This Mach number forms a parameter which describes a posteriori the length of the nozzle. By choosing different values of M_E, optimum contours for different lengths can be obtained. Optimum nozzle contour for any particular desired length can then be obtained by interpolation. For zero ambient pressure, Equation [14] reduces to

$$\sin 2\theta_E = \frac{2}{\gamma M_E^2} \cot \alpha_E \quad [16]$$

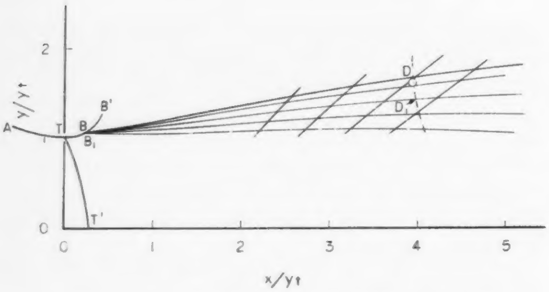

Fig. 2 Selection of the extent of initial expansion

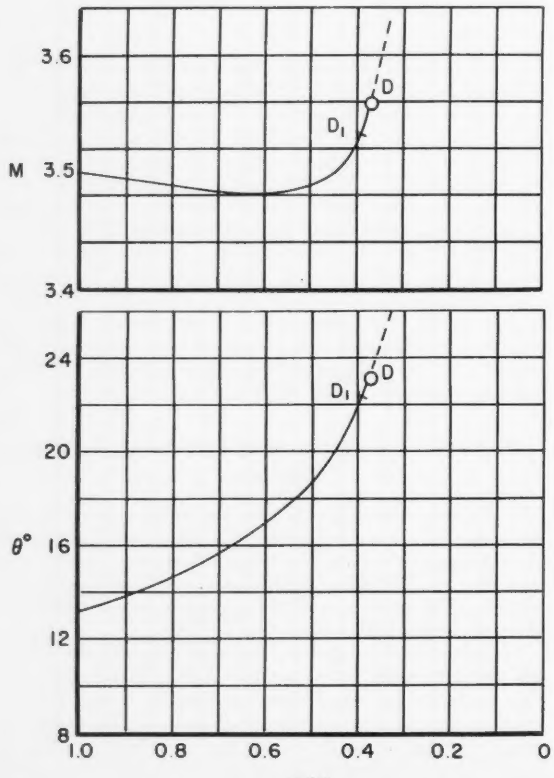

Fig. 3 Mach number and flow angle along the control surface

For the present numerical example $M_E = 3.5$ is chosen and the above equation yields the necessary wall slope $\theta_E = 13.22$ deg. Equations [12, 13] govern M and θ along the control surface, and the constants λ_2 and λ_3 can be evaluated by inserting $M_E = 3.5$ and $\theta_E = 13.22$ deg at $y = y_E$. Equations [12, 13] can be rewritten as

$$M^* \frac{\cos(\theta - \alpha)}{\cos \alpha} = M_E^* \frac{\cos(\theta_E - \alpha_E)}{\cos \alpha_E} \quad [17]$$

where

$$M^* = \left[\frac{1}{\gamma - 1 + \frac{2}{M^2}}\right]^{1/2}$$

and

$$\frac{y}{y_E} M^2 \left(1 + \frac{\gamma - 1}{2} M^2\right)^{-\gamma/(\gamma-1)} \sin^2\theta \tan\alpha = M_E^2 \left(1 + \frac{\gamma - 1}{2} M_E^2\right)^{-\gamma/(\gamma-1)} \sin^2\theta_E \tan\alpha_E \quad [18]$$

The above two equations can easily be solved by first choosing pairs of M, θ values satisfying Equation [17] and then obtaining corresponding values of y/y_E from Equation [18]. Fig. 3 shows the values of M and θ thus obtained as functions of y/y_E. These relations can be computed even though one does not yet know the position of the control surface DE (see Fig. 1).

The next step is to find the point in the characteristics net (shown in Fig. 2) which would define the end point on the control surface. Consider the flow conditions along the right characteristic from any point B_1 on the prescribed contour TB'. Pick a point D_1 on the right characteristic such that the values of M and θ at D_1 satisfy Equation [17]. The dashed line shown in the figure is the locus of all such points. From the values of M and θ at D_1, the value of y/y_E at D_1 can be found from Fig. 3. Conservation of mass requires the mass flow crossing the right characteristic B_1D_1 to be equal to the mass flow crossing the control surface from D_1 to E, the end point on the nozzle wall. That is

$$2\pi y_t^2 \rho_t W_t \int_{B_1}^{D_1} \frac{\rho W \sin\alpha}{\rho_t W_t \cos(\theta - \alpha)} \frac{y}{y_t} d\left(\frac{x}{y_t}\right) = 2\pi y_E^2 \rho_t W_t \int_1^{D_1} \frac{\rho W \sin\alpha}{\rho_t W_t \sin(\theta + \alpha)} \frac{y}{y_E} d\left(\frac{y}{y_E}\right) \quad [19]$$

It should be remembered that the integration on the left-hand side is carried out along B_1D_1 in Fig. 2, whereas the integration on the right-hand side depends upon the control surface, as described in Fig. 3, and the point D_1. Also the ratio of y_E/y_t in the above depends upon the choice of the point D_1.

The above equation can be satisfied by a few trials and by noting the error for each choice of the point D_1. In the present example the point D shown encircled in Figs. 2 and 3, satisfies the above equation, [19]. By interpolating between known right characteristics shown in Fig. 2, the right characteristic BD through the point D, with respective values of M and θ on it is found. This characteristic line BD is shown in Fig. 4, indicated as extent of "kernel" since the assumed initial expansion occurs up to this right line. The location of the point D as represented in Figs. 3 and 4 yields the ratio y_E/y_t. Equation [11] indicates that the control surface DE is a left characteristic and this property is used to find X/y_t for respective values of M, θ, and y/y_t along DE. Thus the information given in Fig. 3 can be translated to define the control surface DE in terms of y_t as shown in Fig. 4. The length of the nozzle is given by the x-coordinate of the point E and is found to be 8.19 y_t for this example.

Starting with the above derived flow conditions along lines

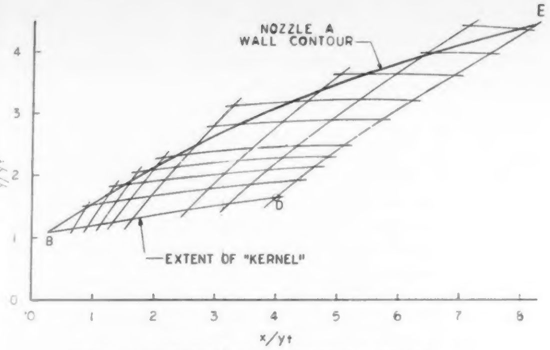

Fig. 4 Construction of the nozzle contour

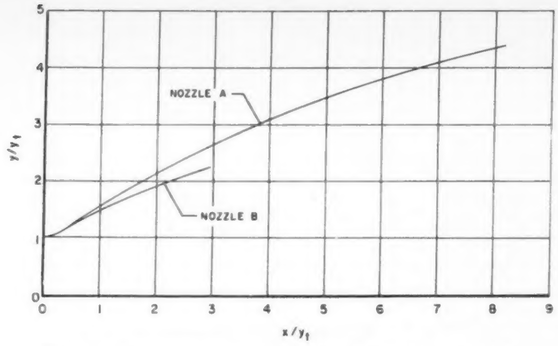

Fig. 5 Optimum nozzle contours—$P_a = 0$; $\gamma = 1.23$

BD and DE, the characteristics net is completed in the region between the two lines as shown in Figure 4. With the flow field in this region known, the streamline passing through B and E is drawn. This streamline shown in Fig. 4 then forms the required contour for nozzle length of 8.19 y_t. As mentioned before, optimum nozzle contours for different lengths can be designed by choosing different values for wall Mach number at the point E.

Typical Nozzle Configurations

The nozzle configuration computed in the preceding section is shown in Fig. 5 and represents the contour for optimum thrust when zero ambient pressure and a length of 8.19 y_t are prescribed. The coordinates of wall points, Mach number and wall slopes at the points are listed in Table 1. By choosing $M_E = 2.6$ and zero ambient pressure a shorter nozzle of length 2.94 y_t is designed and is also shown in Fig. 5. The coordinates of wall points of this nozzle are listed in Table 2.

Table 1 Optimum thrust nozzle A
($P_a = 0$, $\gamma = 1.23$, $L = 8.19Y_t$)

X/Y_t	Y/Y_t	M	Wall slope θ, deg
0.25	1.08	2.11	34.4
0.33	1.13	2.19	32.8
0.94	1.52	2.42	32.0
1.03	1.58	2.45	31.7
1.17	1.66	2.48	31.2
1.47	1.84	2.57	30.4
1.88	2.07	2.67	29.0
2.31	2.30	2.77	27.5
3.37	2.82	2.96	24.0
4.20	3.16	3.08	21.6
5.43	3.32	3.24	18.5
6.50	3.95	3.35	16.2
7.98	4.34	3.48	13.5
8.19	4.40	3.50	13.1

Table 2 Optimum thrust nozzle B
($P_a = 0$, $\gamma = 1.23$, $L = 2.94Y_t$)

X/Y_t	Y/Y_t	M	Wall slope θ, deg
0.21	1.05	1.96	28.7
0.29	1.10	2.01	27.8
0.63	1.27	2.12	26.9
0.91	1.41	2.20	26.1
1.52	1.70	2.34	23.7
2.30	2.01	2.49	20.4
2.94	2.23	2.60	17.9

The thrust coefficients of these nozzle configurations, computed from wall pressures, are shown in Table 3, and are compared with conical nozzles having the same lengths and area ratios. Thrust coefficient is defined as

$$C_T = \frac{\text{thrust}}{p_c A_t}$$

and the maximum attainable value depends only upon the ambient pressure and γ, the ratio of specific heats. For zero ambient pressure

$$C_{T_{\max}} = \gamma \left(\frac{\gamma + 1}{2}\right)^{-\gamma/(\gamma-1)} \sqrt{\frac{\gamma + 1}{\gamma - 1}}$$

and one should remember that this value can only be obtained with a nozzle of infinite length and infinite exit area. The thrust coefficients of the optimum nozzles are also shown in Table 3 as percentages of the above maximum attainable value.

Table 3 Comparison of thrust coefficients

	Nozzle A of Fig. 5	Nozzle B of Fig. 5	Contour A shortened to length of nozzle B
Length-throat radius	8.19	2.94	2.294
Exit area-throat area	19.36	4.973	6.838
Thrust coefficient	1.7676	1.5829	1.5688
One-dimensional thrust for the area ratio, %	98.58	96.93	93.5
Thrust of conical nozzle of same length and area ratio, %	102.3	100.5	102.1
Maximum available thrust, %	82.7	74.1	73.4

Results presented in Table 3 show that nozzle A yields 2.3 per cent more thrust than a conical nozzle of the same length and area ratio. On the other hand, nozzle B, of much shorter length and smaller exit area, yields only 0.5 per cent more thrust than the equivalent conical nozzle. If nozzle contour A were cut off at a length of 2.94 y_t (i.e., the length of nozzle B) one obtains a thrust coefficient of 1.5688. As can be expected this value is lower than the thrust coefficient of the nozzle B which was designed to yield maximum thrust for the length.

To estimate the effect of γ on the optimum nozzle shape, $\gamma = 1.4$ is used, and for zero ambient pressure a nozzle is designed having a length of 9.19 y_t. This nozzle contour is shown in Fig. 6, and differs considerably from the contour computed for $\gamma = 1.23$. Increasing the value of γ reduces the exit area of optimum thrust nozzle.

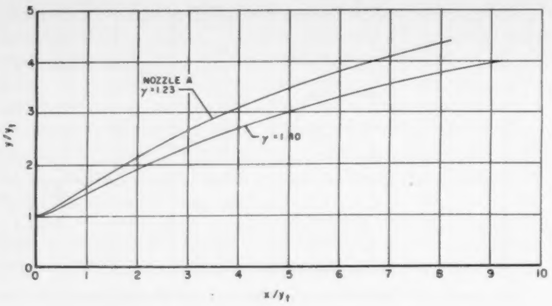

Fig. 6 Optimum nozzle contours—$P_a = 0$

It should be remembered that the nozzle contours shown in Figs. 5 and 6 are computed for inviscid isentropic flow. Similar to the methods used in wind tunnel nozzle design, one may compute the displacement thickness of the boundary layer along the nozzle wall and apply the correction to the contours shown in Figs. 5 and 6. Increasing the radial coordinates of the wall contour by the amount of the boundary layer thickness would yield the exit flow for which the nozzle is designed.

Conclusions

By applying the calculus of variations a method is developed for designing the wall contour of an optimum thrust nozzle. The ambient pressure, length of the nozzle and wall contour in the throat region appear as governing conditions in the formulation and solution of the problem. Typical nozzle contours are presented in Figs. 5 and 6.

A nozzle contour obtained for a given length and ambient pressure will also be the contour yielding maximum thrust when the length and the corresponding exit area are the prescribed conditions. For example, nozzle A shown in Fig. 5 will also be the optimum contour if, in addition to length of $L/y_t = 8.19$, an exit area of $A/A_t = 19.36$ is the condition prescribed in place of zero ambient pressure.

The nozzle contours presented in Fig. 5 show the difference between the optimum nozzles computed for the two different lengths. On the contrary, Guderley and Hantsch (4) concluded from their computations that for a given ambient pressure all optimum nozzles of different lengths can be represented by a single contour. This may be a coincidence due to either the sharp-corner expansion he considered, or the complicated nature of his solution.

The ratio of specific heats, γ, of the exhaust gases has considerable effect on the optimum nozzle contour as can be seen from Fig. 6.

Comparison of thrust coefficients shown in Table 3 indicates that the advantage of contoured nozzles is greater at larger area ratios.

References

1 Foelsch, K., "The Analytical Design of an Axially Symmetric Laval Nozzle for a Parallel and Uniform Jet," *Journal of the Aeronautical Sciences*, March 1949.

2 Dillaway, R. B., "A Philosophy for Improved Rocket Nozzle Design," Jet Propulsion, vol. 27, Oct. 1957, p. 1088.

3 Fraser, R. P., and Rowe, P. N., "The Design of Supersonic Nozzles for Rockets," Imperial College of Science, South Kensington, England, Report JRL No. 28, Oct. 1954.

4 Guderley, G., and Hantsch, E., "Beste Formen für Achsensymmetrische Uberschallschubdusen," *Zeitschrift für Flugwissenschaften*, Brauschweig, Sept. 1955.

5 Sauer, R., "General Characteristics of Flow Through Nozzles at Near Critical Speeds," NACA TM 1147.

6 Shapiro, A. H., "The Dynamics and Thermodynamics of Compressible Fluid Flow," Ronald Press, New York, pp. 676–680.

Prediction of the Explosive Behavior of Mixtures Containing Hydrogen Peroxide

E. S. SHANLEY[1] and J. R. PERRIN[2]

Becco Chemical Division, Food Machinery & Chemical Corporation, Buffalo, N. Y.

This paper concerns a relationship between thermal properties and explosive properties for mixtures containing hydrogen peroxide, water and soluble organic compounds. It has been known for some time that certain mixtures of this kind are explosive. In the present study it has been found that sensitivity to initiation is about the same for all mixtures having the same heat of reaction. This relationship is demonstrated for five different organic constituents and for three methods of initiation. The findings provide an easy basis for predicting the likely range of explosive compositions of untested mixtures containing hydrogen peroxide.

Introduction

Ternary mixtures containing hydrogen peroxide, water and soluble organic compounds are used in rocket propulsion, in synthetic organic chemistry, and for other purposes Mixtures of this kind are explosive within certain concentration limits. The range of explosive compositions has been determined empirically in a few cases.[3] This is a laborious undertaking, so that a way was sought to predict the properties of untested mixtures. The present communication shows the correlation found between explosive behavior and ΔH, the calorimetric heat of reaction. This correlation can be used to predict the range of explosive compositions for untested mixtures.

Experimental Part

Mixtures containing hydrogen peroxide, water and several different combustible materials were tested. Only soluble "fuels" were used, so as to avoid the complications of two-phase systems. Tests for sensitivity were carried out with blasting caps, drop weights and static sparks, as described

Received Sept. 9, 1957.

[1] Present address: Arthur D. Little, Inc., Cambridge, Mass. Mem. ARS.

[2] Present address: Marquardt Aircraft Company, Van Nuys, Calif.

[3] Shanley, E. S., and Greenspan, F. P., "Highly Concentrated Hydrogen Peroxide," *Ind. Eng. Chem.*, vol. 39, 1947, pp. 1536–1543.

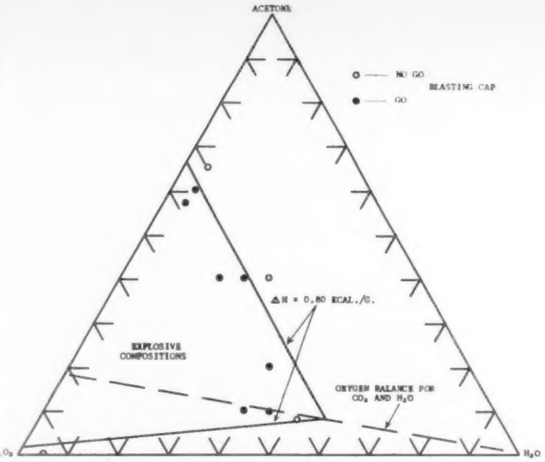

Fig. 1 Explosive compositions of acetone, hydrogen peroxide and water; blasting cap initiation

below. Tests were carried out at ordinary room temperature unless otherwise specified.

Blasting Cap Tests

Blasting cap tests were carried out as follows: The desired proportions of fuel and aqueous hydrogen peroxide were measured into separate containers and then mixed behind a suitable barricade. The resulting mixture, about 10 ml in all, in a 15 × 150 mm test tube was placed in a 7-in. section of ¾ in. ID lead pipe having a ¼ in. wall thickness. The lead pipe was supported upright on a 1-in.-thick steel plate. A fuse-ignited No. 6 aluminum shelled blasting cap was lowered into the test tube and supported in such a way that the shell of the cap was about half immersed. The effect was judged by the condition of the lead pipe after the shot. The cap alone only bulged the pipe, while complete fragmentation occurred if the mixture detonated. In addition, complete absence of liquid residue was taken as evidence for detonation.

Dropweight Tests

Dropweight tests were carried out in a Bureau of Mines type falling weight machine. A few drops of the sample were confined in a tool steel cylinder beneath a piston. The freely falling 3-kg weight was dropped from a height of one meter directly on the piston. The effect was judged by the sound, these mixtures producing a very loud noise upon detonation. Points noted as "no go" denote no positive tests and a minimum of four negative tests on separate portions of a given composition.

Static Spark Tests

Static spark tests were carried out with an apparatus patterned after the one described in Bueau of Mines Report of Investigation No. 3852: "Sensitivity of Explosives to Initiation by Electrostatic Discharges," by Brown, Kusler and Gibson. These tests were carried out by placing a few drops of the sample in a special cell made by inserting a ¾ in. piece of a ¼ in. diam aluminum rod part way into a piece of Saran tubing ¾ in. long. This "cup" was supported upright and grounded by inserting the protruding portion of the aluminum rod into a hole in a steel plate. A phonograph needle connection to a charged condenser was then lowered into the cup until the condenser discharged into the bottom of the cup. In these tests the charging voltage was always 5000 volts. The energy in the discharge was about 25 joules, obtained by the use of a 2.0 mfd. condenser. Some idea of the intensity of the spark may be gained by comparison with the Bureau of Mines' findings that a man's body may accumulate enough static electricity to produce a 0.015-joule discharge. Only

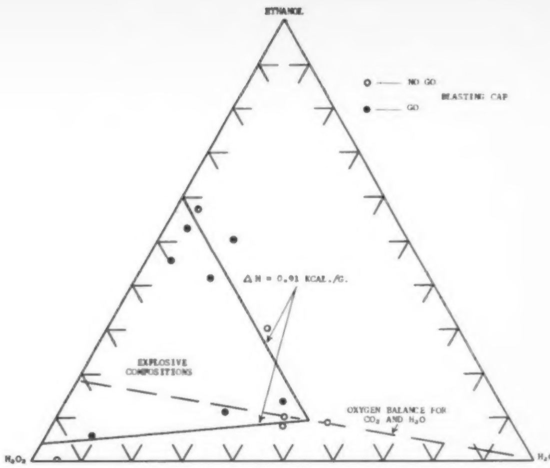

Fig. 2 Explosive compositions of ethanol, hydrogen peroxide and water; blasting cap initiation

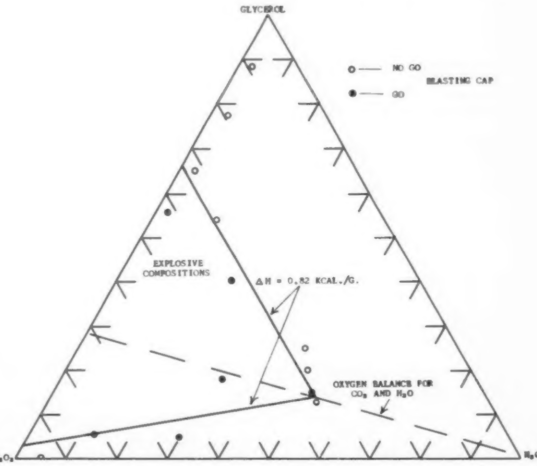

Fig. 3 Explosive compositions of glycerol, hydrogen peroxide and water; blasting cap initiation

glycerol-peroxide and ethanol-peroxide mixtures were tested in this way.

Test Results

Test results are represented by the points on Figs. 1–7. The dashed lines on these figures represent all compositions of the correct proportion to yield CO_2 and H_2O, i.e., zero oxygen balance. The solid lines are isoenthalpy lines derived from the thermal calculations described in the next section.

Thermal Calculations

Since explosive behavior depends upon a high content of chemical energy, some limit will exist below which the energy contained will be insufficient to support propagation. In addition, the behavior of potentially explosive compositions is known to depend upon the intensity of the initiating impulse. This implies a relation between energy content and *sensitivity* to initiation and propagation. It seems reasonable to look for a correlation with the calorimetric heat of reaction, for initiation and propagation of explosive reactions are most probably thermal in nature.[4, 5]

[4] Parlin, R. B., Duffy, G., Powell, R. E., and Eyring, H., "The Theory of Explosion Initiations," OSRD Report 2026, Nov. 13, 1943.

[5] Bowden and Yoffe, "Initiation and Growth of Explosions," Cambridge University Press, 1952.

Fig. 4 Explosive compositions of ethanol, hydrogen peroxide and water; drop weight and static spark initiation

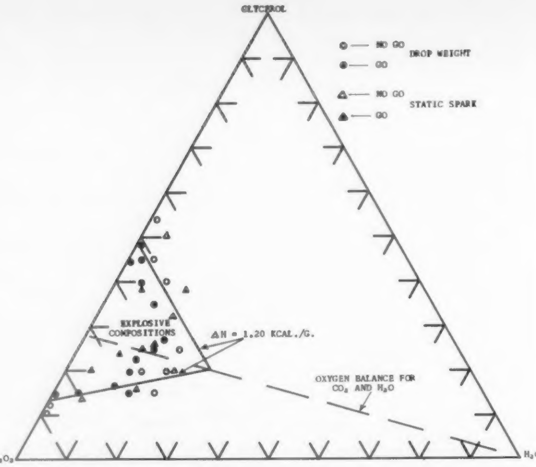

Fig. 5 Explosive compositions of glycerol, hydrogen peroxide and water; drop weight and static spark initiation

In the present cases, correlation has been noted between the experimental behavior of explosive mixtures and the calculated values for the enthalpy change at room temperature. Heats of reaction have been calculated on various assumptions as to the reaction path. The best correlations have resulted from calculations based upon the scheme

$$\text{all } H_2O_2 \rightarrow H_2O \text{ (liquid)} + O_2 \text{ (gas)}$$
$$O_2 + \text{fuel} \rightarrow CO_2 \text{ (gas)} + H_2O \text{ (liquid)}$$

Any remaining fuel is assumed to be unchanged, in the liquid state. This sequence is thermally identical with direct reaction between fuel and hydrogen peroxide, with remaining H_2O_2 in oxidant-rich mixtures decomposed, and with remaining fuel in fuel-rich mixtures remaining unchanged. Sample calculations for illustration are shown in Table 1.

Using the sequence in Table 1, ΔH values were calculated for large numbers of points within the triangular charts representing mixtures of hydrogen peroxide, water and various fuels. Using these points, isoenthalpy lines were drawn on each chart. For blasting cap initiation, it was possible in each case to select an enthalpy value which gave good agreement between the isoenthalpy envelope and the experimentally determined sensitive area. For the different ternary mixtures tested, this enthalpy value varied from 0.8 kcal per gram to 0.9 kcal per gram, depending on the fuel in the mixture. In each case, the envelope had a single discontinuity, located at a composition of zero oxygen balance to CO_2 and H_2O. This is in agreement with the shape of the sensitive area as determined experimentally.

Drop weight tests and static spark tests set off only those mixtures with still higher energy content. The isoenthalpy envelope most nearly fitting the drop weight tests turned out to be about 1.2 cal per gram. The spark test data are limited in number but suggest sensitivity at enthalpy values slightly higher than 1.2 kcal per gram.

Several alternate schemes for calculating ΔH were tried, but gave less satisfactory agreement with the experimental results. For example, one may assume the same reactions as those outlined above, but take the products in the vaporized state. This produces a marked dependence of the enthalpy line for fuel-rich mixtures on the ratio of fuel to water. It is abundantly clear from the experimental evidence that the sensitivity is constant, on the fuel rich side, with constant peroxide content. This fact is most easily explainable on the thesis that the reaction products immediately following the detonation are still in a condensed state.

A conventional way to handle thermal calculations of this kind is to assume that the constituents first break down to very simple parts and then recombine with each other. In the present instance, one might assume that all of the fuel broke down to carbon, hydrogen and water, while all the peroxide yielded oxygen and water. The hydrogen would then combine with the oxygen to form water. After oxidation of the hydrogen, the carbon would begin to oxidize and so on until the oxygen-rich region was reached. This and related methods of calculation lead to predictions of several discontinuities in the envelope which are not observed experimentally. Also, the predicted carbon residue has not been observed in our studies of fuel rich mixtures. Secondary reaction might account for the disappearance of the carbon, and calculations on this more conventional basis might correlate well with the power or rate of the explosion. In fact, the preferred reaction

Table 1 Sample calculations

$$H_2O_2 \rightarrow \tfrac{1}{2}O_2 + H_2O \qquad \Delta H_{(298)} = -0.67 \text{ kcal/g}$$
$$C_2H_5OH + 3O_2 \rightarrow 2CO_2 + 3H_2O \qquad \Delta H_{(298)} = -7.11 \text{ kcal/g}$$

	Composition, wt %			Ethanol consumed by O_2 from H_2O_2, grams	Heat liberated, kcal		
	H_2O_2	H_2O	Ethanol		From ethanol combustion	From H_2O_2 decomposition	Total/100 grams of mixture
Fuel rich	40	15	45	9.0	64.0	26.8	90.8
Oxygen rich	85	9	6	6.0	42.7	56.9	99.6

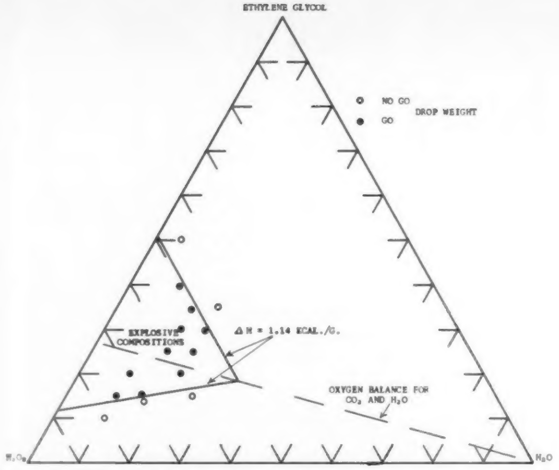

Fig. 6 Explosive compositions of ethylene glycol, hydrogen peroxide and water; drop weight tests

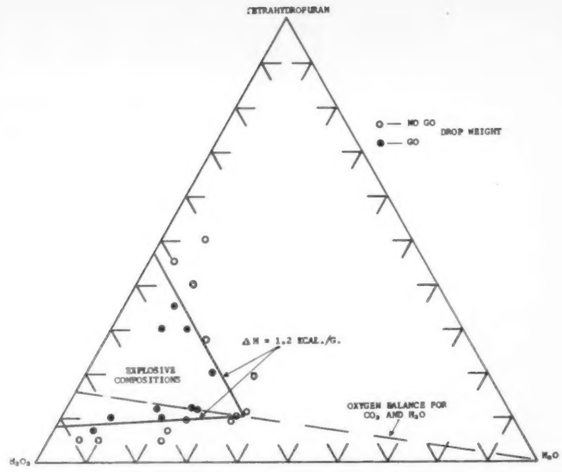

Fig. 7 Explosive compositions of tetrahydrofuran, hydrogen peroxide and water; drop weight tests

scheme detailed above may be valid only for the initial stages, in the critical period between the initiating impulse and the establishment of a propagating reaction.

Temperature Coefficient of the Explosion Limit

If the heat content is the decisive factor in sensitivity, warmer solutions should have wider explosive limits than cooler solutions. Such behavior has been demonstrated for a few peroxide compositions. For example, it is known that 95 per cent aqueous hydrogen peroxide can be detonated under very special conditions (very high confinement and a powerful booster charge). It can be shown that 85 per cent peroxide possesses about the same sensitivity if warmed to 100 C. Now, the heat of decomposition for 95 per cent aqueous peroxide is about 650 cal per gram and for 85 per cent peroxide is 580 cal per gram. The specific heat of 85 per cent H_2O_2 is about 0.68 cal per gram per degree C, so that warming from 25 to 100 C adds about 51 cal per gram. This is nearly equivalent to the heat deficit of 70 cal per gram resulting from the smaller amount of peroxide in the 85 per cent solution.

A very few observations on mixtures containing fuels have shown that raising the temperature does indeed increase the sensitivity. However, the area representing sensitive compositions seems to increase more than can be accounted for by the direct addition of sensible heat. At any rate, a given mixture of this kind seems certain to be more sensitive at higher temperatures.

Precautions in the Use of Explosion Limit Data

In using data for explosion limits it is necessary to bear certain limitations in mind. For example, points marked "no go" on these charts indicate no positive effects in a few attempts. In a long series of attempts on a composition near the indicated limits, it is probable that some explosions would occur. Also, the strength of the initiator, the degree of confinement, the temperature, the quantity of material and possibly other factors may affect the sensitivity. In short, the boundaries shown are not to be taken as literal limits beyond which no hazards exist. To provide a margin of safety, tests should be made under conditions more severe than those expected in practice. For example, compositions immune to the effect of a blasting cap are very unlikely to be set off during ordinary transportation and handling.

Summary

A method has been described for predicting the range of explosive compositions in certain systems containing hydrogen peroxide, water and a soluble fuel. Using calculations based upon arbitrary but reasonable assumptions about the course of the reaction, it has been shown that the isoenthalpy line for 0.8 kcal per gram of mixture is almost identical with the experimental limit of sensitivity to blasting cap initiation. In the same way, the isoenthalpy line for 1.2 kcal per gram of mixture is in good agreement with the experimental limit of sensitivity to the drop weight test. On the basis of a few tests, the 1.2 kcal per gram limit, or perhaps a slightly higher value, also seems valid for initiation with a 25-joule static spark.

The results obtained in this investigation indicate that sensitivity to initiation is related to enthalpy content. In the case of ternary mixtures containing hydrogen peroxide, water and a fuel, more highly energetic compositions are relatively easy to detonate and vice versa, while mixtures of the same energy content always appear to have the same sensitivity. It is suggested that other fuel-oxidizer compositions may have similar properties

Some Properties of a Simplified Model of Solid Propellant Burning[1]

LEON GREEN Jr.[2]

Aerojet-General Corp., Azusa, Calif.

A thermal model of solid propellant burning is postulated, in which the complex chemical reaction and heat conduction problem in the gas phase is replaced by a simplified boundary condition which assumes convective heat transfer to the surface from a parallel flow of gas at flame temperature. The effective heat transfer coefficient is assumed to be an inverse function of propellant burning rate, which in turn is assumed to be an Arrhenius function of the surface temperature. This model permits calculation of steady-state propellant temperatures, burning rates and temperature gradients which show the proper qualitative dependence upon the propellant and gas-flow parameters and which, for the assumed values of these parameters, appear to be of the proper order of magnitude. The nonsteady behavior of the model is analyzed, assuming that the nonsteady variations in heat flux, surface temperature and burning rate may be expressed as small perturbations from the steady-state values, and considering that a small time interval is required for completion of the phase change or disordering of the propellant matter from the solid to a homogeneous, gaseous state in a thin zone comprising the burning "surface." The results indicate that, when the simplified transfer coefficient assumed to govern heat flow to the surface is subject to fluctuation at high frequencies as a result of "sonance" in the grain cavity, conditions can exist under which a coupling between the heat transfer fluctuation and the decomposition reaction can cause large-amplitude oscillations of the surface temperature. In such a "resonance" condition, significant deviations in the burning rate from its nominal steady-state value may be effected.

Nomenclature

A = complex constant defined in Equation [21], cm^{-2}
B = frequency factor in burning-rate equation, cm/sec
C = complex constant defined in Equation [23], cm^{-1}
c = heat capacity of solid, cal/g °K
c_p = average heat capacity of gas in film at constant pressure, cal/g °K
D = constant defined in Equation [24], °K/cm
E = activation energy in burning-rate equation, cal/mole
F = film-coefficient factor, $F = K\rho_1 v_1/\rho_\pi l$, cal/cm sec^2 °K
F_1 = amplitude of ΔF, cal/cm sec^2 °K
f = function of x
G = complex constant defined in Equation [31], cm^{-1}
h = heat transfer coefficient, cal/cm^2 sec °K
K = total thermal conductivity of gas in film, $K = k_g + \rho c_p \epsilon_H$
k = thermal conductivity of solid, cal/cm sec °K
k_g = average molecular thermal conductivity of gas in film, cal/cm sec °K
L = heat of phase change, cal/g
l = length parameter characteristic of parallel gas flow, ft

Presented at the ARS 11th Annual Meeting, New York, N. Y., Nov. 26-30, 1956.

[1] This research was supported by the U. S. Air Force through the Office of Scientific Research of the Air Research and Development Command.

[2] Principal Engineer, Nuclear Projects Department. Mem. ARS.

q = heat flux per unit area, cal/cm^2 sec
R = universal gas constant, cal/mole °K
r = burning rate of propellant, cm/sec
T = temperature, °K
t = time, sec
v_1 = main-stream velocity of parallel gas flow, fps
x = linear dimension, cm
α = thermal diffusivity of solid, cm^2/sec
Δ = small perturbation in a quantity
δ = effective film thickness, cm
ϵ_H = average eddy diffusivity of heat in film, cm^2/sec
η = function of x
λ = root of Equation [26], cm^{-1}
ρ = average mass density of gas in film, g/cm^3
ρ_1 = mass density of gas in main stream, g/cm^3
ρ_π = mass density of solid, g/cm^3
τ = time lag defined in Equation [19d], sec
φ = phase angle defined in Equation [30], rad
ω = angular frequency, rad/sec

Subscripts

f = flame
i = initial
o = steady state
s = surface ($x = 0$)

Introduction

THEORETICAL investigations of the mechanism of solid propellant combustion conventionally consider the problem of steady, one-dimensional heat conduction in the moving solid and gas phases; these phases are sometimes further subdivided into zones where different types of reaction prevail.[3] When the facts that chemical reactions in the combustion zones produce some components and consume others and that the reactants diffuse away from the surface are taken into account, and when arbitrary heat release patterns are assumed, this approach becomes mathematically complex. Consequently, it cannot easily be extended to treat the problems of "erosive" and "resonant" burning, phenomena which are encountered only where a finite gas velocity (steady and nonsteady, respectively) prevails parallel to the burning surface. The purpose of the present study, accordingly, is to examine the behavior of a model of propellant burning in which a gross simplification of the burning mechanism is attempted; the problem is represented as one of one-dimensional heat conduction in the solid phase, with the gas-phase problem replaced by a boundary condition assuming convective heat transfer from a parallel flow of gas at flame temperature.

Formulation of Problem

Idealized Continuity Condition at Boundary

It is assumed that the complex situation prevailing in the gas phase at the boundary (involving transport of heat and reacting chemical species both by molecular diffusion and by

[3] A comprehensive review of theories concerning solid propellant combustion has been provided by Geckler, Reference (1).

turbulent exchange) may be idealized by a convective boundary condition, according to which the rate of heat transfer from a turbulent stream at flame temperature T_f to the receding surface at temperature T_s is governed by a simplified equation of the film coefficient type

$$q = h(T_f - T_s) = \frac{K}{\delta}(T_f - T_s) \quad \text{[1]}$$

where δ is an effective "film" thickness, as depicted in Fig. 1, and K is a mean value of the total thermal conductivity of the gas in the layer δ. It is also assumed that the decomposition of the solid occurs as a change of phase directly to the gaseous state,[4] and is endothermic, requiring a constant heat of phase change L. This quantity is not a latent heat in the usual sense, since the solid-phase decomposition does not take place at a specific value of T_s.

The effect of the mass flux $\rho_\pi r$ from the boundary (the gas density is here neglected in comparison to that of the solid) is to increase the effective film thickess δ and hence to decrease the value of the heat-transfer coefficient.[5] The exact dependence involved is not accurately known, so a simplified approximation showing a qualitatively proper inverse relationship is assumed

$$\delta \cong \frac{\rho_\pi r l}{\rho_1 v_1} \quad \text{[2]}$$

where l is a length parameter characteristic of the mainstream flow at a given station. It is presumed l will be approximately proportional to the distance from the mainstream stagnation point (fore end of the propellant grain) to the station in question.[6] The film coefficient h can thus be written as $h \cong F/r$, where the multiplier

$$F = \frac{K\rho_1 v_1}{\rho_\pi l} \quad \text{[3]}$$

is a "film-coefficient factor," a measure of the degree to which the heat transfer coefficient is influenced by the properties of the parallel gas flow. The assumption of Equation [2] thus permits a heat balance at the surface $x = 0$ to be made; the heat transferred from the parallel flow to the surface by convection must equal the heat absorbed by the phase change and transported out, plus the heat conducted away in the solid

$$\frac{F}{r}(T_f - T_s) = \rho_\pi r L - k\left.\frac{\partial T}{\partial x}\right|_s \quad \text{[4]}$$

Heat Conduction in Solid Phase

It is assumed that the burning solid propellant, idealized as a one-dimensional slab, moves in the $-x$ direction with the same absolute velocity $|r|$ at which the burning surface regresses in the $+x$ direction, so that the burning surface is fixed at the coordinate $x = 0$. In order to simplify the problem, heat generation by reactions proceeding within the solid is disregarded, and the conduction of heat in the moving solid is thus governed by the equation

$$\frac{\partial T}{\partial t} = \alpha\frac{\partial^2 T}{\partial x^2} + r\frac{\partial T}{\partial x} \quad \text{[5]}$$

[4] Refinement of this assumption is required later in discussion of the nature of the time lag, τ, which enters into the nonsteady solution.

[5] The effect of mass addition on the thickness of boundary layers is currently the subject of active investigation, Reference (2). Although δ is a thermal film thickness, the present simplified approach will consider it to be of the "displacement" type as far as its dependence upon r is concerned, with a magnitude governed by continuity requirements alone, i.e., determined by the velocity field, with no consideration given to the enthalpy of the mass added.

[6] If so, Equation [2] is thus analogous to the asymptotic expression for the displacement thickness of a laminar boundary layer in an incompressible flow along a flat plate with fluid injection, Reference (3).

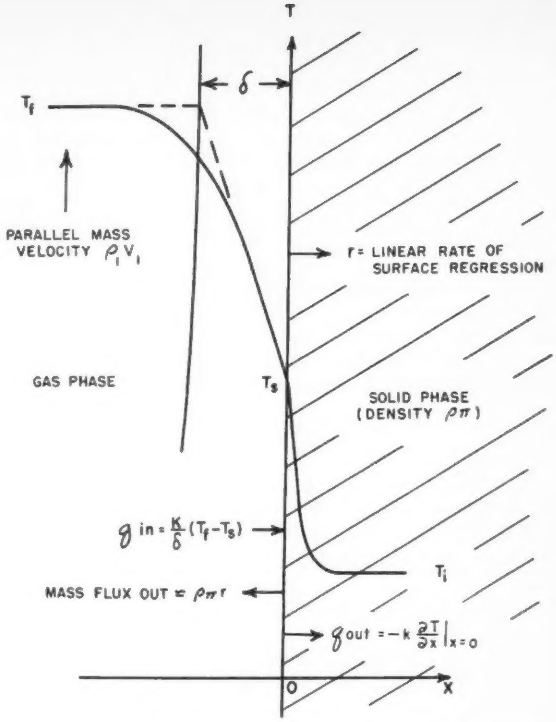

Fig. 1 Hypothetical situation obtaining at surface of burning solid propellant

subject to the boundary conditions

$$T(0, t) = T_s \qquad T(\infty, t) = T_i \quad \text{[6a], [6b]}$$

where the thermal diffusivity α (equal to $k/\rho_\pi c$) is assumed to be independent of temperature. It is also assumed that the nonsteady variations in temperature and burning rate can be expressed as small perturbations from a steady-state condition

$$T = T_o(x) + \Delta T(x, t) \quad \text{[7a]}$$

$$T_s = T_{so} + \Delta T_s(t) \quad \text{[7b]}$$

$$r = r_o(T_{so}) + \Delta r(\Delta T_s) \quad \text{[7c]}$$

in terms of these variables, the heat-flow Equation [5] becomes

$$\frac{\partial}{\partial t}(T_o + \Delta T) = \alpha\left(\frac{\partial^2 T_o}{\partial x^2} + \frac{\partial^2 \Delta T}{\partial x^2}\right) + (r_0 + \Delta r)\frac{\partial}{\partial x}(T_o + \Delta T) \quad \text{[8]}$$

also assuming that the film-coefficient factor can be expressed as $F = F_o + \Delta F(t)$, the heat-flux continuity condition at $x = 0$ becomes

$$k\left(\left.\frac{dT_o}{dx}\right|_s + \left.\frac{\partial \Delta T}{\partial x}\right|_s\right)(r_o + \Delta r) = \rho_\pi L(r_o + \Delta r)^2 - (F_o + \Delta F)(T_f - T_{so} - \Delta T_s) \quad \text{[9]}$$

Steady-State Problem

Collection of the zero-order terms in Equation [8] defines the steady-state heat conduction problem

$$\alpha\frac{d^2 T_o}{dx^2} + r_o\frac{dT_o}{dx} = 0 \quad \text{[10]}$$

where

$$T_o(0) = T_{so} \qquad T_o(\infty) = T_i \ldots . \text{[11a], [11b]}$$

Equation [10] is nonlinear in the sense that $r_o = r_o(T_{so})$. Therefore, it will first be assumed that T_{so} and r_o are known constants, and the dependence of T_o upon these values will be calculated from the "linearized" equation. The solution of this problem is

$$\frac{T_o - T_i}{T_{so} - T_i} = \exp\left(-\frac{r_o x}{\alpha}\right) \ldots\ldots\ldots\ldots [12]$$

Using the temperature gradient at the surface $x = 0$ computed from Equation [12] in the steady-state form of Equation [9], the steady-state surface temperature may be related to the known properties of the propellant, the propellant burning rate and the conditions of the parallel flow

$$\frac{F_o(T_f - T_{so})}{\rho_\pi c r_o^2} = \frac{L}{c} + T_{so} - T_i \ldots\ldots\ldots\ldots [13]$$

Following Wilfong, Penner and Daniels (4),[7] it is assumed that the dependence of the steady-state burning rate r_o upon the steady-state surface temperature T_{so} may be approximated by an Arrhenius rate relation

$$r_o = B \exp\left(-\frac{E}{RT_{so}}\right) \ldots\ldots\ldots\ldots\ldots [14]$$

It is recognized that this type of approximation is accurate only over a limited range of temperatures. In view of the prefatory nature of the present study, however, use of this approximation over the entire temperature range does not appear inconsistent with the drastic assumptions previously introduced. Substitution of the assumed relation into Equation [13] yields an expression which relates the steady surface temperature to the propellant properties and the parallel flow condition as manifested by the film-coefficient factor F_o

$$\frac{\rho_\pi c B^2}{F_o}\left[\frac{\dfrac{L}{cT_f} + \dfrac{T_{so}}{T_f} - \dfrac{T_i}{T_f}}{1 - \dfrac{T_{so}}{T_f}}\right] = \exp\frac{2\left(\dfrac{E}{RT_f}\right)}{\left(\dfrac{T_{so}}{T_f}\right)} \ldots\ldots [15]$$

Solutions of this equation for the dimensionless temperature ratio T_{so}/T_f vs. $\rho_\pi c B^2/F_o$ with T_i/T_f, E/RT_f, and $L/c\,T_f$ as parameters, obtained by trial-and-error numerical calculations, are presented in Fig. 2.

Magnitude of Parameters

Owing to the extremely high temperature gradients prevailing at the surface of a burning solid propellant, precise measurement of the surface temperature is difficult. Experiments employing fine thermocouples in the propellant have been attempted and have yielded surface temperature values in the range from 500 to 1500 C, depending upon the propellant and the pressure level. The validity of these measurements is questionable, however, since even a fine thermocouple wire is very large compared to the dimensions of the zone of maximum temperature gradient. For composite propellants, this situation is complicated by the nonhomogeneous, granular nature of the solid. In the absence of reliable experimental data on propellant burning rate as a function of surface temperature, a range of values for the activation energy E and the frequency factor B in Equation [14] was estimated on the basis of the measured rate parameters characterizing the thermal decomposition of typical organic and inorganic constituents of a composite solid propellant. Values of B in the range 1 to 10^3 cm/sec, and values of $E/RT_f = 1.0$ and 2.0 were selected.

[7] Numbers in parentheses indicate References at end of paper.

In the numerical solutions subsequently discussed, the decomposing solid was assumed to have the following properties: mass density, $\rho_\pi = 1.7$ gm/cm³; specific heat, $c = 0.3$ cal/gm°K; initial temperature, $T_i = 300$°K $(T_i/T_f = 0.1)$; heat of phase change, $L = 0$ and 100 cal/gm.

The magnitude of quantity F defined by Equation [3], a factor by which the conditions of pressure and velocity prevailing in the gas phase are manifested, is not easy to estimate with precision. In the first place, the mean effective total conductivity K of the hypothetical film region is the sum of the molecular and eddy conductivities in that region, i.e., turbulent motion is assumed to vanish only at the solid surface

$$K = k_g + \rho c_p \epsilon_H \ldots\ldots\ldots\ldots\ldots\ldots [16]$$

and the eddy conductivity term is itself a function of pressure and velocity. In the case of steady flow past an inert solid surface, expressions for the eddy diffusivity of momentum (for a gas, approximately equal to that of heat) have been derived but little can be said about the corresponding diffusivities prevailing under conditions of oscillatory flow past a surface from which mass is being added to the stream at a significant rate. For purposes of the present study, accordingly, it was assumed that the molecular and eddy conductivities are of the same order of magnitude, and that the dependence of the total conductivity upon pressure and velocity is mild; an approximate mean value of the order of 1×10^{-3} cal/cm sec°K was selected. It may be seen that F will assume its maximum value under conditions where a large value of v_1 obtains at the fore-end of a propellant charge $(l \rightarrow 0)$ during periods of a high-amplitude gas-phase oscillation in a transverse mode, and where a high mean pressure (high ρ_1) prevails. From a rough calculation arbitrarily taking $v_1 = 10^3$ fps and $l = 0.1$ ft, it was estimated that the upper limit of F_o would be of the order of 1.0 cal/cm sec² °K. Conversely, a lower limit of the order of 10^{-3} cal/cm sec² °K appeared reasonable.

Steady-State Calculations

Using the values of the propellant properties given above, the steady surface temperature T_{so} was calculated as a function of F_0 from the nondimensional curves of T_{so}/T_f presented in Fig. 2 for the cases where $L/c\,T_f = 0.1$ and $E/RT_f = 1.0$ and 2.0, and with the frequency factor B as a parameter. These calculated results are presented in Fig. 3, from which it may be seen that not only do the surface temperatures show the proper qualitative dependence upon F_o (increasing with increasing pressure and velocity), but are generally of the right order of magnitude.[8] The steady burning rates corresponding to the temperatures shown in Fig. 3 are presented in Fig. 4. Again, with the exception of the case $B = 1.0$ cm/sec, these rates appear to be of the magnitude normally associated with ammonium perchlorate propellants, at least for the higher values of F_o.

From the data of Figs. 3 and 4, the rates of heat conduction away from the surface were computed by Equation [12] and are shown in Fig. 5 for the case of $E/RT_f = 1$. The tendency shown therein for the curves computed for the low values of B to cross over those for higher values of B appeared inconsistent at first glance. Accordingly, a cross computation was performed, and the heat-flow data are presented in Fig. 6 vs. the frequency factor B, with the film-coefficient factor F_o as a parameter. It is seen therein that the maximum rate of heat conduction occurs at a value of B which varies with the flow

[8] The temperatures calculated for the case of $B = 1.0$ cm/sec appear too high, indicating that such a low estimate of the frequency factor, included for purposes of comparison, is not realistic. A low frequency factor might be characteristic of slow-burning ammonium nitrate propellants, for which the ratio T_{so}/T_f would be expected to be greater than in the case of fast-burning ammonium perchlorate propellants. In such a case, however, the estimate that T_f equals 3000 K is too high, and the group E/RT_f might be of the order of 3–5 rather than 1–2.

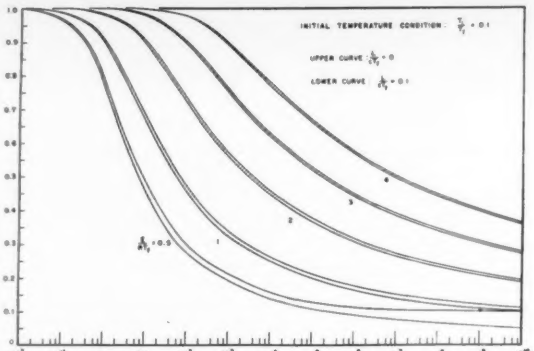

Fig. 2 Nondimensional solutions to the steady-state surface temperature, Equation [15], T_{so}/T_f vs. $\rho_\pi c B^2/F_o$

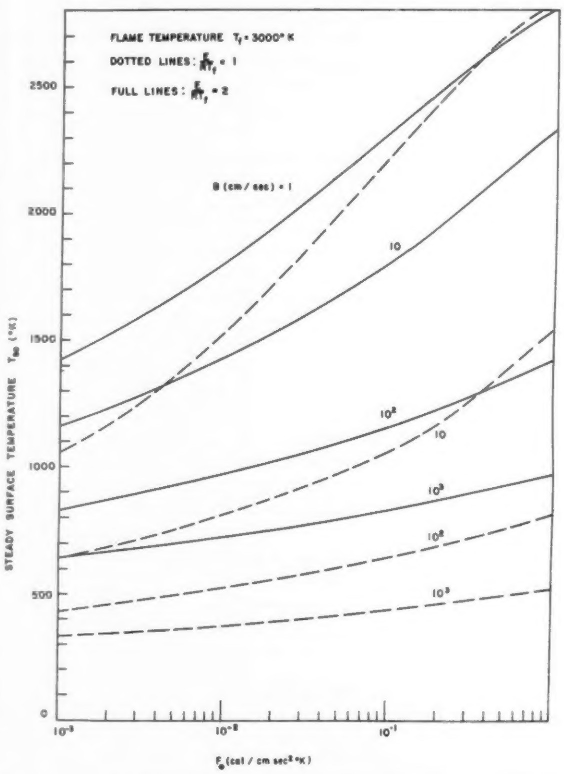

Fig. 3 Steady-state surface temperatures vs. film coefficient factor for T_f = 3000 K

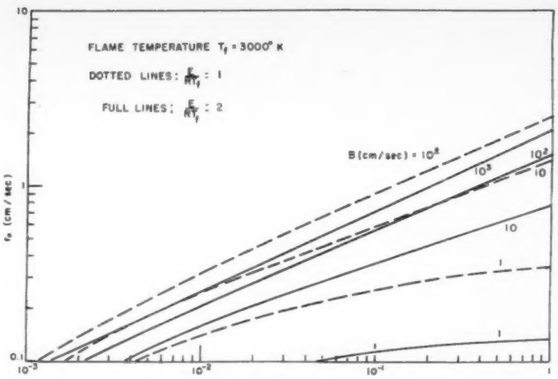

Fig. 4 Steady-state linear burning rate vs. film coefficient factor for T_f = 3000 K

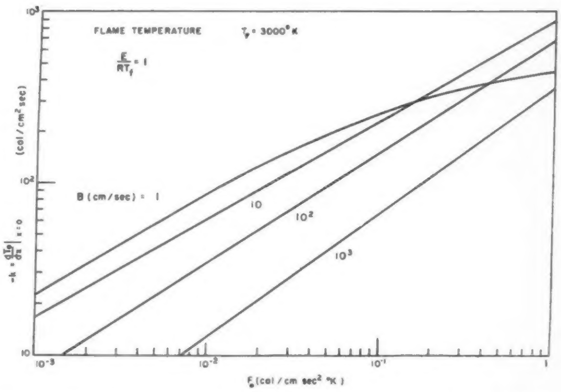

Fig. 5 Conduction heat flux at surface vs. film coefficient factor for T_f = 3000 K and E/RT_f = 1

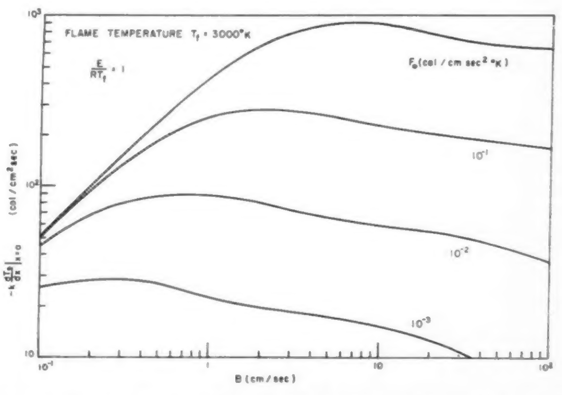

Fig. 6 Conduction heat flux at surface vs. frequency factor for T_f = 3000 K and E/RT_f = 1

condition (F_o value), thus producing the cross-over tendency shown in Fig. 5. As an additional check, curves of the heat flux to the surface, $h_o(T_f - T_{so})$, were also computed as a function of F_o, and it was found that the data satisfy the heat balance of Equation [4] with reasonable accuracy. Similar behavior was also confirmed in the case $E/RT_f = 2$.

Nonsteady Problem

It has been seen that the proposed simplified model permits calculation of steady-state surface temperatures, burning rates and temperature gradients which show the proper qualitative dependence upon the propellant and gas-flow parameters, and, for the values of these parameters assumed, appear to be of the proper order of magnitude. In view of this encouraging result, it was desired to investigate the nonsteady behavior of the model, in an effort to attack the unsolved problem of periodic deflagration (5). It has been postulated that, under certain nonsteady conditions, a coupling between the heat transfer oscillation and the solid decomposition reaction may cause an increase in the average burning rate (6). This postulate was advanced as an explanation for the fact that the occurrence of high frequency acoustical pressure oscillations within a burning grain cavity ("sonant" burning,

sustained by the gas-phase reaction) is a condition necessary, but not sufficient, to effect "resonant" burning, or a deviation in the average solid burning rate from its nominal value (6).

Collection of the zero-order terms of Equations [8 and 9] defined the steady-state problem, solutions for which were presented above. The nonsteady problem is represented by the first-order terms, which yield the expressions

$$\frac{\partial \Delta T}{\partial t} = \frac{\partial^2 \Delta T}{\partial x^2} + r_o \frac{\partial \Delta T}{\partial x} + \Delta r \frac{dT_o}{dx} \qquad [17]$$

$$\left.\frac{\partial \Delta T}{\partial x}\right|_s + \left.\frac{dT_o}{dx}\right|_s \frac{\Delta r}{r_0} = \frac{2\rho_\pi L \Delta r}{k} + \frac{F_o}{kr_o}\Delta T_s - \frac{\Delta F}{kr_o}(T_f - T_{so}) \qquad [18]$$

It is now assumed that the variation in the film coefficient factor F is periodic, thus producing a periodic variation in the solid temperature

$$\Delta F = F_1 e^{i\omega t} \qquad [19a]$$

$$\Delta T = f(x)e^{i\omega t} \qquad [19b]$$

$$\Delta T_s = f(0)e^{i\omega t} \qquad [19c]$$

and that the variation in burning rate follows the variation in surface temperature, after a time lag, τ, required for the completion of the phase change

$$\Delta r = \left.\frac{dr}{dT_s}\right|_{T_{so}} \Delta T_s(t - \tau) + \ldots$$

$$\cong r_o \frac{E}{RT_{so}^2}\Delta T_s(t - \tau) = r_0 \frac{E}{RT_{so}^2} f(0)e^{i\omega(t-\tau)} \qquad [19d]$$

Substitution of these expressions in Equations [17 and 18], together with use of Equation [12], yields the following equations for the space function of the temperature variation

$$f'' + \frac{r_o}{\alpha}f' - \frac{i\omega}{\alpha}f = Af(0)e^{-r_o x/\alpha} \qquad [20]$$

where

$$A = \left(\frac{r_o}{\alpha}\right)^2 \frac{E(T_{so} - T_i)}{RT_{so}^2} e^{-i\omega\tau} \qquad [21]$$

and for the boundary condition on this space function at the burning surface

$$f'(0) - Cf(0) + D = 0 \qquad [22]$$

where

$$C = \frac{r_o E}{RT_{so}^2}\left[\frac{T_{so} - T_i}{\alpha} + \frac{2\rho_\pi L}{k}\right] e^{-i\omega\tau} + \frac{F_o}{kr_o} \qquad [23]$$

and

$$D = \frac{F_1}{kr_o}(T_f - T_{so}) \qquad [24]$$

Finally, there exists the additional requirement that the amplitude of the perodic temperature fluctuation approach zero at large values of x, as the temperature "wave" resulting from the oscillatory surface heat flux is dissipated; i.e., $f(\infty) = 0$.

The particular solution to Equation [20] is

$$\eta(x) = i\frac{\alpha}{\omega}Af(0)e^{-r_o x/\alpha} \qquad [25]$$

A substitution of type $f = \text{const}\ e^{\lambda x}$ in the homogeneous equation yields the characteristic equation

$$\lambda^2 + \frac{r_0}{\alpha}\lambda - i\frac{\omega}{\alpha} = 0 \qquad [26]$$

with the roots

$$\lambda = \frac{r_0}{2\alpha}\left[-1 \pm \sqrt{1 + i\frac{4\omega\alpha}{r_o^2}}\right] \qquad [27]$$

For simplicity, it is convenient to classify the solutions into two limiting cases: (a) the low frequency regime (ω small), where the imaginary term in the radical of Equation [27] is small compared to unity; and (2) the high frequency regime (ω large) where the imaginary term is dominant.

Low Frequency Regime

In the case where the frequency of the heat transfer oscillation is low, i.e., when $(4\omega\alpha/r_o^2) \ll 1$, it is found that the amplitude of the surface temperature excursion $|\Delta T_s|$ is approximated in the form

$$|\Delta T_s| \cong \frac{D}{|C| + \frac{\alpha|A|}{r_o} + \frac{r_o}{\alpha}} \qquad [28]$$

with an insignificant phase lag between the heat transfer and surface temperature oscillations. Consideration of the order of magnitude of the parameters characterizing a typical propellant-burning situation indicates that this type of solution is valid when the frequency $\omega/2\pi$ is less than about 10 cps. Although A and C, as given in Equations [21 and 23] are, in general, complex constants depending upon ω, they are substantially real for the small values of ω considered here, since τ is also small, i.e., the factor $e^{-i\omega\tau}$ is very nearly unity.

In order to establish the order of magnitude of this fluctuation, values of the various parameters estimated to be reasonable for a burning solid propellant charge were chosen as follows: $T_f = 3000$ K; $E/RT_f = 2.0$ ($E = 11{,}900$ cal/-mole); $B = 100$ cm/sec; $\alpha = 10^{-3}$ cm²/sec; $T_i = 300$ K; $k = 5 \times 10^{-4}$ cal/cm sec °K; $\rho_\pi = 1.7$ gm/cm³; $L = 100$ cal/gm; $F_o = 10^{-1}$ cal/cm sec² °K; $F_1 = 10^{-2}$ cal/cm sec² °K. By use of Figs. 3 and 4, the steady-state surface temperatures and burning rate, and hence the values of the constants A, C and D were computed as follows: $T_{so} = 1150$ K; $T_{so} - T_i = 850$ K; $r_o = 0.56$ cm/sec; $|A| = 1.21 \times 10^6$ cm⁻²; $|C| = 4.24 \times 10^3$ cm⁻¹; $D = 3.70 \times 10^4$ °K/cm. Substitution of these values in Equation [28] indicates that the amplitude of the surface temperature excursion would be 5.3 K, corresponding to a burning-rate variation of

$$|\Delta r| \cong r_o \frac{E}{RT_{so}^2}|\Delta T_s| = 0.013 \text{ cm/sec}$$

or a maximum instantaneous variation of the order of only 2 per cent from the steady-state value. It is concluded that, in the model of propellant burning here considered, heat transfer oscillations (i.e., variations in the film coefficient factor F) at low frequencies do not lead to a significant deviation of the instantaneous burning rate, much less the mean effective burning rate, from the steady-state value.

High Frequency Regime

In the case where the frequency of the heat transfer oscillation (variation of the film coefficient factor F) is high, i.e., $\omega > 10^4$ radians/sec, it is found that the surface temperature excursion, ΔT_s, may be approximated in the form

$$\Delta T_s \cong \frac{De^{i(\omega t + \varphi)}}{\left[\left(G\cos\omega\tau + \frac{F_o}{kr_o} - \frac{r_c}{2\alpha} + \sqrt{\frac{\omega}{2\alpha}}\right)^2 + \left(G\sin\omega\tau - \sqrt{\frac{\omega}{2\alpha}}\right)^2\right]^{\frac{1}{2}}} \qquad [29]$$

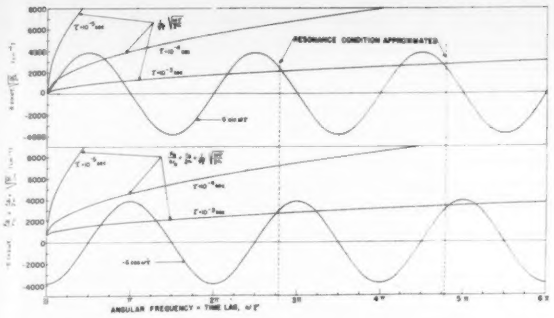

Fig. 7 Illustration of resonance condition occurrence of approximation

where

$$\tan\varphi = \frac{G \sin\omega\tau - \sqrt{\dfrac{\omega}{2\alpha}}}{G\cos\omega\tau + \dfrac{F_o}{kr_o} + \dfrac{r_o}{2\alpha} + \sqrt{\dfrac{\omega}{2\alpha}}} \qquad [30]$$

and

$$G = \frac{\rho_\pi r_o E}{kRT_{so}^2}\,[c(T_{so} - T_i) + 2L] \qquad [31]$$

It may be seen that, in contrast to the low frequency case, double-eigenvalue situations can exist where the denominator of Equation [29] may become small, thus producing a large-amplitude variation in surface temperature (in which case, of course, the small-perturbation assumption becomes invalid).

In order to illustrate this behavior, graphs of the two groups comprising the denominator of Equation [33] were plotted vs. $\omega\tau$, using the values of the various parameters employed earlier. These curves are presented in Fig. 7. Three arbitrary values of the time lag were considered: $\tau = 10^{-3}$, 10^{-4} and 10^{-5} sec. It may be seen that no true "resonance" points, or conditions where the denominator of Equation [29] becomes zero, are shown by the curves of Fig. 7. The nearest approaches to such a condition occur at $\omega\tau \cong 2.8\pi$ and 4.8π (indicated by dashed vertical lines) for the case of $\tau = 10^{-3}$ sec. At the point $\omega\tau \cong 2.8\pi$, the amplitude $|\Delta T_s|$ of the surface temperature variation is calculated to be 105 K, using the numerical values of the parameters assumed previously. Although this amplitude is appreciable, the corresponding deviation of the mean effective burning rate from its steady-state value r_o is still not great. It thus illustrates that the resonance condition must be approached very closely before the amplitude of the surface temperature excursion becomes great enough to effect a manifold increase in the mean effective burning rate. Fig. 7 shows that such a condition would obtain near the point $\omega\tau = 2.78\pi$, for example, if either G were slightly smaller than the value assumed therein, or if τ were slightly less than 10^{-3} sec.

To illustrate the sensitivity of the resonance condition to small changes in the time lag, Fig. 8 presents curves of $|\Delta T_s|$ vs. ω for the case of $\tau = 1 \times 10^{-3}$ sec, as considered in Fig. 7, and for $\tau = 7.88 \times 10^{-4}$ sec, in which case a true resonance condition is achieved. Similarly, another resonance condition ($\tau = 10^{-4}$ sec, $\omega\tau = 0.8\pi$) would be obtained if G were larger (of the order of 5000/cm), and so forth. From the strongly nonlinear rate-vs.-temperature dependence shown in Fig. 9, it is apparent that a high-amplitude fluctuation around the mean value for the case considered would effect a significant net increase in the mean burning rate, averaged over a complete cycle.

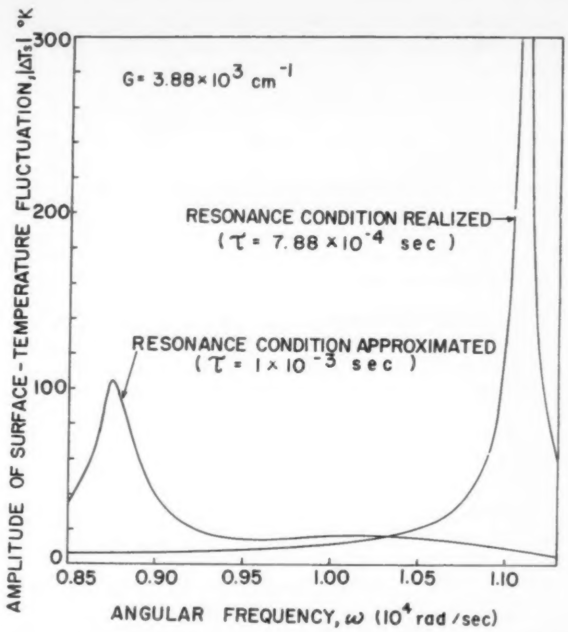

Fig. 8 Amplitude of surface temperature fluctuation under resonance and near-resonance conditions

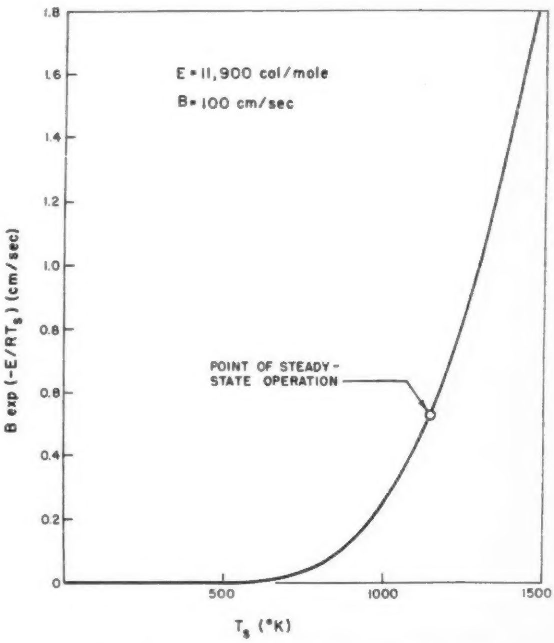

Fig. 9 Burning rate vs. surface temperature relationship

Nature of the Time Lag

In setting up the simplified model of a burning propellant, the steady-state analysis implied that the change of phase from the solid to the gaseous state takes place at a well-defined surface at a temperature T_s. Since the change of phase at constant temperature across a mathematical "surface" would be instantaneous, the time lag defined by Equation [19d] might seem to be an artificial device introduced in order to permit an oscillatory solution to the nonsteady problem. However, the physical nature of τ can be seen if it is

recognized that what has heretofore been called the "surface" of the solid propellant is not really a surface in the mathematical sense, but is actually a zone of small but finite thickness, in which the propellant matter exists in a semi-ordered state (presumably as a liquid, containing gas bubbles) and the "surface" temperature T_s is the mean temperature in this zone. Accordingly, the "time lag" is the time interval required for the propellant matter to pass from an ordered solid state at a temperature $(T_s - \theta)$, where θ is a relatively small temperature difference, through this semi-ordered region to a disordered gaseous state at a temperature $(T_s + \theta)$. In the case of composite propellants, τ may also include the time required for diffusion and mixing of the fuel and oxidizer components in the semi-ordered surface region, since the "surface" temperature in the model represents an average between the fuel and oxidizer temperatures in this region, which may differ appreciably.

Conclusion

The foregoing analysis has indicated that the simplified thermal model of solid propellant burning under consideration exhibits both steady and nonsteady behavior which appears consistent with the known burning characteristics of solid propellants. Under certain situations in which the frequency of parallel velocity fluctuations resulting from "sonant" burning are properly related to the thermal and ballistic properties of the propellant, a "resonant" condition can exist (or be closely approached), which gives rise to large-amplitude fluctuations in surface temperature and, consequently, to increased mean effective burning rates. Although detailed analysis is reserved for future discussion (7), it may be stated that the occurrence of a resonance condition appears to be favored by a low thermal conductivity in the solid phase, a large heat of phase change, a high flame temperature, a low activation energy and a high frequency factor. Resonance appears to be favored by a low initial propellant temperature except that a very high initial temperature might also favor resonance by reducing the activation energy requirement. These observations appear to be in qualitative agreement with the known resonance-burning tendencies of actual propellants. However, one aspect of the model behavior deserves emphasis here: The resonance condition must be approached very closely before large deviations in the mean effective burning rate are encountered, and seemingly small variations in propellant properties or operating conditions can be important in determining whether or not such a situation is realized. This prediction is interesting in view of the sporadic nature of the occurrence of resonant burning in tests of actual propellant charges. Whereas some propellants never exhibit such behavior, and a few consistently do (at least at extreme conditioning temperatures), resonant burning in many propellants is a seemingly random phenomenon, sometimes occurring for no obvious reason in the testing of a usually "well-behaved" formulation. In other cases, resonant burning apparently can often be avoided by making relatively small changes in the oxidizer particle-size distribution or concentration, in the charge configuration, or by including relatively small amounts of certain additives in the formulation. The indicated sensitivity of the resonance condition to small changes in the time lag suggests that variations in this parameter may be associated with the observed effectiveness of such seemingly small formulation changes in suppressing resonance burning.

Despite its rather drastic assumptions, it is believed that the proposed simplified model exhibits nonsteady behavior realistic enough to justify its use as a guide for the design and interpretation of combustion-stability experiments. One assumption which needs further refinement is the steady-state approximation of Equation [2], which is also employed as an instantaneously valid relation in formulating the nonsteady problem. Recent investigations of heat transfer to bodies in oscillating, longitudinal, laminar flow by Lighthill (8) and Stuart (9), however, indicate that, when the frequency of oscillation is high, a phase lag exists between the stream-velocity fluctuation and the heat transfer fluctuation. It is suggested that further pursuit of the present problem may profit from an analysis of heat transfer through a turbulent boundary layer to a plate emitting fluid, in the case where an oscillating, transverse velocity component is superposed upon a steady, longitudinal flow with a velocity increasing linearly from zero at the fore end of the plate. Consideration of the heat generated within the solid may also be desired. Finally, the nature of the time lag and its possible dependence upon diffusion times should be clarified.

Acknowledgments

The foregoing analysis followed lines of approach suggested by H. J. Stewart, who also reviewed the assumptions and results. The numerical solutions of Equation [15] and many of the other computations were carried out by M. Lipow. In addition, the author has benefitted from helpful discussions with R. D. Geckler, R. W. Lawrence and S. S. Penner. Finally, the author is indebted to many of his associates in the solid propellant field, especially W. Nachbar, for reviewing the manuscript and suggesting improvements or corrections.

References

1 Geckler, R. D., "The Mechanism of Combustion of Solid Propellants," Selected Combustion Problems, Fundamentals and Aeronautical Applications, AGARD Combustion Colloquium, Cambridge University, Butterworths Scientific Publications, London, 1954.

2 Mickley, H. S., Ross, R. C., Squyers, A. L., and Stewart, W. E., "Heat, Mass, and Momentum Transfer for Flows Over a Flat Plate with Blowing or Suction," NACA TN 3208, July 1954.

3 Schlichting, H., "Lecture Series 'Boundary Layer Theory,' Part I—Laminar Flows," NACA TM 1217, April 1949.

4 Wilfong, R. E., Penner, S. S., and Daniels, F., "An Hypothesis for Propellant Burning," *Journal of Physical and Colloid Chemistry*, vol. 54, 1950, pp. 863–872.

5 Geckler, R. D., "Unsolved Problems in Solid-Propellant Combustion," Fifth Symposium (International) on Combustion, Reinhold Publishing, New York, 1955, pp. 29–40.

6 Green, L., Jr., "Observations on the Irregular Reaction of Solid-Propellant Charges," Jet Propulsion, vol. 26, 1956, pp. 655–659.

7 Nachbar, W., and Green, L., Jr., "Analysis of a Simplified Model of Solid Propellant Resonant Burning," to be submitted for publication.

8 Lighthill, M. J., "The Response of Laminar Skin Friction and Heat Transfer to Fluctuations in the Stream Velocity," *Proceedings of the Royal Society of London*, Series A, vol. 224, 1954, pp. 1–23.

9 Stuart, J. T., "A Solution of the Navier-Stokes and Energy Equations Illustrating the Response of Skin Friction and Temperature of an Infinite Flat Plate Thermometer to Fluctuations in the Stream Velocity," *Proceedings of the Royal Society of London*, Series A, vol. 231, 1955, pp. 116–130.

Evidence for the Wrinkled Continuous Laminar Wave Concept of Turbulent Burning[1]

J. K. RICHMOND,[2] W. F. DONALDSON,[3] D. S. BURGESS[4] and J. GRUMER[5]

U.S. Department of the Interior, Bureau of Mines, Pittsburgh, Pa.

Several investigators have attempted to explain and evaluate turbulent burning rates by assuming the turbulent flame brush to be a zone traversed by a wrinkled continuous laminar flame front. Others have argued that the brush consists of a distributed reaction zone characterized by turbulent energy transport and diffusion of active species. A third point of view is that of visualizing the brush as a region containing disconnected flamelets of varying chemical composition. The purpose of the present paper is to state the case for the wrinkled wave concept and to place limits on the regime of its applicability. Experiments indicate that the distributed reaction zone model applies to conditions of incomplete burning within the flame brush. It is suggested that the transition from wrinkled wave to distributed reaction zone corresponds to the breakdown of full turbulent flames through the incidence of "holes." New photometric evidence is presented.

Introduction

IN ORDER to understand turbulent flame propagation, it is necessary to have a flame model which represents the actual combustion processes over a useful range of conditions. The only such model to find wide acceptance for laboratory burner flames has been the wrinkled laminar flame structure (1, 2, 3, 4),[6] and the range of applicability of this model has been subject to much speculation.

Karlovitz et al. (5) considered the structure to be applicable up to such high approach flows that the continuous flame front becomes disrupted by the action of velocity gradients, giving "holes" that were observed by electronic probe. Grumer et al. (6) inspected short-duration direct photographs of laboratory flames and proposed that the flame brush is a zone of discontinuous flamelets. Summerfield et al. (7, 8) postulated an extended reaction zone wherein exist smooth spatial variations of the time-average values of composition and temperature, somewhat as in a thickened laminar flame; evidence for such a structure in burner flames has been based largely on observations that seemed contradictory to the wrinkled flame model. Summerfield (9) and Wohl (10) have discussed a criterion originated by Kovasznay (11), that

$$(u'/\lambda)/(S_L/\delta) > 1$$

at the point of break-up of laminar burning; S_L/δ and u'/λ are described as the typical velocity gradients in a laminar flame and in the turbulent flame under consideration, respectively.

The purpose of this paper is to present experimental evidence for the existence of a continuous laminar flame within a turbulent flame brush and to suggest that this structure is applicable to much more highly turbulent flames than is commonly supposed. The most persuasive evidence to date is obtained by photometric measurement of the transient radiation from flames, whereby a definite correlation with a laminar flame has been observed.

Experimental Techniques

Range of Experiments

Long, vertical, cylindrical burners were used in all experiments, with three different inside diameters: $\frac{9}{16}$, $1\frac{1}{4}$ and 2 in. In each instance the flame was stabilized on the burner by a tiny annular pilot flame of a stoichiometric hydrogen-air mixture whose flow rate never exceeded 1 per cent of that in the burner tube. The flames were surrounded by a concentric flow of secondary air to help isolate the flame from external disturbances. Tests were made with pipe-flow turbulence (1 to 2 per cent) and grid-induced turbulence. The grids used were similar to those employed by Hottel, Williams and Levine (12), who measured the resulting turbulence intensity (about 3 to 6 per cent for the present range of experiments).

The flow conditions ranged from a laminar flow at Re = 4000 (possible because of the long, smooth burner tube) to a turbulent flow at Re = 5000 on the $\frac{9}{16}$-in. burner tube; turbulent flows from Re = 10,000 to Re = 100,000 on the $1\frac{1}{4}$-inch burner tube; and from Re = 10,000 to Re = 160,000 on the 2-in. burner tube. The average approach velocity ranged from about 14 to 155 fps, with rms turbulent fluctuation velocities from 0 to 9 fps. Estimated values of scale of turbulence varied from about 0.06 to about 0.20 in. The pilot flame could be varied so that the main flame was either full (100 per cent combustion) or incomplete (less than 100 per cent combustion, with "holes"). The main flame in this set of experiments was a stoichiometric mixture of Pittsburgh natural gas (about 92 per cent methane) and air, the flow being metered by standard orifices.

Fig. 1 shows the arrangement of the burner and measuring equipment. The flame shown is the largest and most highly turbulent employed in this study.

Flame Radiation Photometer

The flame photometer has been described previously (13) but has been redesigned to improve the reliability of measurements of spatial distribution of light intensities and to improve the signal-to-noise ratio. The present design consists of a large lens which produces a real image of the flame in the plane of a circular aperture of 0.02-in. diam, immediately behind which is a 1P21 photomultiplier tube. The entire system moves as a unit, surveying the flame in the manner of a traveling telescope. The photometer is used in two ways: (a) To measure time-average values of light intensity by means of a sensitive galvanometer connected to the phototube, and (b) to measure transient fluctuations of light intensity by means of a cathode ray oscilloscope connected to the phototube.

Presented at the ARS 12th Annual Meeting, New York, N. Y., Dec. 2–6, 1957.

[1] This research was supported by the U. S. Air Force through the Air Force Office of Scientific Research of the Air Research and Development Command, under Contract CSO-680-57-14.

[2] Physicist, Flame Research Section, Division of Explosives Technology. Mem. ARS.

[3] Physicist, Flame Research Section, Division of Explosives Technology.

[4] Physical chemist. Chief, Branch of Physical Sciences, Division of Explosives Technology.

[5] Physical chemist. Chief, Flame Research Section, Division of Explosives Technology.

[6] Numbers in parentheses indicate References at end of paper.

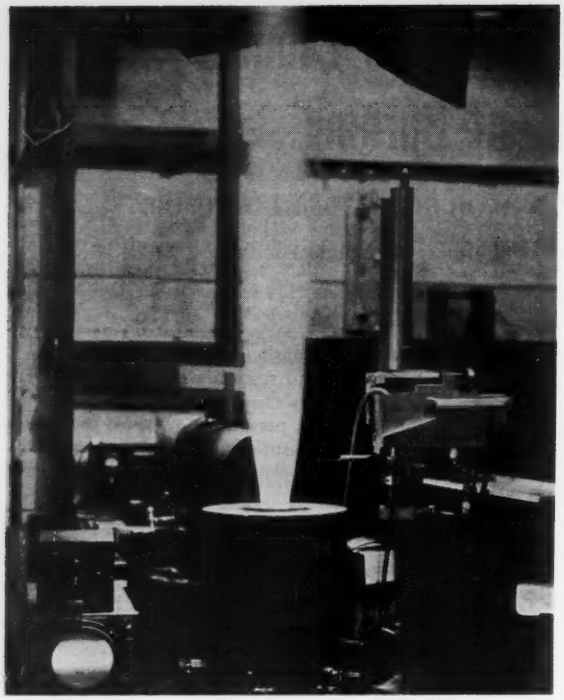

Fig. 1 General view of experimental arrangement

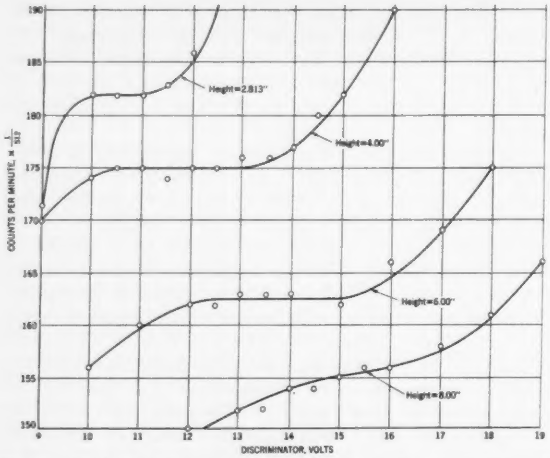

Fig. 2 Typical plateaus with electronic probe measurement Re = 50,000, 1¼-in. burner

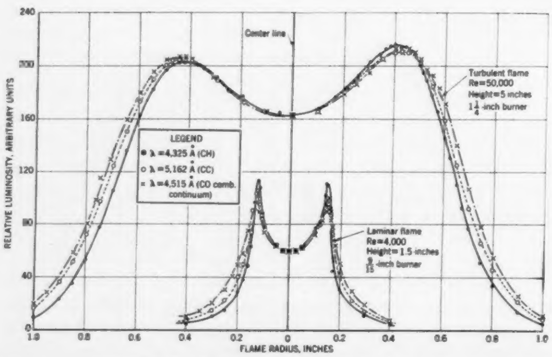

Fig. 3 Horizontal distribution of radical emission (uncorrected for cylindrical curvature and normalized to center-line values)

For the time-average light measurements it was found that the photometer could discriminate between line sources of light 0.030-in. apart in such a way that the photocurrent reached zero as the photometer observed points between the two sources. In order to study the spatial distribution of the various emitter species in the flame, three interference filters were used whose pass-bands centered at 4325, 4515, and 5162 Å for studying the emission due to the CH radical, the continuum due to CO combustion, and the CC radical, respectively. These filters all have pass-band widths of 75 Å at the half-power level. Rectangular coordinates in the flame cross section could be established and calibrated to within 0.002-in.

The time resolution of the photometer when used for transient measurement was determined by means of a chopper wheel interrupting the light from a steady source. Since the main limitation to the frequency response of the equipment was the cable connecting the photomultiplier to the oscilloscope, the length of this cable and the value of its terminating impedance were adjusted so that the over-all response to a square-wave light signal was flat from 0 to 4000 cps, and down about 5 per cent at 7500 cps. Because of the low light levels resulting from the small apertures used, the bandwidth had to be limited because of shot noise in the photomultiplier. The depth of focus for this type of experiment was extended to cover the entire thickness of the flame brush by stopping down the lens to f/6. The photometer was focused on a point in the front side of the flame, while the light from the opposite side of the flame was blocked by a small baffle at the axis of flow.

Electronic Probe

The electronic probe as used in this laboratory has been described in (5 and 14); it consists of a bare wire inserted into the flame to pick up fluctuations in flame ionization, and is equipped with suitable detecting and analyzing circuits. An essential feature of this probe is a pulse-height discriminator by means of which it is possible to distinguish between the high level of ionization associated with the combustion process and the low-level thermal ionization existing in the burned gas. It is also possible, by means of a current integrating and counting circuit, to measure the relative amount of time the flame is on or off the probe wire, as well as the frequency of fluctuations of ionization level.

Smoke Photography

Smoke photography, wherein a subliming or dissociating smoke is carried in the approach flow, has been used to study turbulent flames. The smoke disappears when heated by the flame, and flash photographs may be taken of light reflected from the remaining smoke. Two smokes have been used in this laboratory: Ammonium chloride smoke, dissociating around 325 C, traces a low temperature contour; zinc oxide smoke, subliming appreciably at about 1300 C, delineates a temperature contour much closer to that associated with the most luminous portion of a laminar flame.

Experimental Results and Discussion

Electronic Probe Measurements

While some caution is required in the interpretation of probe results because of the necessity of pulse height discrimination, the following points seem to be clear-cut:

The instantaneous values of probe current are not completely random as argued by Summerfield et al. (7) but comprise high level values suggestive of the ionization peak behind a laminar flame front as well as low levels of current such as might be derived from thermal ionization in the burned gas (5). This is the sense of Fig. 2 wherein the frequency of pulses that pass the discriminator is plotted against discriminator voltage, the probe tip being located at the flame's

mean position. There is a well-defined plateau in each curve which can only refer to a discontinuity in the amplitudes of the current pulses. The plateau tends to disappear in the flame zone above the apex of the inner cone.

The continuity of the ionization peak to form a fluctuating sheath around the flame is demonstrated by thrusting the probe wire through the entire thickness of the flame brush, whereupon the frequency of counts becomes zero; i.e., some part of the probe wire is constantly in contact with the high level ionization. Because of the probe's finite dimensions, there could still be undetected small gaps in the ionization sheath, that is, "holes" in the flame front. Such holes become readily observable as the flame tends toward instability either because of high turbulence levels or of inadequate piloting.

In terms of the Kovasznay criterion, "holes" in well-piloted flames have not yet been observed for values of $(u'/\lambda)/(S_L/\delta)$ below 5–10. To arrive at these values, S_L, the laminar burning velocity, is taken as 40 cm/sec; δ, laminar flame thickness, as 0.02 cm; u', the rms turbulent fluctuation velocity, as 200 cm/sec; λ, the microscale of turbulence, as 0.01–0.02 cm at the critical height for appearance of "holes," about 6 cm above the burner rim on a $1\frac{1}{4}$-in.-diam burner.

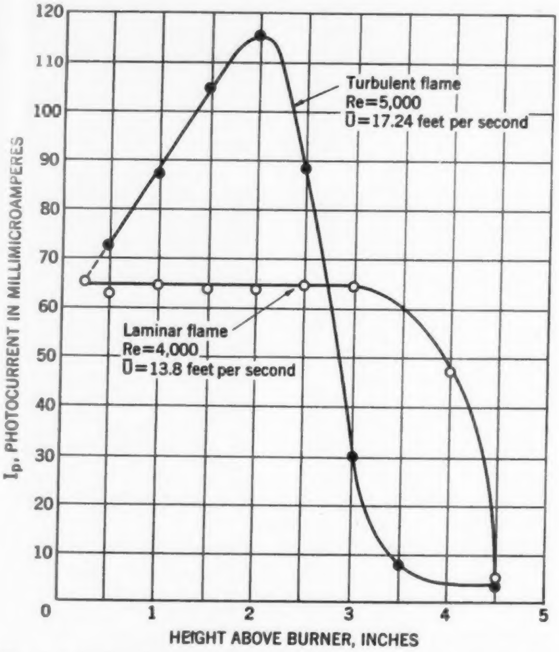

Fig. 4 (a) Luminosity as a function of height above $\frac{5}{16}$-in.-diam burner for laminar and turbulent flames

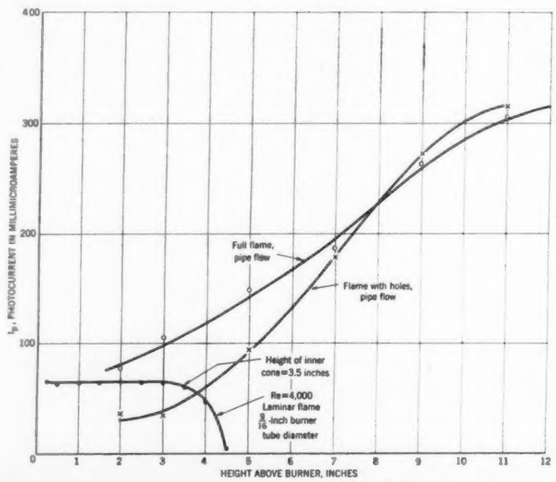

Fig. 4 (b) Luminosity as function of height above $1\frac{1}{4}$-in.-diam burner for full and incomplete flames at Re = 100,000

Horizontal Distribution of Radiations

An objection to the wrinkled flame concept can be based on any real displacement of emissions from their relative positions in a laminar flame. For this reason, horizontal traversals of laminar and turbulent flames were performed with the photometer and the three filters. Typical data are shown in Fig. 3, where the time-average distribution curves due to the different emitters have been normalized to the same value at the center line. It will be seen that the spatial separations of the peak luminosities of the different emitters are greater for the turbulent flame than for the laminar flame; however, this is not surprising if one also considers the distribution curves for these same emissions in a laminar flame. A recent theoretical treatment of this problem by Williams and Fuhs (15) shows that the change in relative distribution of emission due to CH and H_2O in turbulent flames as compared to laminar flames (7) is that which would be predicted from a wrinkled laminar flame model. Any difference in the shapes of emitter distribution curves in an undisturbed laminar flame would be greatly exaggerated in a wrinkled laminar flame. The same kind of analysis would seem to apply to distributions due to CH, CC, and continuum due to CO combustion.

Vertical Distribution of Luminosity

Fig. 4(a) shows a plot of time-average photocurrents (which are proportional to time-average luminosities) as measured with the 4325 Å filter vs. distance from the port. The lines of sight pass through the flame axis. The luminosity of the primary cone of a stoichiometric laminar flame is essentially constant over its whole height and serves as the standard of comparison for turbulent flames. The luminosities of the turbulent flames, however, increase almost linearly with height and are nearly proportional to flame brush thickness, as defined in (13).

Of particular interest to this discussion is the minimum luminosity level of the turbulent flame, which approaches that of a laminar flame slightly above the burner rim.

Fig. 4(b) compares the luminosities of flames at relatively high Reynolds number with and without "holes." In the full flame, the luminosity decreases toward that of a laminar flame as the base of the flame is approached. When the flame has "holes" (incomplete combustion resulting from an inadequate pilot) the luminosity near the base of the flame is much less than that due to a laminar flame, but may increase rapidly with height and even exceed that from a full flame.

Ratio of CH/CC Intensities

Clark and Bittker (16) and John et al. (17) have suggested the use of the CH/CC intensity ratio as an indication of the local stoichiometry, since in laminar flames this ratio increases slowly to its maximum value at about stoichiometric. Fig. 5 is a plot of the ratio of photocurrents obtained with the CH filter to those with the CC filter (hereafter called CH/CC ratio) as a function of height, along the center line, in various flames. In the laminar flame, this ratio is constant over most of the flame height but decreases rapidly at the tip, apparently because of the more rapid decay of the CH radical. This same trend is observed in the turbulent flames as far as the tip of the inner cone, where again the ratio decreases. The numerical value of this ratio in a laminar flame is also equal to that of the turbulent flames at small and moderate flows. This result is consistent with the wrinkled laminar flame model and does not admit of mixing of the

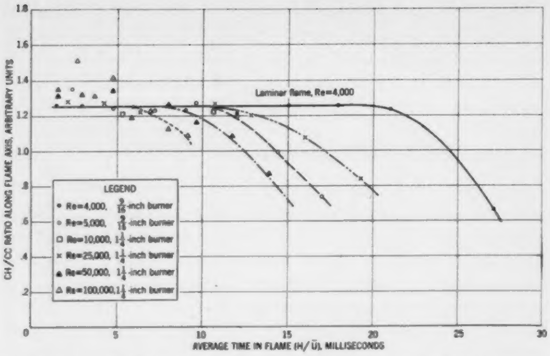

Fig. 5 CH/CC ratio as a function of average time in flame

flame with entrained air. Clark and Bittker (16) say that this similarity of CH/CC ratio indicates similar chemical kinetics in laminar and turbulent flames. John and Summerfield (8) state that a small sensitivity of radical radiation to turbulence can only mean that radical formation follows the same chemical path as in a laminar flame. The values of CH/CC ratio found in the flames at higher flows do seem to be anomalously large although the scatter of experimental data is also worse in these experiments. No explanation is offered as yet for these high values.

Smoke Photography

Previous evidence for the wrinkled laminar wave concept has employed schlieren photography. The ambiguity of these tests has been discussed (6). Difficulties arise from the emphasis obtained by schlieren photographs of flames on low temperature contours, around 300 C. The same questionable emphasis on a low temperature contour results from the use of ammonium chloride smoke to trace flame surfaces in a turbulent flame brush. However, a high temperature smoke such as zinc oxide is far less objectionable. Tests have shown this smoke to sublime in flames at around 1300 C (6). This temperature is still removed from the theoretical temperature (approximately 1950 C) of the stoichiometric flames used in this study, but close enough to give weight to photographic evidence obtained with this smoke. Typical photographs of laminar and turbulent flames are shown in Fig. 6. In a low temperature flame (Fig. 6(a)) the laminar front is poorly defined and some of the smoke passes through unsublimed; at a higher flame temperature the flame is sharply outlined (Fig. 6(b)). The smoke passes through a low temperature turbulent flame as might be expected (Fig. 6(c)), but in a stoichiometric turbulent flame, one obtains the familiar wrinkled pattern that one expects from the continuous flame front model. Although the instantaneous temperature profile to be expected from a distributed reaction zone model is not clear to the authors, it seems that smoother contours than seen in Fig. 6(d) must be obtained to distinguish the model from that of a wrinkled laminar front. The test does not support the concept of flamelets but the results are not necessarily inconsistent with this concept if the zinc oxide smoke, subliming several hundred degrees below flamelet temperature, is incapable of passing unsublimed between closely occurring flamelets.

Photometric Transients

The most persuasive evidence to date for the continuous wrinkled laminar flame model is represented by photometer oscillograms, typical examples of which are shown in Figs. 7, 8 and 9. In these oscillograms, the vertical displacements are proportional to light intensity in a small region of the flame brush, while the horizontal displacement is proportional to time. The fluctuations in the trace made from the

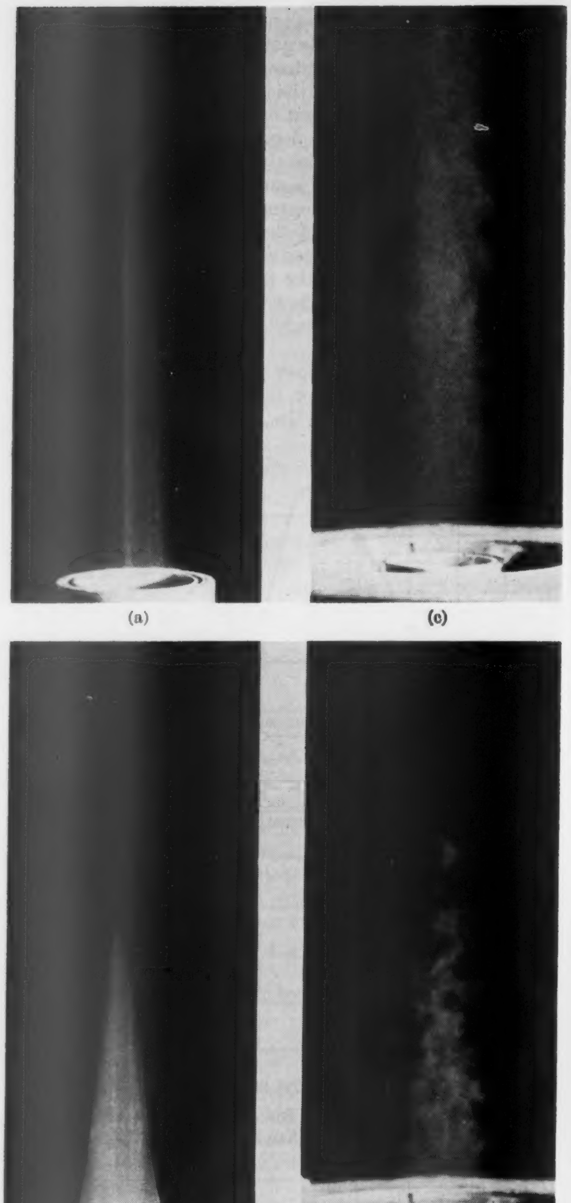

	(a)	(b)	(c)	(d)
Mixture composition, fraction of stoichiometric	0.6	0.75	0.6	1.0
Adiabatic flame temperature, °K.	1550	1930	1550	2230
Reynolds number	2000	2000	25,000	25,000

Fig. 6 Natural gas-air flames of different compositions with zinc oxide smoke injected into approach flow

laminar flame are due to shot noise in the photomultiplier tube and depend only on the value of the photocathode current and the band width of the detecting system. In the cases of the oscillograms made from full turbulent flames, the minimum light intensity is in the range of that due to a single sheet of laminar flame of the same equivalence ratio. A logical explanation for this minimum value is that it repre-

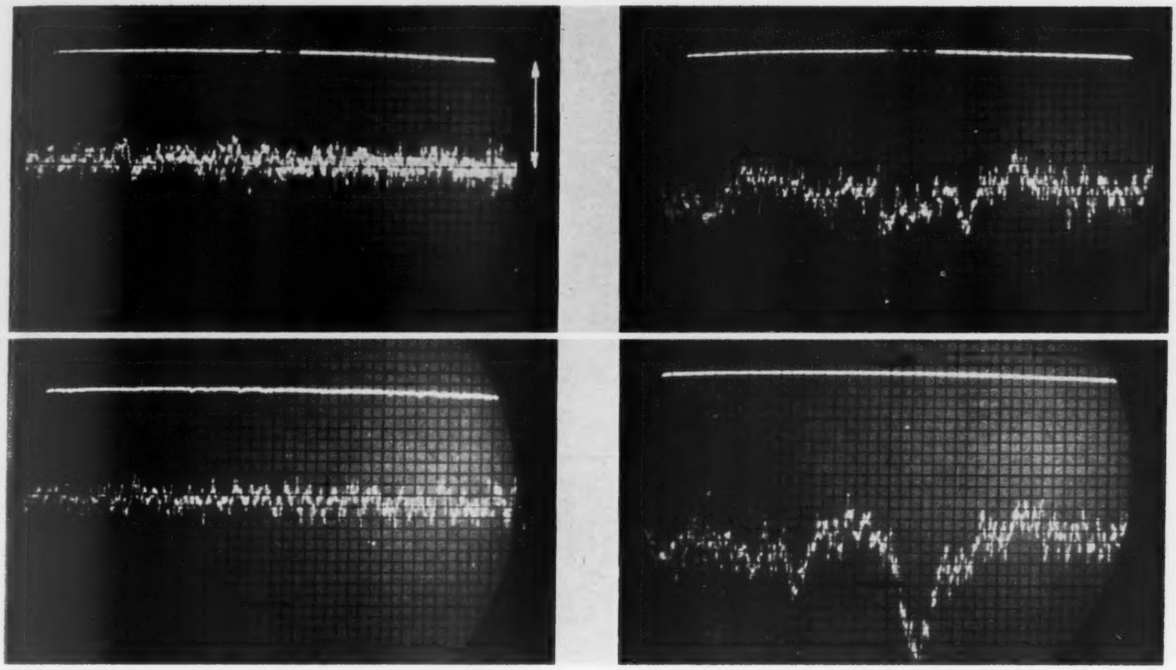

(a)
Laminar flame
$Re = 4000$
$U = 13.8$ fps

(b)
Turbulent flame
$Re = 5000$
$U = 17.2$ fps

Fig. 7 Representative luminosity transients from a laminar and a turbulent flame on a $\frac{9}{16}$-in. burner tube, as observed at 1.5 in. above burner. Time scale = 100 μ sec/small division; average amplitude for laminar flame front indicated by ↕

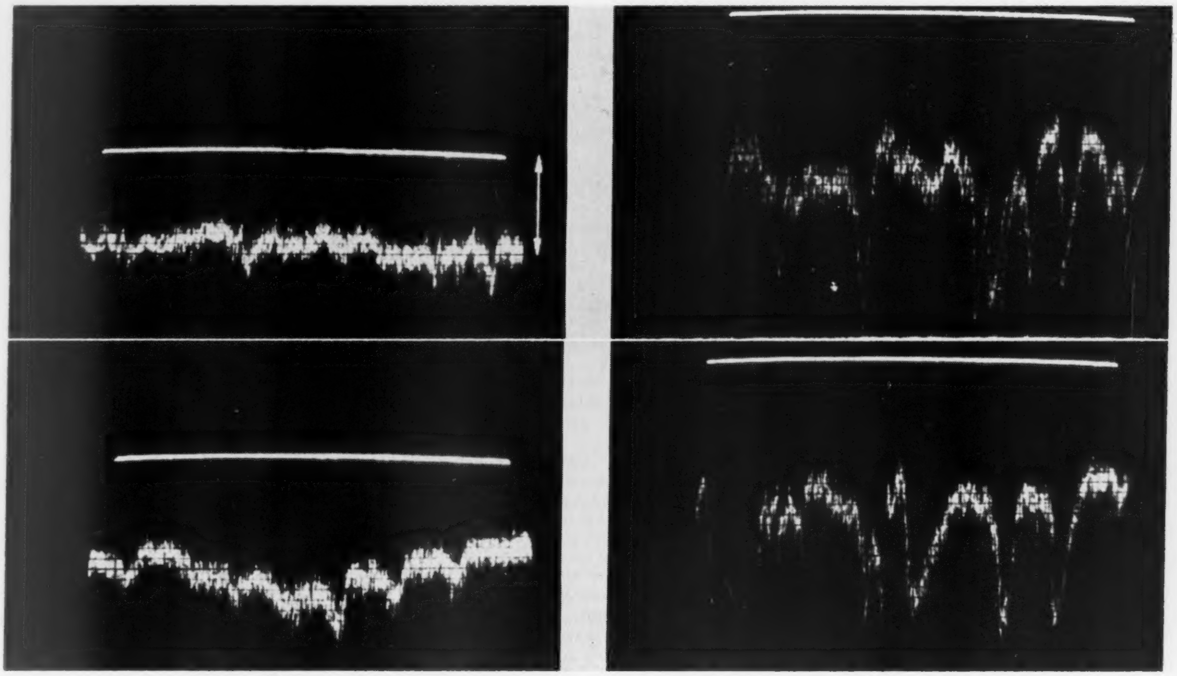

(a)
Height = 0.5 in.

(b)
Height = 2 in.

Fig. 8 Representative luminosity transients of a turbulent flame at Re = 10,000. 2-in. burner tube; pipe-flow turbulence; $\overline{U}$ = 9.7 fps; time calibration = 700 μ sec/small division; average amplitude for laminar flame front indicated by ↕

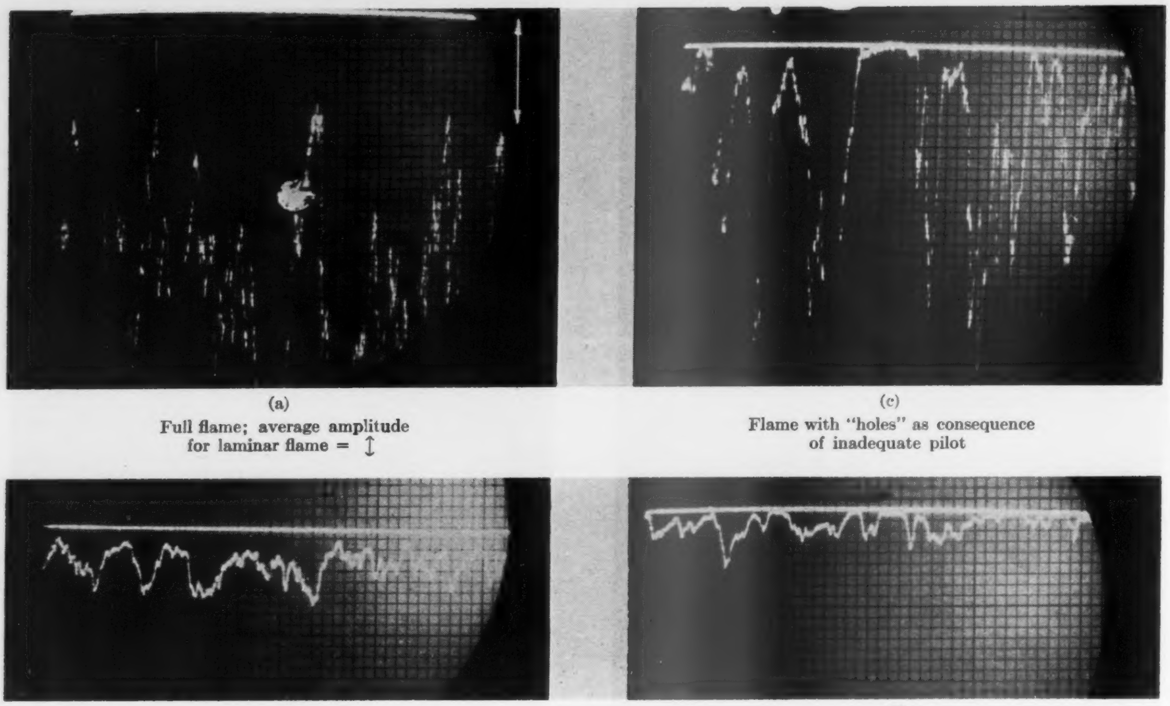

(a)
Full flame; average amplitude for laminar flame = ↕

(c)
Flame with "holes" as consequence of inadequate pilot

(b)
Same as (a) except photo-current attenuated 10:1

(d)
Same as (c) except photo-current attenuated 10:1

Fig. 9 Representative luminosity transients of turbulent flames at Re = 160,000—2-in. burner tube; height = 4 in. above burner; turbulence induced by 0.1-in. mesh grid; $\overline{U}$ = 155 fps; rms turbulence = 9 fps.; time calibration = 200 μ sec/small division

sents the broad side of a single laminar flame sheet. Since the light from full turbulent flames never goes below this value, one must also infer that the flame is continuous. The transients in excess of this minimum may represent light levels gathered from a laminar sheet inclined along the optical path of the photometer, plus perhaps islands of flame.

These results modify the observations made by means of direct short exposure photographs of turbulent flames (6). In spite of the test for adequate film sensitivity, the direct photographs did not register the light levels corresponding to broadside views of laminar flame surfaces and only registered higher light levels.

Fig. 9 (Re = 160,000) compares a full flame with grid-induced turbulence and a similar flame with "holes" resulting from an inadequate pilot. In the latter case, the light level is frequently seen to fall to zero, indicating breaks in the flame front, while the value of the maximum fluctuation, although occurring less often, is unaffected. Under these conditions the time-average specific light emission from a turbulent flame may drop below the laminar value. The "holes" seen photometrically in Fig. 9(c) have been correlated with "holes" found by simultaneous measurement by the electronic probe. The record in Fig. 9(c) appears to be relatable to the work of John and Summerfield (8). These authors noted that the specific emittance of a propane-air flame decreases as the approach flow turbulence reaches high values.

Conclusions

Measurements on flames by means of an electronic probe and a photometer and smoke photography have been combined to show that a turbulent flame may contain a wrinkled continuous laminar combustion wave. Of all the evidence consistent with the wrinkled laminar flame model of turbulent flame structure, the photometer oscillograms seem most nearly to fit the requirement for a crucial experiment to distinguish between the various models in existence. The correlation which these oscillograms show between the light from a steady laminar flame and the minimum light transients from a turbulent flame strongly indicates that the wrinkled laminar flame model is pertinent over the entire range of conditions extending to pipe flows up to 150 fps through a 2-in. ID tube and turbulence intensities up to 6 per cent.

Acknowledgments

The participation of J. M. Singer and J. R. Oxendine in obtaining the smoke photographs is gratefully acknowledged.

References

1 Damköhler, G., "The Effect of Turbulence on the Flame Velocity in Gas Mixtures," NACA TM 1112, 1947.

2 Schelkin, K. I., "On Combustion in a Turbulent Flow," NACA TM 1110, 1947.

3 Karlovitz, B., Denniston, D. W., Jr., and Wells, F. E., "Investigations of Turbulent Flames," *Journal of Chemical Physics*, vol. 19, 1951, p. 541.

4 Scurlock, A. C., and Grover, J. H., "Propagation of Turbulent Flames," in Fourth Symposium (International) on Combustion, Williams and Wilkins, Baltimore, 1953, p. 645.

5 Karlovitz, B., Denniston, D. W., Jr., Knapschaefer, D. H., and Wells, F. E., "Studies on Turbulent Flames. A. Flame Propagation Across Velocity Gradients. B. Turbulence Measurement in Flames," in Fourth Symposium (International) on Combustion, Williams and Wilkins, Baltimore, 1953, p. 613.

6 Grumer, J., Singer, J. M., Richmond, J. K., and Oxendine, J. R., "Photographic Studies of Turbulent Flame Structure,"

Industrial and Engineering Chemistry, vol. 49, 1957, p. 305.

7 Summerfield, M., Reiter, S. H., Kebely, V., and Mascolo, R. W., "The Physical Structure of Turbulent Flames," JET PROPULSION, vol. 24, 1954, p. 254.

8 John, R. R., and Summerfield, M., "Effect of Turbulence on Radiation Intensity from Propane-Air Flames," JET PROPULSION, vol. 27, 1957, p. 169.

9 Summerfield, M., "Turbulent Flames in Gases," JET PROPULSION, vol. 26, 1956, p. 485.

10 Wohl, K., and collaborators, "The Structure of Turbulent Flames," in Sixth Symposium (International) on Combustion, Reinhold, New York, 1957, p. 333.

11 Kovasznay, L. S. G., "A Comment on Turbulent Combustion," Remarks at the Conference on Combustion in Turbulent Flow, The Johns Hopkins University, 1955. JET PROPULSION, vol. 26, 1956, p. 480.

12 Hottel, H. C., Williams, G. C., and Levine, R. S., "Influence of Isotropic Turbulence on Flame Propagation," in Fourth Symposium (International) on Combustion, Williams and Wilkins, Baltimore, 1953, p. 636.

13 Richmond, J. K., Singer, J. M., Cook, E. B., Oxendine, J. R., Grumer, J., and Burgess, D. S., "Turbulent Burning Velocities of Natural Gas-Air Flames with Pipe Flow Turbulence," in Sixth Symposium (International) on Combustion, Reinhold, New York, 1957, p. 303.

14 Denniston, D. W., Jr., Oxendine, J. R., Knapschaefer, D. H., Burgess, D. S., and Karlovitz, B., "Applications of the Electronic Probe to the Study of Turbulent Flames," *Journal of Applied Physics*, vol. 28, 1957, p. 70.

15 Williams, F., and Fuhs, A. E., "Apparent Emission Intensities from a Turbulent Flame Composed of Wrinkled Laminar Flames," California Institute of Technology, Technical Report 20, June 1957.

16 Clark, T. P., and Bittker, D. A., "A Study of Radiation from Laminar and Turbulent Open Propane-Air Flames as a Function of Flame Area Equivalence Ratio, and Fuel Flow Rate," NACA RM E54F29, 1954.

17 John, R. R., Wilson, E. S., and Summerfield, M., "Studies of the Mechanism of Flame Stabilization by a Spectral Intensity Method," JET PROPULSION, vol. 25, 1955, p. 535.

Artificial Satellites—A Bibliography of Recent Literature Part Two—1957–1958[1]

MILDRED BENTON[2]

U. S. Naval Research Laboratory, Washington, D. C.

1957

Aberdeen Proving Ground, Ballistic Research Laboratories, Aberdeen, Md.

On the Motion of a Satellite of an Oblate Planet, by B. Garfinkel. 33 pp., July 1957. (Rpt. 1018.) Orbit calculation.

Orbit Measurements of an Artificial Earth Satellite (Sputnik II) from Photographs Taken with a Tracking Ballistic Telescope System, by D. Reuyl. ¼ in. thick, Nov. 1957. (Tech. Note 1156.) A brief résumé of optical methods for measurement of artificial earth satellites. Observations of the third stage rocket of Sputnik I and II with tracking ballistic telescope systems, based on SMT and IAOR instruments are described.

Theory of the Spin of a Conducting Satellite in the Magnetic Field of the Earth, by J. P. Vinti. 70 pp., July 1957. (Rpt. 1020.) A theoretical investigation of spin.

Aeronautics

Are Earth Satellites Illegal? 36: 37–38, Aug. 1957. Refers to legal "squabble" over necessity and means of legalizing satellites.

Air Force. Wright Air Development Center, Dayton, Ohio

Transfer Between Vehicles in Circular Orbits, by B. H. Paiewonsky. 9 pp., Aug. 1957. (Tech. Note 57-267.) Development of a method for calculating the initial angular separation between two vehicles in circular orbits, required for the orbital transfer of a commuter rocket with a minimum expenditure of fuel.

Arnowitz, Leonard

The Vanguard Control System. ASTRONAUTICS 2: 34–36, 84, illus., Oct. 1957. How scientists working on the project plan to handle the job of getting the artificial earth satellite into orbit.

ASTRONAUTICS

Eyes on the Sky. 2: 40–41, 76–77, illus., Dec. 1957. A brief description of the optical and visual tracking program being used to establish the Sputnik orbits, based on a paper by F. L. Whipple and J. A. Hynek presented at the IAF Barcelona meeting.

Automatic Control

Satellite Computing Center Opened. 7: 53–56, illus., Aug. 1957.

Bates, D. R., and Moore, Patrick, ed.

Space Research and Exploration. 224 pp., London, Eyre. 1957. The earth satellite program by H. S. W. Massey, Chapter 7, and Appendix XVII, pp. 100–124, 218–219.

Berger, W.

Ueber Die Verwendung Von Photoelementen in Kuestlichen Erdsatelliten (Application of Photoelectric Devices to Satellite Vehicle Instrumentation). Rakententech. u. Raumfahrtforsch. 1: 22–23, Apr. 1957. In German.

Berkeley, E. C.

Satellites and Computers—and Psychology. Computers and Automation 6: 6–8, 14, 1957. The field of information-handling mechanisms for unmanned space vehicles without doubt will become one of the important and fascinating subdivisions of automatic computers and data automation.

Bizony, M. T., and Griffin, R., ed.

The Space Encyclopaedia. A Guide to Astronomy and Space Research. 287 pp., and Suppl., illus., New York, Dutton, 1957. A guide to the nomenclature of astronomy and space research. The artificial earth satellite program, pp. 20–34. The Russian earth satellite, Supplement, pp. 1–4.

Black, T. W.

Tooling for the Satellite. Tool Eng. 38: 83–85, Mar. 1957.

Blitzer, Leon

Apsidal Motion of an IGY Satellite Orbit. J. Appl. Phys. 28: 1362, Nov. 1957. Notes that nodal regression and apsidal motion both increase with orbit eccentricity in the same manner.

Effect of Earth's Oblateness on the Period of a Satellite. JET PROPULSION 27: 405–406, Apr. 1957. For a satellite at an altitude of 300 miles, the difference in period between a polar and an equatorial orbit is found to be 12 sec.

Blitzer, Leon, and Wheelon, A. D.

Oblateness Perturbation of Elliptical Satellite Orbits. J. Appl. Phys. 28: 279, Feb. 1957. The formulas of nodal regression of earth-satellite orbits (due to the oblateness of the earth) in the case of elliptical orbits are deduced, thus extending the analysis of a previous paper. (See Blitzer in Part One—1956[1] references).

Bloom, A. L., and Johnson, L. E.

A Magnetometer for the Satellite. Electron. Indus. and Tele-Tech. 16: 76–78, 148, 150, 152, 154, 156, 158, Aug. 1957. The characteristic frequency of precessing protons in a weak magnetic field can serve as a measure of the earth's field in space. Data from rocket-borne magnetometers have been extrapolated to produce a tentative design for a satellite magnetometer.

Brit. Comm. and Electron.

British Radio Observation of the Satellite. 4: 770–772, Dec. 1957. Report of observations of the Russian Sputniks.

Brown, R. R., Green, P. E., Jr., Howland, B., and Others

Radio Observations of the Russian Earth Satellite. Inst. Radio Engrs. Proc. 45: 1552–1553, Nov. 1957. Reports observations

Received March 11, 1958.

[1] Part One of this Bibliography covering 1956 appeared in May 1958 JET PROPULSION, p. 301.

[2] Consultant in Research Information.

made at Lincoln Laboratory, beginning Oct. 5, 1957.

Burgess, Eric

Satellites and Spaceflight. 160 pp., illus., London, Chapman and Hall, 1957. A factual survey of developments in the field of rocket propulsion, interplanetary travel and the establishment of satellite bodies.

Burghardt, J. E.

Chemical Rocket Propulsion in the Vanguard Satellite Launching Vehicle. Chem. Eng. Prog. 53: suppl., 86, 88, 90–91, Oct. 1957. Includes illustrations of first and second stage propulsion systems.

Caidin, Martin

Vanguard, the Story of the Man-Made Satellite. 288 pp., New York, Dutton, 1957. Touches upon various phases of Project Vanguard and the scientific topics that can be explored by shooting rockets around the moon. Essentially the same material as Clarke's *The Making of a Moon,* but with less emphasis on scientific theory.

California Institute of Technology, Jet Propulsion Laboratory, Pasadena, Calif.

Equations of Motion of a Missile and a Satellite for an Ablate-Spheroidal Rotating Earth, by B. E. Kalensher. 36 pp., Apr. 12, 1957. (Memo. 20-142.) The motion of a satellite is determined directly from the equation of motion of the missile, the former being considered a special case of the latter.

Canadian Mining Journal

Tracking Down the Synthetic Satellite. U. S. Navy Project Vanguard. 78: 82, illus., July 1957. Details expected use of a Varian magnetometer, a device which measures the earth's magnetic field.

Canney, H. E., and Ordway, F. I.

The Uses of Artificial Satellite Vehicles. Astronautica Acta 2: 147–174, 1956: 3: 1–15, 1957. Astronomical and astrophysical advantages of the artificial satellite are covered, as are the benefits to the biological and medical sciences deriving from a space station. The satellite as an observation and military base, a communications relay station, and a radar beacon, and navigational fix are also considered.

Carter, L. J., ed.

Realities of Space Travel. 431 pp., London, Putnam, 1957. Contains 24 selected papers published during the last decade in the Journal of the British Interplanetary Society. There are eleven chapters, one entitled "The Satellite Vehicle." American ed. New York, McGraw-Hill, 1958.

Chemical and Engineering News

Sputnik II—A Prelude to the Moon? 35: 27, Nov. 11, 1957. Some vital statistics of Russia's artificial satellites.

Chemical Week

Chemical Showcase in Space. 81: 58–64, illus., July 27, 1957. A descriptive article which not only gives fabrication details to indicate why the satellite is "a colossal chemical showcase" but also includes details of how it will be hurled into space.

Clark, Evert

Programs for Future Sputniks Detailed by Russian Scientists. Aviat. Wk. 67: 32–33, Dec. 16, 1957.

Clarke, A. C.

The Making of a Moon. The Story of the Earth Satellite Program. 205 pp., illus., New York, Harper, 1957. Satellite prehistory, the inception of Project Vanguard, and some technical details and plans.

A New Moon is Born. Holiday 22: 60–61, 104–106, Nov. 1957. The Vanguard Project; its background; current activity; and possible technical achievements of a satellite.

Visit to Vanguard. Spaceflight 1: 27–29, July 1957. Some over-all impressions obtained during a visit to most of the contractors and agencies involved in the Earth Satellite Program.

Coombs, Charles

Rockets, Missiles and Moons. 256 pp., New York, Morrow, 1957. A broad survey of the government's program to launch unmanned, earth-circling satellites.

Cox, Donald

Men of Project Vanguard. ASTRONAUTICS 2: 32–33, 68–70, illus., Oct. 1957. Personalities on the Navy and Martin teams.

Croome, Angela, Compiler

The International Geophysical Year Month by Month. Discovery 18: 526–528, illus., Dec. 1957. Includes remarks on tracking the Russian satellite; rocket survival; discovery that atmosphere is thinner and colder; increasing British observations and Sputnik I help ionospheric studies.

Cross, C. A.

Satellite Paradox. Spaceflight 1: 48, Jan. 1957. Concerns velocity of satellite vehicles.

The Satellite Paradox. Brit. Interplan. Soc. J. 16: 110–111, Apr./June 1957. Refers to two papers (see items under King-Hele and Cross) in which authors have independently made the point that when a satellite encounters air resistance it is speeded up, instead of slowed down as might have been expected. This paradox has led the writer to speculate on the behavior of a composite satellite, made up of a light sphere and a dense one linked by a thin cord.

Crouse, V. J.

Vanguard Instrumentation System. Signal 12: 33–34, 36, illus., Sept. 1957. A discussion of the system, how it works, and what it is expected to do.

Danilin, B. S., Mikhnevich, V. V., and Others

Zadacha Izmereniia Davleniia I Plotnosti Vysokikh Sloev Atmosfery S Pomoshchiu Iskusstrennogo Sputnika Zemli. (*The Problem of Measuring Pressure and Density of the Upper Atmospheric Layers with the Aid of an Artificial Earth Satellite*). Usp. Fiz. Nauk. 63 (lb): 205–225, Sept. 1957. In Russian. Deals with an analysis of the physical control of the problem pertaining to measurements of the pressure and density of high altitude layers of the atmosphere with the use of a satellite for this purpose.

Das, Anadijiban

The Artificial Satellite and the Relativistic Red Shift. Prog. Theor. Phys. 18: 554–555, Nov. 1957. Refers to formula derived by Singer and extended by Hoffman, which, according to the author, does not follow directly from the solution of the field equation. This the author proceeds to do.

Daugherty, B. W.

Buying for the Earth Satellite. Aero. Purchasing 1: 22–23, illus., Oct. 1957. Gives an idea of the miscellaneous items acquired by The Martin Company from twelve major suppliers in connection with Project Vanguard. Relates, in particular, the making of the mouse-trap spring.

De Groat, G. H.

Building the Space Satellites. Am. Mach. 101: 101–106, Jan. 14, 1957. Vanguard production details.

Detra, R. W., Kemp, N. H., and Riddell, F. R.

Addendum to 'Heat Transfer to Satellite Vehicles Re-entering the Atmosphere.' JET PROPULSION 27: 1256–1257, Dec. 1957. Original article is by N. H. Kemp and F. R. Riddell.

Devienne, M.

Temperature Reached by a Missile Moving in the Upper Atmosphere. Fusées 2: 43-47, Mar. 1957. In French.

"Two problems are considered: (a) what is the equilibrium temperature reached by a satellite or missile on its trajectory and the range of variations at this condition; (b) at what height does a given missile become incandescent or reach a given temperature. At the altitudes discussed (80 to 120 km) the flow regimes are those of a rarefied gas. The characteristics of such flows are briefly discussed. The results of experiments simulating these conditions for a plate and a sphere are summarized. It is shown that on such results calculations for the above problems can be based, and particularly for bodies of cylindroconical form." (Index Aeronauticus 7: 32, July 1957.)

Dickinson, T. A.

Earth Satellite No. 1. Weld. and Metal Fabric. 25: 289, 305, illus., Aug. 1957. Importance of welding in construction of the satellite.

Easton, R. L.

Calibration of the Mark II Minitrack Using Radio Stars as Signal Sources. QST 41: 42–44, illus., Apr. 1957. Outlines the necessary requirements of the receiving equipment and lists the stars that will be useful.

Mark II Minitrack Base-Line Components Constructional Details of Antenna System for Satellite Tracking. QST 41: 37–41, illus., Sept. 1957.

The Mark II Minitrack System. In Am. Astronautical Soc. Proc., 3rd Annual Meeting, Dec. 6–7, 1956, pp. 53–58, New York, The Society, 1957. A brief history of the preliminary design leading to final specifications for the Vanguard satellite radio tracking program.

Radio Tracking of IGY Satellite: The Mark II Minitrack System. J. Astronautics 4: 31–32, 39, illus., Summer 1957. Describes the interferometer system and the present status of the radio tracking.

Edelbaum, T. N.

Comments on the Powered Flight Trajectory of a Satellite. JET PROPULSION 27: 1260–1261, Dec. 1957. Points out significance of centrifugal force.

Eggers, A. J., Jr.

Performance of Long-Range Hypervelocity Vehicles. JET PROPULSION 27: 1147–1151, illus., Nov. 1957. The paper concludes with some observations on satellite vehicles which are treated as a limiting case of the ballistic vehicles previously discussed.

Electronic Equipment

Opticians Aid Electronics. 5: 40–41, illus., July 1957. Concerns the telescopic photographic recorder (TPR) used to test missiles in flight and miniaturized components used in the earth satellite program to aid in weather forecasting.

Electron. Indus. and Tele-Tech.

"Sputnik." What Are Its Technical Implications? 16: 70–71, 73, 149–150, 1957. Sputnik history, propaganda value and what industry officials said about it. U. S. satellite experiments are reviewed and an indication given of what the U. S. scientific satellite will accomplish. It is prophesied that the "satellite promises to profoundly affect the future of the electronic industry and over-all defense effort."

Electronics

Transistor Inverters Power Vanguard Rocket. 30: 203–204, Apr. 1, 1957. Incorporation of high-power transistors into power-supply design has made possible a 300-volt, lightweight inverter for use with servos in the second-stage rocket for the Vanguard Project. The block diagram is shown.

Vanguard's Center Gets Rehearsal. 30: 7–8, illus., Nov. 1, 1957. Describes operation of the IBM center, under contract to Vanguard, after the launching of the Soviet Sputnik on October 4, 1957.

Electroplating

Gold Plating of Magnesium. 10: 319–321, Oct. 1957. Vanguard construction detail.

Emmons, R. H.
Satellite-Tracking Practice in a Planetarium. Sky and Telescope 16: 170–171, illus., Feb. 1957. Description of a satellite-tracking simulator devised by a North Canton, Ohio, Moonwatch team.

Engineering
Practical Aspects of Earth Satellites. 184: 484–486, illus., Oct. 18, 1957. Discusses energy requirements; energies available; value of accuracy; satellite uses; research; and utilitarian advantages.

Faust, Heinrich
Aufgaben Fuer Messatelliten (Applications for Satellite Vehicles). Weltraumfahrt 8: 9–12, Feb. 1957. In German. Includes a discussion of various satellite problems, such as the presence of meteors and cosmic rays, and information that may be obtained directly or deduced from research satellites.

Fedorov, E. K., and Skuridin, G. A.
Rakety I Iskusstvennye Sputniki Zemli V Issledovaniiakh Verkhnei Atmosfery (Rockets and Artificial Satellites in Studies of the Upper Atmosphere). Akad. Nauk. SSSR. Vestnik 27: 37–48, Aug. 1957. In Russian.
"Survey of work done in the U.S.A. and Soviet Union in studying the upper atmosphere, and use of rockets in these studies. Description of several possible types of future artificial satellites." (Battelle Tech. Rev. Abs. 7: 82, Jan. 1958.)

Fejer, J. A.
Life-Time of an Artificial Satellite. Nature 180: 1413, Dec. 21, 1957. A simple expression is derived which predicts the approximate lifetime from initially measured values of the rate of change of height at apogee and the difference between the heights at apogee and perigee.

Felt, N. E.
The Vanguard Satellite Launching Vehicle. Brit. Interplan. Soc. J. 16: 27–29, Jan./Mar. 1957. Summary of talk given at Seventh International Astronautical Congress in Rome, Sept. 1956.

Ferri, Antonio, Feldman, Lewis, and Daskin, Walter
The Use of Lift for Re-entry from Satellite Trajectories. Jet Propulsion 27: 1184–1191, Nov. 1957. The combined use of lift and heat sinks in the re-entry problem is studied in this paper. Three types of trajectory were investigated. The results of the analysis show that the combination of reasonable amounts of lift and heat capacity, with properly chosen trajectories, can greatly alleviate the aerodynamic heating problems.

Firor, J.
A Radio Telescope. QST 41: 32–36, Sept. 1957. The antenna system described is a type suitable for tracking the earth satellite.

Franklin Institute Journal
Computing Facility for Project Vanguard. 263: 275–277, Mar. 1957.
Instruments for Satellites. 264: 258–259, Sept. 1957. A description of the Varian magnetometer, a device which measures the earth's magnetic field, and which will be one of the instruments carried in the earth satellite.

Fraser, Ronald
Once Around the Sun. 160 pp., London, Hodder and Stoughton, 1957. Chapter 9 deals with satellites and rockets.

Fried, B. D.
On the Powered Flight Trajectory of an Earth Satellite. Jet Propulsion 27: 641–643, June 1957. The problem of programming the powered flight trajectory of an earth satellite to obtain maximum orbit altitude is investigated.

Friedman, Herbert
Scientific Experiments in IGY Satellites. Yale Sci. Mag. pp. 1–5, May 1957. A summary of the problems being overcome and the information to be gleaned from the launching of the first man-made satellite.
Scientific Instrumentation in IGY Satellites. Elec. Eng. 76: 470–474, June 1957. Possibilities for experimental instrumentation in connection with the IGY satellites are discussed. (Also issued as AIEE Paper CP57-213.) Summary in Midwest Eng. 9: 21, Feb. 1957.
Brief paper with same title appears also in Instr. Soc. Am. Proc. 11 (Pt. 2), IGY, 1 p., 1956.
The Vanguard Instrument Package. Astronautics 2: 66–69, 104–105, illus., Aug. 1957. Tells how 10 lb of tiny but reliable instruments will permit IGY scientists to perform major experiments in the fields of solar radiation, cosmic rays, geomagnetism and meteorology.

Gatland, K. W., Kunesch, A. M., and Dixon, A. E.
Minimum Satellite Vehicles. In Carter, L. J., ed. *Realities of Space Travel. Selected Papers of the British Interplanetary Society,* pp. 67–79, London, Putnam, 1957. Project Vanguard, pp. 75–78.

Gatland, K. W.
Rockets and Artificial Satellites in the IGY. Spaceflight 1: 130–138, illus., July 1957. The scope and objectives of the IGY and background histories of the rockets and artificial satellites, including Vanguard, that will play vital roles in the biggest and most intensive program of research ever attempted by man.

Gazley, Carl, Jr., and Masson, D. J.
Designing a Recoverable Scientific Satellite. Aviat. Age 28: 44–51, Aug. 1957. A recoverable orbiting body appears to be the logical sequel to the IGY satellite project. At first such a body would closely resemble the 21.5-lb, 20-in.-diam IGY sphere, the only "payload" being its own skin and a radio beacon.

Ginzburg, V. L.
Ispol'zovanie Iskusstvennikh Sputnikov Zemli Dlya Proverki Obshche Teorii Otnositel'nosti (Utilization of Artificial Earth Satellites for the Re-check of the General Theory of Relativity). Usp. Fiz. Nauk 63(1a): 119–122, Sept. 1957. In Russian. Previously published in Priroda 45: 30–39, Sept. 1956.
Ueber die Verwendung Kuenstlicher Erd-Satelliten zur Pruefung der Allgemeinen Relativitaetstheorie (On the Use of the Artificial Earth Satellite to Prove the General Theory of Relativity). Exp. Tech. Physik 5: 89–92, 1957. In German. Paper given at the International Geophysical Year, Rocket and Satellite Conference, Washington, D. C., Sept. 30–Oct. 5, 1957. In a suggestion for measuring the gravitational displacement of frequency it is proposed that one measures not the frequency but the difference between the readings on clocks on earth and the readings on clocks on the satellite.

Goldman, D. T., and Singer, S. F.
Studies of a Minimum Orbital Unmanned Satellite of the Earth (MOUSE). III. Radiation Equilibrium and Temperature. Astronautica Acta 3: 110–129, 1957. Presents the problem of predicting the equilibrium temperature of an artificial earth satellite and methods for designing and controlling its temperature under all types of conditions. The results for the equilibrium temperature are presented in the form of convenient nomograms to aid in preliminary design.

Grammer, George
Sat llite 40-mc Converter. Sensitivity and Stability in a Design for Use with Amateur-Band Receivers. QST 41: 25–28, Dec. 1957.
What to Do About Satellites. QST 41: 14–15, 174, Dec. 1957. What to do at a launching; afterward; telemetering; and experiments. Suggestions for amateurs.

Great Britain. Royal Aircraft Establishment, Farnborough
The Effect of the Earth's Oblateness on the Orbit of a Near Satellite, by D. G. King-Hele and D. M. C. Gilmore. 40 pp., figs., Oct. 1957. (Tech. Note GW 475.) The equations of motion of a satellite in an orbit over an oblate earth in vacuo are solved analytically by a perturbation method.

Gringaus, K. I., and Zelikhman, M. K.
Ismerenie Kontsentralsii Polozhitel'nykh Ionov Vdol'orbity Iskusstvennogo Sputnika Zemli (Measurement of the Concentration of Positive Ions Along the Orbit of an Artificial Earth Satellite). Usp. Fiz. Nauk 63(1b): 239–252, Sept. 1957. In Russian. Concerns possibility of utilizing the earth satellites as a means of investigating the structure of the ionosphere.

Grupp, G. W.
Electroplating is an Important Step in the Construction of a Man-Made Satellite. Metal Finish. 55: 40–44, illus., July 1957. Outlines the preplating procedure and the gold-plating cycle for the satellite constructed for Project Vanguard.

Gunther, Max
Tracking the Man-Made Satellite. Radio and TV News 58: 31–33, illus., July 1957. A complex and elaborate recording system will be used to keep track of the tiny sphere after it is launched in space.

Gustavson, John
Meteoritic Dust. Jet Propulsion 27: 207–208, Feb. 1957. Present limited knowledge of abundance and energy distribution of meteoritic dust may be alleviated by use of the IGY earth satellite as a research vehicle to determine the actual intensity of micro-meteroid impact.

Hass, G. H.
The Coatings That Go on the Satellite. Mag. Magnesium, pp. 4–5, illus., Aug. 1957. The application and effect of the four exterior coatings applied to the Vanguard satellite sphere.

Hagen, J. P.
Radio Tracking, Orbit and Communication for the Earth Satellite. Aero. Eng. Rev. 16: 62–66, May 1957. A chain of receiving stations create a radio fence which will intercept a satellite each time it circles the earth.

Haviland, R. P.
What the Future Holds for the Earth Satellite. In American Astronautical Society Proceedings, 3rd Annual Meeting, Dec. 6–7, 1956, pp. 77–87, New York, The Society, 1957. The satellite's inherent characteristics suggest early application in three major fields: Mapping and geodesy, weather charting and forecasting, and communications. Previously published in Gen. Elec. Rev. 59: 10–16, Sept. 1956. Also in J. Astronautics 4: 41–45, 51, Autumn 1957.
For comment, see Stehling, K. R., Space Flight Notes. Jet Propulsion 26: 48, Jan. 1956.

Hawkes, Russell
Camera Ready to Track Soviet Satellite. Aviat. Wk. 67: 123, 125, 127, illus., Oct. 28, 1957. Describes design and operation of first of twelve tracking cameras intended as part of the satellite tracking network in IGY Project Vanguard.

Henry, I. G.
Lifetimes of Artificial Satellites of the Earth. Jet Propulsion 27: 21–24, Jan. 1957. The effect of variations in upper-atmosphere density on the lifetimes of satellites in elliptical and circular orbits, calculated from kinetic theory.

Hersey, Irwin
The Meaning of "Sputnik." Astronautics 2: 22–25, 83–86 Nov. 1957. A chronological review of the launching of the Russian earth satellite and what happened after-

(Continued on page 418)

Technical Notes

Wall Temperature Instability for Convective Heating With Surface Radical Recombination

DANIEL E. ROSNER[1]

Daniel & Florence Guggenheim Jet Propulsion Center, Princeton University, Princeton, N. J.

WHILE one can often formally construct "steady-state" solutions to engineering problems, a demonstration of the physical *existence* of such steady-state solutions necessarily involves static stability considerations. We call attention here to an interesting instability which, for example, may arise in the problem of aerodynamic heating for the range of altitudes and flight speeds in which shock-produced radical concentrations are significant.

One may formally compute the steady-state local heat flux for each flight condition, geometry, and choice of both wall material and temperature T, by accounting for (a) energy transport q_c to the wall by ordinary molecular conduction, and (b) energy transport q_D by radical diffusion followed by wall recombination. We make the assumption here that the contribution made by radiation to the wall is small compared to mechanisms (a) and (b), although this is not essential to the following discussion. For definiteness consider the technically important case of stagnation point heat transfer to a thin, internally cooled wall with a chemically frozen boundary layer. Then, as recently shown by Lees (1),[2] Fay & Riddell (2) and Goulard (3),[3] when the wall is catalytic the energy transfer rates q_c and q_D are of comparable magnitude, for wall temperatures, surfaces and flight conditions of interest. Goulard has further indicated that each of q_c and q_D has its own distinct wall temperature dependence. In particular, q_D depends largely upon a catalytic rate parameter which is essentially the ratio of the characteristic time to diffuse across the boundary layer to a time characteristic of the reaction process at the wall. Because of the strong positive wall temperature dependence of the catalytic rate constant for metals and oxide layers, this parameter may itself have a strong wall temperature dependence, over a wide range of temperatures. Studies (4) have shown that this increase in surface activity may persist up to wall temperatures of the order of 1300 K or higher. This indicates that the catalytic contribution, q_D, to the heat transfer can *rise* appreciably as higher wall temperatures are contemplated, particularly for combinations of flight conditions and wall temperatures such that wall reaction rates are "chemically controlled."

However, as in conventional heat transfer problems involving cooled bodies in hot streams, the conductive contribution q_c *decreases* with the choice of higher wall temperatures. In early heat transfer practice, when q_c was the principal contributor to the heat flux, one chose a coolant flow such that the highest wall temperature consistent with structural safety was achieved, and, because q_c is monotone decreasing with increasing wall temperature, this required the smallest practical coolant flow. Now, with q_D becoming an important contributor to the total heat flux, there arises the possibility that the sum $q = q_c + q_D$ may pass through minima and exhibit regions of positive slope for wall temperatures below the melting point. The steady-state wall temperature then becomes a multivalued function of the heat input to the wall and, depending upon the nature of the cooling system, a wide range of surface temperatures may not be statically stable. We examine these possibilities here.

For a given flight condition, consider the superposition of the resulting steady-state aerodynamic heat input curve $q(T)$, with coolant capacity curves, having non-negative slopes and parametrized by the coolant mass flow $\dot{m}$, as shown in Fig. 1. Intersections locate all eligible steady-state combinations of heat flux and wall temperature. However, all couples (q, T) at which the slope of the heat input curve exceeds that of the relevant cooling capacity curve (such as at E) are unstable in the sense that perturbations in the wall temperature or coolant flow rate, in the absence of additional controls on the coolant flow, will cause the system to wander to the nearest eligible steady-state solution.

Adopting a quasi-steady approach we briefly indicate here possible consequences of a situation such as that shown in Fig. 1. Owing to the existence of two stable wall temperatures for each mass flow $\dot{m}$ between $\dot{m}^*$ and $\dot{m}^{**}$, it is necessary to consider the circumstances under which each stable point can be attained. For simplicity, consider the internally cooled surface of a vehicle entering the atmosphere of a planet in a trajectory such that the aerodynamic heat input curve is substantially unaltered in times comparable to the time required for the following changes to take place. Suppose, first, that the external surface in question is cooler than T_A although the internal coolant mass flow is initially fixed at $\dot{m}_A > \dot{m}^*$. This implies that a series of transient states will be passed through with the stable operating point T_A finally being achieved. If, for example, one now decreased the coolant flow to $\dot{m}_c > \dot{m}^*$ then the wall temperature would approach the steady value T_c; that is, further reductions in $\dot{m}$ lead to a continuous sequence of increasing wall temperatures until $\dot{m}^*$ is reached, at which point the coolant mass flow curve is tangent to the heat input curve. A slight reduction in coolant mass flow then causes a comparatively sudden jump in wall temperature to the value T_H. Of course, if structural failure occurs for T such that $T_H > T > T_D$, then this slight decrease in coolant mass flow would lead to sudden destruction of the surface.

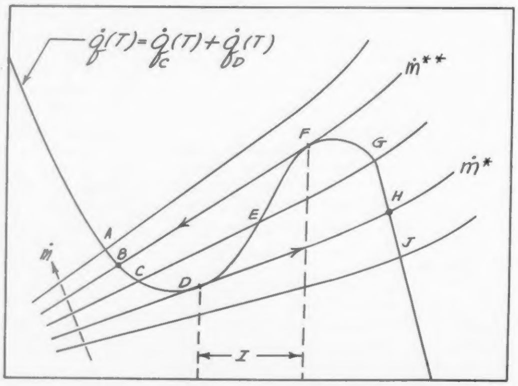

Fig. 1 Superposition of aerodynamic heat input curve $q(T)$ with coolant capacity curves showing an unstable operating point E and the region I of wall temperature instability

Received Feb. 25, 1958.

[1] General Electric Co., Charles A. Coffin Fellow, 1957–1958. Mem. ARS. Present address: AeroChem Research Laboratories, Inc., P.O. Box 12, Princeton, N. J.

[2] Numbers in parentheses indicate References at end of paper.

[3] Added in proof: See also Scala, S. M., *J. Aero. Sci.*, vol. 25, no. 4, 1958, pp. 273-275.

EDITOR'S NOTE: The Technical Notes and Technical Comments sections of JET PROPULSION are open to short manuscripts describing new developments or offering comments on papers previously published. Such manuscripts are published without editorial review, usually within two months of the date of receipt. Requirements as to style are the same as for regular contributions (see masthead page).

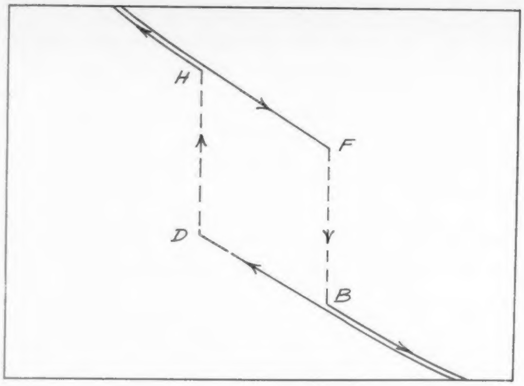

Fig. 2 **Wall temperature T as a function of coolant mass flow $\dot{m}$ showing temperature jumps D-H, F-B and hysteresis loop D-H-F-B**

Consider now the reverse case of entry with a wall temperature initially higher than the equilibrium temperature corresponding to the pre-existing coolant mass flow, say $\dot{m}_J < \dot{m}^{**}$. Then the wall temperature will approach the steady value T_J. If the coolant mass flow is now continuously increased, then a continuous decrease in steady-state wall temperature is effected until the mass flow passes through $\dot{m}^{**}$ at which point the wall temperature will suddenly drop from the value T_F to the value T_B.

The resulting wall temperature-coolant mass flow curve displays the hysteresis shown in Fig. 2. It is clear from this figure that no stable wall temperature T such that $T_F > T > T_D$ can be reached from either direction. This is consistent with the relative slopes shown in Fig. 1.

The behavior described here bears a striking resemblance to the Frank-Kamenetskii quasi-steady theory of thermal ignition and extinction of combustion occurring at solid surfaces. If one considers the case of an exothermic reaction taking place at the surface of a solid body placed in a combustible gaseous stream, and, for simplicity, disregards both radiation away from the body and conductive heat flux *into* the body, then steady-state conditions are determined by a balance between heat convected *away* from the surface into the gaseous stream and heat released at the surface as a result of chemical reaction. Again, each of these has its own wall temperature dependence, and eligible steady-state conditions, as before, are determined by finding appropriate intersections. The consequences of this approach have been investigated by Frank-Kamenetskii (5) in an effort to interpret ignition and extinction data under such conditions. Here we briefly indicate the similarities of the two situations.

The analog of the aerodynamic heat input curve $q(T)$ is now the heat release rate by virtue of surface reaction, except that the latter is considered to be a monotone increasing function of surface temperature. For very low surface temperatures the rate of heat evolution by chemical reaction is "chemically controlled" and comparatively small. At higher wall temperatures, but still within the "chemically controlled" regime, the heat evolution curve displays a rapid rise, with characteristic exponential wall temperature dependence. At sufficiently high surface temperatures the regime passes over to "diffusion controlled" and the heat evolution again becomes relatively insensitive to temperature changes, being more sensitive to changes in hydrodynamic conditions.

The analog of the family of cooling capacity curves is now the family of curves (one for each hydrodynamic condition, say free stream velocity U) which give the heat convected away from the surface as a function of the surface temperature. As before, for a particular range of hydrodynamic conditions three stationary states are possible, of which, however, only the upper and lower are stable. Furthermore hysteresis phenomena resembling Fig. 2 are exhibited if one considers the quasi-steady attainment of stable operating points with, say, U replacing $\dot{m}$. The jumps in surface temperature are now interpreted as "ignition" and "extinction" and are therefore associated with the sudden passage of the reaction from the kinetic to diffusional regime.

Ignition experiments carried out in Russia by Buben (6), who used electrically heated platinum wires to study the catalytic oxidation of hydrogen-air and other fuel-air mixtures, did in fact exhibit the sudden jumps in temperature and the hysteresis described above. Whether the corresponding behavior is to be expected in the case of convective heating with surface radical recombination for engineering materials and wall temperature ranges of interest can, in principle, be analytically determined by integration of the boundary layer equations subject to the appropriate hydrodynamic, thermal and chemical kinetic boundary conditions. For this purpose one must have access to catalytic data over the range of wall temperatures below the melting point.

References

1 Lees, L., "Laminar Heat Transfer over Blunt-Nosed Bodies at Hypersonic Flight Speeds," Jet Propulsion," vol. 26, April 1956, pp. 259–269.

2 Fay, J. A., and Riddell, F. R., "Theory of Stagnation Point Heat Transfer in Dissociated Air," *Journal of the Aeronautical Sciences*, vol. 25, Feb. 1958, p. 73.

3 Goulard, R., "On Catalytic Recombination Rates in Hypersonic Stagnation Heat Transfer," ARS Preprint 544-57, 1957.

4 Buben, N., and Schechter, A., "Chemische Reaktionen in Elektrischen Entladungen. IV. Rekombination von Stickstoffatomen an Metallen," *ACTA Physicochimica*, U.R.S.S., vol. X, no. 3, 1939, p. 371.

5 Frank-Kamenetskii, D. A., "Diffusion and Heat Exchange in Chemical Kinetics," translated from the Russian edition by N. Thon, Princeton University Press, 1955, Ch. IX, pp. 285 ff.

6 Buben, N., "Sbornik rabot po fizicheskoi Khimii" (Collected Works on Physical Chemistry), Supplementary volume to *Zhur. Fiz. Khim.*, 1946; 1947, pp. 148, 154.

Combined Effects of Unsteady Flight Velocity and Surface Temperature on Heat Transfer

E. M. SPARROW[1]

NACA, Lewis Flight Propulsion Lab., Cleveland, Ohio

Introduction

It is frequently desired to compute the heat transfer to a vehicle whose flight velocity and surface temperature are both changing with time. A considerable simplification is introduced into the problem by supposing that quasi-steady conditions exist. Under this assumption, the heat transfer is found by instantaneous application of steady-state relationships. In reality, however, there will always be some difference between the actual instantaneous heat transfer and the quasi-steady value. The extent of this deviation depends upon the response characteristics of the boundary layer as well as on the rapidity of the changes in flight velocity and surface temperature.

The aim of the note is to find the first and second order deviations of the instantaneous heat transfer from the quasi-steady value. A particular utility of the results is that they provide a simple quantitative means for determining whether a given set of flight velocity and surface temperature data leads to essentially quasi-steady heat transfer.

The system chosen for analysis is a semi-infinite flat plate pictured schematically in Fig. 1.

The surface temperature and the free stream velocity are

Received Feb. 13, 1958.

[1] Research Scientist.

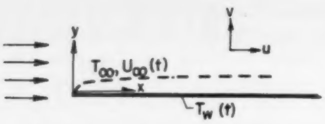

Fig. 1 Semi-infinite flat plate

permitted to take on arbitrary, but differentiable, variations with time. Spatial uniformity is assumed for the surface temperature. The flow is taken to be laminar, and viscous dissipation and variable fluid properties are included. Those who are primarily interested in results are invited to pass over the analysis section to Equation [9a].

Readers interested in nonquasi-steady boundary layers are referred to the work of Moore (1)[2] and Ostrach (2), who considered the effects of unsteady flight velocity alone; and to Sparrow and Gregg (3), who investigated the effects due to unsteady surface temperature alone.

Analysis

We begin by writing the equations expressing conservation of mass, momentum and energy for unsteady laminar boundary layer flow over a flat plate

$$\frac{\partial}{\partial x}(\rho u) + \frac{\partial}{\partial y}(\rho v) + \frac{\partial \rho}{\partial t} = 0 \ldots\ldots\ldots\ldots [1]$$

$$\rho\left[\frac{\partial u}{\partial t} + u\frac{\partial u}{\partial x} + v\frac{\partial u}{\partial y}\right] = \rho\frac{dU_\infty}{dt} + \frac{\partial}{\partial y}\left(\mu\frac{\partial u}{\partial y}\right) \ldots [2]$$

$$\rho c_p\left[\frac{\partial T}{\partial t} + u\frac{\partial T}{\partial x} + v\frac{\partial T}{\partial y}\right] = \frac{\partial}{\partial y}\left(k\frac{\partial T}{\partial y}\right) + \mu\left(\frac{\partial u}{\partial y}\right)^2 \ldots\ldots [3]$$

Time is denoted by t and the static temperature by T.

The conservation of mass equation is satisfied by a stream function ψ defined by (1)

$$u = \frac{\rho_\infty}{\rho}\frac{\partial \psi}{\partial y}, \qquad v = -\frac{\rho_\infty}{\rho}\left[\frac{\partial \psi}{\partial x} + \frac{\partial}{\partial t}\int_0^y \frac{\rho}{\rho_\infty}\,dy\right] \ldots\ldots [1a]$$

Then, by replacing u and v in favor of ψ and introducing the following new variables

$$\theta = \frac{T - T_\infty}{T_w - T_\infty}, \qquad X = x, \qquad Y = \int_0^y \left(\frac{\rho}{\rho_\infty}\right) dy, \qquad \tau = t \ldots [4]$$

we may rephrase Equations [2, 3] as

$$\psi_{Y\tau} + \psi_Y\psi_{XY} - \psi_X\psi_{YY} = \dot{U}_\infty + \nu_\infty\psi_{YYY} \ldots\ldots [2a]$$

$$\theta_\tau + \theta\frac{\dot{T}_w}{T_w - T_\infty} + \psi_Y\theta_X - \psi_X\theta_Y = \frac{\nu_\infty}{Pr}\left[\theta_{YY} + \frac{\mu_\infty/k_\infty}{T_w - T_\infty}(\psi_{YY})^2\right] \ldots [3a]$$

Derivatives with respect to X, Y, and τ are denoted by subscripts, while $\dot{T}_w$ and $\dot{U}_\infty$, respectively, represent the time derivatives of the surface temperature and the free stream velocity. The free stream temperature T_∞ is taken to be constant.

As has already been noted, our goal is to investigate the deviations of the actual instantaneous heat transfer from the quasi-steady value. With this in mind, it is natural to seek a solution for the temperature and velocity distributions in the form of series expansions about the quasi-steady state. A set of parameters ζ_n has been constructed in (1 and 2) to serve as a measure of the promptness with which the boundary layer responds to impressed variations of free stream velocity. A second group of parameters β_n is given in (3) to characterize the promptness of the response to changes in wall temperature. These same ζ_n and β_n will also serve as expansion parameters in a series solution of our present problem in which time-variations of both the flight velocity and surface temperature are permitted.

So, the stream function ψ and the dimensionless temperature θ are written in the form

$$\psi = \sqrt{\nu_\infty U_\infty X}\,[F(\eta) + \zeta_0 f_0(\eta) + \zeta_1 f_1(\eta) + \ldots] \ldots\ldots\ldots [5a]$$

$$\theta = \theta_0(\eta) + \beta_1\theta_1(\eta) + \beta_2\theta_2(\eta) + \ldots + \zeta_0 h_0(\eta) + \zeta_1 h_1(\eta) + \ldots + \frac{U_\infty^2}{2c_p(T_w - T_\infty)} \times [S(\eta) + \zeta_0 s_0(\eta) + \zeta_1 s_1(\eta) + \ldots] \ldots\ldots [5b]$$

where

$$\eta = \frac{Y}{2X}\sqrt{\frac{U_\infty X}{\nu_\infty}} \ldots\ldots\ldots\ldots\ldots\ldots [6a]$$

$$\zeta_0 = \frac{\dot{U}_\infty}{U_\infty}\left(\frac{X}{U_\infty}\right), \qquad \zeta_1 = \frac{\ddot{U}_\infty}{U_\infty}\left(\frac{X}{U_\infty}\right)^2, \ldots \qquad \ldots [6b]$$

$$\beta_1 = \frac{\dot{T}_w}{T_w - T_\infty}\left(\frac{X}{U_\infty}\right), \qquad \beta_2 = \frac{\ddot{T}_w}{T_w - T_\infty}\left(\frac{X}{U_\infty}\right)^2, \ldots \qquad \ldots [6c]$$

The variable η is immediately recognized as the Blasius similarity variable, while F, θ_0, and S are associated with the quasi-steady velocity and temperature distributions. When the ζ_n and β_n are very small (corresponding to prompt response to impressed changes), the state is essentially quasi-steady.

The series expansions are substituted back into Equations [2a, 3a], and after terms are grouped in the usual way, there results a set of ordinary differential equations for F, f_0, f_1, θ_0, ..., s_1. These differential equations will be omitted here because of space limitations; but they may be found, along with appropriate boundary conditions, in References (2 and 3) as Equations [24–29] and [6–10], respectively. Numerical solutions presently exist for $Pr = 0.72$ and these will be utilized in the heat transfer calculation which follows.

Heat Transfer Results

The instantaneous local heat flux rate at the plate surface, q_{inst}, may be calculated by applying Fourier's law: $q = -[k\partial T/\partial y]_{y=0}$. By introducing the series expansion of Equation [5b] and taking account of the transformed variables of Equations [4, 6a], the expression for q becomes

$$q_{inst} = -\frac{k_\infty}{2}\sqrt{\frac{U_\infty}{\nu_\infty x}}(T_w - T_\infty)\Big\{\theta_0'(0) + \beta_1\theta_1'(0) + \beta_2\theta_2'(0) + \ldots + \zeta_0 h_0'(0) + \zeta_1 h_1'(0) + \ldots + \frac{U_\infty^2}{2c_p(T_w - T_\infty)} \times [S'(0) + \zeta_0 s_0'(0) + \zeta_1 s_1'(0) + \ldots]\Big\} \ldots [7]$$

where $\theta_0'(0)$, ..., $s_1'(0)$ are abbreviations for $[d\theta_0/d\eta]_{\eta=0}$, ... $[ds_1/d\eta]_{\eta=0}$.

The quasi-steady heat transfer, q_{qs}, is given by

$$q_{qs} = -\frac{k_\infty}{2}\sqrt{\frac{U_\infty}{\nu_\infty x}}(T_w - T_\infty) \times \left[\theta_0'(0) + \frac{U_\infty^2}{2c_p(T_w - T_\infty)}S'(0)\right] \ldots [8]$$

The important relationship between the instantaneous and the quasi-steady heat transfer is then found by combining

[2] Numbers in parentheses indicate References at end of paper.

Equations [7 and 8]. After eliminating ζ_n and β_n in favor of physical quantities, we get

$$\frac{q_{inst}}{q_{qs}} = 1 + \frac{x}{U_\infty}\left\{\frac{\dot{T}_w}{T_w - T_{aw,\,qs}}\left(\frac{\theta_1'(0)}{\theta_0'(0)}\right) + \frac{\ddot{T}_w}{T_w - T_{aw,\,qs}} \times \left(\frac{x}{U_\infty}\right)\left(\frac{\theta_2'(0)}{\theta_0'(0)}\right) + \ldots + \frac{\dot{U}_\infty}{U_\infty}\left[\frac{T_w - T_\infty}{T_w - T_{aw,\,qs}}\left(\frac{h_0'(0)}{\theta_0'(0)}\right) + \frac{T_\infty - T_{aw,\,qs}}{T_w - T_{aw,\,qs}}\left(\frac{s_0'(0)}{S'(0)}\right)\right] + \left(\frac{\ddot{U}_\infty}{U_\infty}\right)\left(\frac{x}{U_\infty}\right) \times \left[\frac{T_w - T_\infty}{T_w - T_{aw,\,qs}}\left(\frac{h_1'(0)}{\theta_0'(0)}\right) + \frac{T_\infty - T_{aw,\,qs}}{T_w - T_{aw,\,qs}}\left(\frac{s_1'(0)}{S'(0)}\right)\right]\right\} \ldots [9]$$

where $T_{aw,\,qs}$, the quasi-steady adiabatic wall temperature, is given by

$$T_{aw,\,qs} = T_\infty - \frac{U_\infty^2}{2c_p}\left(\frac{S'(0)}{\theta_0'(0)}\right)$$

Using the following numerical results for $Pr = 0.72$ from References (2 and 3):

$\theta_0'(0) = -0.5913$, $\theta_1'(0) = -1.416$, $\theta_2'(0) = 0.4739$, $h_0'(0) = 0.04093$, $h_1'(0) = 0.2502$, $S'(0) = 0.5013$, $s_0'(0) = 0.02248$, $s_1'(0) = -0.2754$

there is obtained

$$\frac{q_{inst}}{q_{qs}} = 1 + \frac{x}{U_\infty}\left\{2.39\,\frac{\dot{T}_w}{T_w - T_{aw,\,qs}} - 0.801\,\frac{\ddot{T}_w}{T_w - T_{aw,\,qs}} \times \left(\frac{x}{U_\infty}\right) + \ldots - \frac{\dot{U}_\infty}{U_\infty}\left[0.0692\,\frac{T_w - T_\infty}{T_w - T_{aw,\,qs}} - 0.0448\,\frac{T_\infty - T_{aw,\,qs}}{T_w - T_{aw,\,qs}}\right] - \frac{\ddot{U}_\infty}{U_\infty}\left(\frac{x}{U_\infty}\right) \times \left[0.423\,\frac{T_w - T_\infty}{T_w - T_{aw,\,qs}} + 0.549\,\frac{T_\infty - T_{aw,\,qs}}{T_w - T_{aw,\,qs}}\right]\right\} \ldots [9a]$$

where $T_{aw,\,qs} = T_\infty + 0.848(U_\infty^2/2c_p)$.

From the series nature of the solution, it is expected that Equation [9a] would be most accurate for small deviations of q_{inst}/q_{qs} from unity. This suggests that Equation [9a] can serve as an accurate and rapid means for checking whether a given situation may be treated as quasi-steady. When the free stream velocity and surface temperature data of a given situation lead to $q_{inst}/q_{qs} \approx 1$, then that situation can be taken as quasi-steady for heat transfer purposes. It appears evident from Equation [9a] that in high speed flight, the very small values of x/U_∞ will almost always assure quasi-steady heat transfer.

Since the response of a turbulent flow is expected to be more rapid than that of a laminar flow, the results given here may also serve to provide an upper bound for the deviations from turbulent quasi-steady heat transfer.

References

1 Moore, Franklin K., "Unsteady Laminar Boundary Layer Flow," NACA TN 2471, Sept. 1951.

2 Ostrach, Simon, "Compressible Laminar Boundary Layer and Heat Transfer for Unsteady Motions of a Flat Plate," NACA TN 3569, Nov. 1955.

3 Sparrow, E. M., and Gregg, J. L., "Nonsteady Surface Temperature Effects on Forced Convection Heat Transfer," *Journal of the Aeronautical Sciences*, vol. 24, 1957, p. 776.

Optimum Variation of Exhaust Velocity During Burning

R. H. OLDS[1]

Naval Ordnance Test Station, China Lake, Calif.

In the case of a vertically launched rocket with a fixed initial amount of propellant energy the optimum distribution of energy with respect to the propellant results in an exhaust velocity that increases during burning in accordance with the formula, $c = c_0 + v + gt$.

Nomenclature

c = exhaust velocity relative to rocket
c_0 = initial exhaust velocity
E = total energy available for propulsion
g = gravitational acceleration
m = mass of rocket
m_b = mass of rocket at end of burning
m_0 = initial mass of rocket
m_p = initial mass of propellant
$\dot{m}$ = mass rate of discharge of propellant
t = time
t_b = burning time
v = rocket velocity
v_b = burnt velocity of rocket
Φ = a function
λ = a constant

IMPROVEMENT in the burnt velocity of a rocket with a fixed initial amount of propellant energy was shown by Seifert[2] to result from a scheduled increase in the exhaust velocity of the propellant gases during burning. The schedule he chose to investigate consisted in steadily increasing the exhaust velocity during burning by exactly the amount of the rocket velocity, i.e., $c = c_0 + v$. The analysis given here shows that if air drag can be neglected the schedule chosen by Seifert is nearly optimum for a vertically launched rocket.

Neglecting air drag, the following equation describes the motion of a vertically launched rocket

$$m\frac{dv}{dt} = -c\frac{dm}{dt} - mg \ldots\ldots\ldots\ldots [1]$$

in which

$$m = m_0 - \dot{m}t$$

Let the propellant mass discharge rate be constant so that

$$\frac{dm}{dt} = -\dot{m} = \text{const}$$

Then we have

$$v_b = \int_0^{t_b}\left(\frac{\dot{m}c}{m_0 - \dot{m}t} - g\right)dt \ldots\ldots\ldots\ldots [2]$$

The total energy available for propulsion is given by

$$E = \int_0^{t_b} \tfrac{1}{2}\,\dot{m}c^2 dt \ldots\ldots\ldots\ldots [3]$$

We wish to find the function $c(t)$ that yields a maximum

Received March 4, 1958.

[1] Head, Physics Division. Mem. ARS.
[2] Seifert, H. S., "The Performance of a Rocket with Tapered Exhaust Velocity," JET PROPULSION, vol. 27, 1957, pp. 1264–1266.

value for v_b while satisfying the restriction imposed by assigning a value to E. This is a familiar problem in the calculus of variations and is readily solved by applying Euler's equation to the following function composed of the integrands from Equations [2, 3]

$$\phi \equiv \frac{\dot{m}c}{m_0 - \dot{m}t} - g + \frac{\lambda}{2}\dot{m}c^2 \qquad [4]$$

Euler's equation states

$$\frac{\partial \phi}{\partial c} - \frac{d}{dt}\frac{\partial \phi}{\partial \dot{c}} = 0 \qquad [5]$$

in which $\dot{c}$ represents dc/dt. Since $\dot{c}$ does not explicitly appear in ϕ, we have

$$\frac{\partial \phi}{\partial c} = \frac{\dot{m}}{m_0 - \dot{m}t} + \lambda \dot{m}c = 0$$

$$c = -\frac{1}{\lambda(m_0 - \dot{m}t)} \qquad [6]$$

That is, the exhaust velocity varies inversely with the mass of the rocket during burning. Substitution of this expression for c into Equation [3] permits the evaluation of λ as

$$E = \int_0^{t_b} \frac{\dot{m}dt}{2\lambda^2(m_0 - \dot{m}t)^2} = \frac{m_p}{2\lambda^2 m_0 m_b}$$

$$\lambda = \pm\sqrt{\frac{m_p}{2Em_0m_b}} \qquad [7]$$

Therefore

$$c = \frac{1}{m_0 - \dot{m}t}\sqrt{\frac{2Em_0m_b}{m_p}} \qquad [8]$$

The velocity of the rocket may now be determined.

$$v = \int_0^t \left(\frac{\dot{m}c}{m_0 - \dot{m}t} - g\right) dt$$

$$v = \int_0^t \left[\frac{\dot{m}\sqrt{2Em_0m_b/m_p}}{(m_0 - \dot{m}t)^2} - g\right] dt$$

$$v = \left(\frac{1}{m_0 - \dot{m}t} - \frac{1}{m_0}\right)\sqrt{\frac{2Em_0m_b}{m_p}} - \int_0^t g dt \qquad [9]$$

If the variation of gravity with altitude can be neglected, we have

$$c = c_0 + v + gt \qquad [10]$$

Thus we see that the schedule of exhaust velocity chosen by Seifert differs from the optimum schedule by an additive term gt which is small compared to v in most instances.

It is interesting to note that the following relationship from Seifert's paper

$$\frac{v_b'}{v_b} = \frac{(R-1)R^{-0.5} - \gamma_b}{\ln R - \gamma_b} \qquad [11]$$

which he derives as an approximation, becomes an exact equality in the case of the optimum variation of exhaust velocity during burning.

Direct Digital Read-Out of Missile Role From Film Records

O. J. W. CHRIST,[1] and B. B. SMALL,[2]

Patrick Air Force Base, Fla.

Received Feb. 5, 1958.

[1] Planning Engineer, Range Engineering Section, Missile Test Project, RCA Service Co.

[2] Major, Jupiter Project Officer, Army Ballistic Missile Agency. Mem. ARS.

Introduction

A METHOD for the direct read-out of missile roll information in digital form from film records of ballistic missiles is presented. The procedure applies an extension of the encoder techniques used to measure mechanical shaft positions. The method eliminates the necessity for linear measurements and computation of missile roll angles as is the case when using the spiral band paint pattern currently in wide use. The method described, however, does not prevent the possibility of precision machine measurement techniques, if desired.

The digital pattern proposed consists of a number of parallel bands, each interrupted into segments according to a binary scheme. Read-out of roll information is accomplished by counting the digital sum indicated along some reference line, normally the center line on the cylindrical surface. The pattern has the advantages of being unaffected by missile aspect angle and foreshortening due to perspective. It also has the advantage of being only gradually affected by a loss of resolution due to distance from the recording camera, in that when the finest digital band is lost the next less precise band will still be distinguishable, and so forth.

The proposed scheme has the additional feature of providing roll rates without measurements. Read-out of two successive time-correlated roll positions will allow ready computation of rotational rate information for spin-stabilized bodies.

Methods for Determining Roll

The most precise and accurate method for obtaining missile roll information over a considerable flight interval is by means of roll gyros or integrating accelerometers within the missile. Telemetered roll data from these can be obtained to an accuracy of $\frac{1}{4}$ deg very easily and much better accuracies can be obtained with precision gyros. Internal measurements require playback of telemetered signals onto oscillograph or

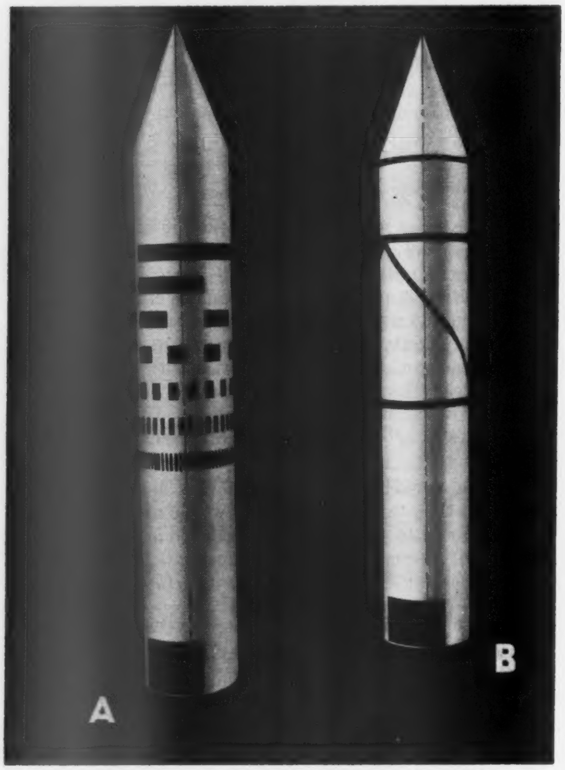

Fig. 1 Model A shows digital painting scheme compared to the commonly used spiral band scheme on model B

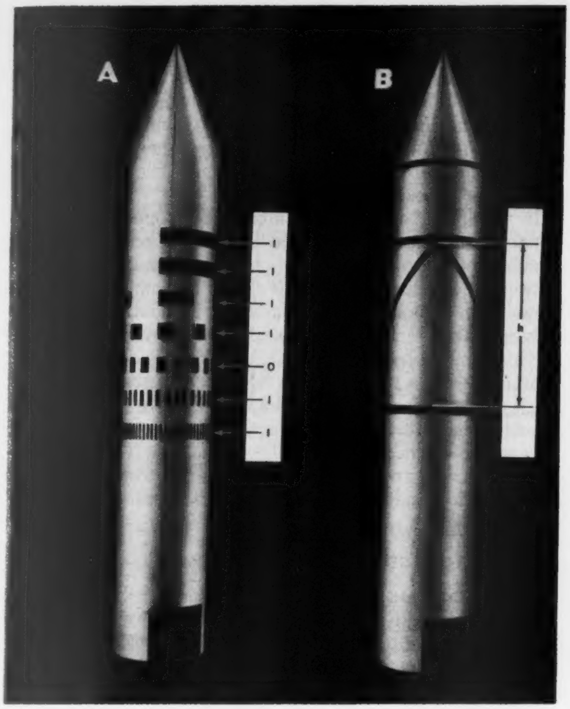

Fig. 2 Method of read-out for digital pattern, model A, and spiral pattern, model B, are compared for approximately identical attitudes

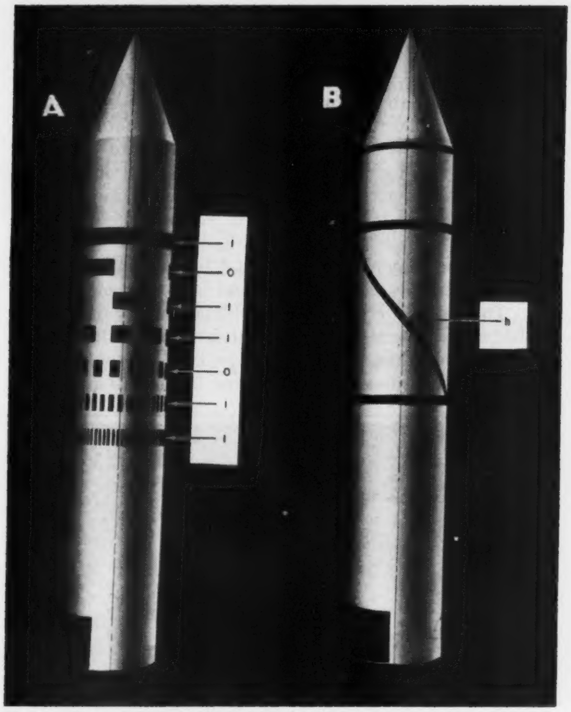

Fig. 3 Comparison of digital and spiral patterns for an approximate 90 deg counterclockwise roll from Fig. 2

other visual records. This is expensive, and requires extensive missile-borne and ground equipment. Internal measurements are subject to the errors of all telemetered measurements contributed by the pickup, the telemetering link itself and the data playback processes. For many reasons internal roll information may be difficult to obtain. External determinations are by far the more reliable and are convenient for quick-look and backup for the internal data. Where high precision is not required and where information is needed for the early periods of flight only, photography provides the simplest and least expensive solution to roll measurement.

Painting Schemes for Photographic Determination of Roll

All photographic systems for determining roll are based upon the appearance of the missile image on the film. To readily detect differences in successive appearances of the missile image, a sharply contrasting paint pattern is applied to the exterior of the missile. Normally the pattern is of a black on white color. The pattern is designed to provide reference marks for determinations. From the changes in appearance of the paint pattern through successive camera views, the pitch, roll and yaw attitudes of the missile can also be determined. The pattern, thus, provides a basis for qualitative data on nonmetric films.

The missile paint schemes may be alternating bands of black and white, checker-board type rectangular bands or patterns composed of several horizontal bands combined with spiral band forms. Whatever the scheme it merely provides sharp boundaries and points of known position and orientation on the missile for measurement reference. Roll information is normally derived by measuring the apparent change in position of these paint pattern images from one film frame to

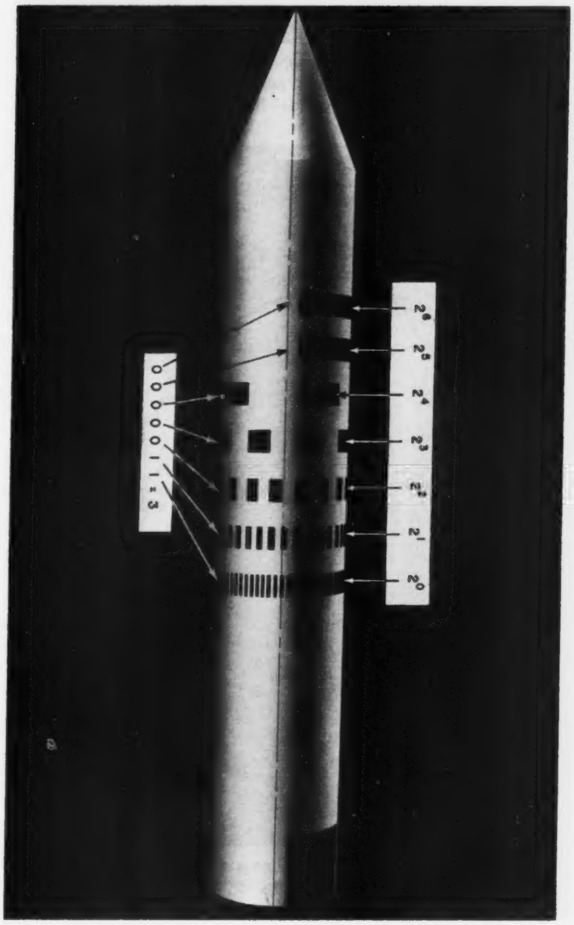

Fig. 4 Digital paint scheme; numbers at the right indicate binary digital values for each band; numbers at the left indicate binary value and decimal equivalent for the attitude shown as read-out on center line reference

another and computing by some geometric or trigonometric relationship the amount of roll necessary to cause such apparent changes. This method can yield reliable roll data to 1 to 2 deg up to several thousand ft distance and by correcting for missile position can perhaps produce roll data to an accuracy of $\frac{1}{2}$ deg up to 400 ft. If raw readings are made using comparators and if the camera geometry is adequate, pitch and yaw can be read to 1 deg under optimum conditions. In special situations for extremely short flight periods, more precise data are possible but the effort to achieve these may be extreme.

The most common painting scheme for vertically launched cylindrical missiles is the spiral band pattern shown in Fig. 1B. This pattern consists of two horizontal bands of black applied some convenient and accurately known distance apart on the missile skin. Between these two horizontal bands are painted two diagonally encircling bands of black which

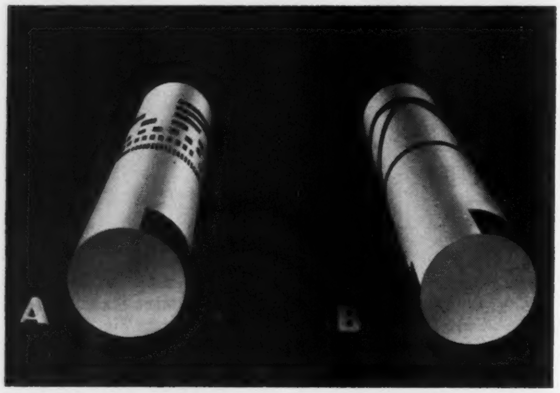

Fig. 5 Models A and B are shown under conditions of poor aspect angle; note distortions due to perspective as affecting model B

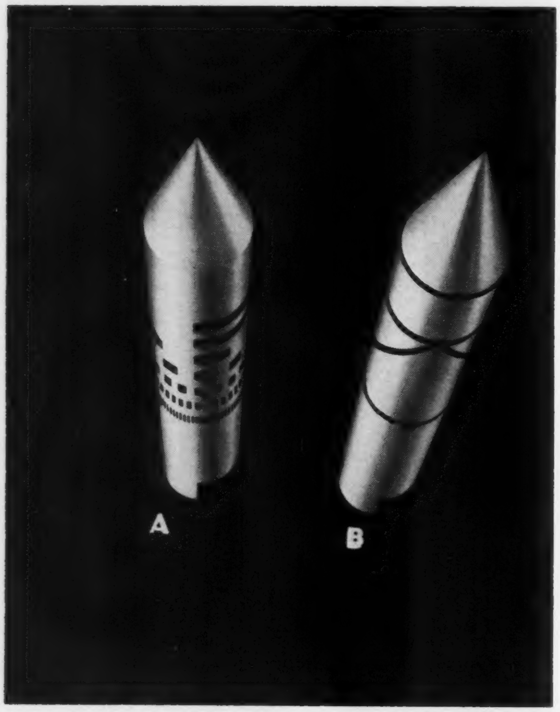

Fig. 6 Models A and B are shown under conditions of even poorer aspect angle than in Fig. 5; the rapid deterioration of model B data can be seen

begin at an accurately known point on the missile and descend around the missile to terminate together on the lower band at another accurately known point 180 deg opposite. The origin and terminal points correspond to some orientation of the missile, normally identified by coinciding with one or other of the missile fins. Most ballistic missiles fly in a stabilized attitude with one fin (or hypothetical fin if the missile is finless) pointed in the direction of the target at liftoff or after take-off stabilization.

In the spiral band pattern, missile roll is indicated by the apparent distance to the spiral band from one of the two circular reference bands. The change in apparent distance between the bands due to roll is shown by comparison of the views of the missile in Figs. 2 and 3. Evaluation of roll involves a measurement using a scale or a microscopic or magnifying film reader. The missile roll angle is determined by computation of a trigonometric relationship involving the roll angle and the apparent change in distance from the horizontal bands to the vertical intercept on the spiral band as compared to a previous film frame (see Figs. 2 and 3). This computation takes time and is subject to errors due to the distortion of the spiral band from perspective and missile-camera relationships.

Digital Painting Scheme

The spiral band pattern can be replaced with the digital pattern shown in Fig. 1A. This pattern is a format of parallel circular bands of increasing digital significance corresponding to a binary sequence. The value of each band segment is a power of the binary base 2 as indicated in Fig. 4. Each of the bands is 6–8 in. wide on large missiles. Each band is successively divided into twice as many segments as the preceding. The first significant band divides the missile circumference into two 180 deg segments; the second band begins exactly below the half segment and divides the circumference into quadrants; the third band is aligned with the two preceding and it divides the circumference into eight 45 deg segments. Succeeding bands divide the missile into sixteenths, thirty-seconds, sixty-fourths, and so on, if desired.

The result of such a scheme is that if the missile turns in aspect as seen on a film record, a center line drawn on its cylindrical surface will intercept different segments of the digital code. The sum of the presences of digital segments along this center line will add up to a certain value representing the aspect of the missile with respect to the camera taking that particular picture (see Fig. 2). The difference between two successive sums will be the amount of roll. Figs. 2 and 3 show the change in appearance of both the binary scheme and the spiral band patterns with an apparent roll of approximately 90 deg. Fig. 2A has a binary count of 1111011 which is equivalent to 123 decimal counts and Fig. 3A has a binary reading of 1011011 which is equivalent to a decimal count of 91. Roll displacement from Figs. 2A to 3A is indicated by the count difference of $1111011 - 1011011 = 0100000$ or a decimal count difference of 32. This represents a roll of 32×2.8 deg or 89.6 deg. Figs. 2B and 3B show a corresponding roll for a spiral band pattern.

The digital painting scheme is more complex than others and requires some pains in application. It is unique in the respect that it would enable a rapid computation of roll within the accuracy of the 2.8 deg least bit value.

The simpler painting schemes such as rectangles of alternating black and white or other contrasting colors normally use a tail marking in conjunction with the tip of the nose cone for the establishment of a reference origin for the reading of roll values. This means that it is necessary to see one of the tail segments to identify the quadrant and also to see the nose to establish the surface center line. The spiral band pattern is not similarly ambiguous as to orientation but suffers greatly from distortions of perspective and resolution difficulties (see Figs. 5 and 6).

In the digital pattern when the lowest or finest band is lost

through failure to be resolved on the film, the reader merely loses one order of precision and jumps to the next digital band where resolution is still possible. This continues in a series of steps until the roll can be read to half a turn only. This provides a progressive step-like data dilution rather than an abrupt and discrete inability to read any data beyond a certain point.

In using the digital design, like any other, it should be above any body region affected by cryogenic frosting or other changes due to fueling or launching. The scheme is, of course, not applicable to any missile of noncircular cross section. A cylinder of oval shape cannot use such a binary pattern.

Determination of Spin Rates

The digital scheme has a further application in that it can be used to determine rotational speeds of spinning bodies. Readings from one film frame to another, the times of both being known, can reveal rps or rpm directly. This feature may be useful where telemetering space is not available or where economy may prevent sophisticated telemetering.

Technical Comments

Comments on 'An Approximate Specific Impulse Equation for Condensable Gas Mixtures'

D. J. ZIGRANG[1]

North American Aviation, Inc., Downey, Calif.

In a recent note Wilde[2] derived the expression

$$I_{sp} = \frac{1}{g}\left\{\frac{2}{\bar{M}}\left[\bar{C}_p T_c\left(1 - \left(\frac{P_e}{P_c}\right)^{R(1-y_{lc})/\bar{C}_p} \times \exp\left(\frac{y_{gc}\Delta H_v}{\bar{C}_p T_{be}} + \frac{y\Delta H_f}{\bar{C}_p T_f} - \frac{R}{\bar{C}_p}(1 - y_{gc})\ln(1 - y_{gc})\right)\right) + y_{gc}\Delta H_v + y\Delta H_f\right]\right\}^{1/2}$$

for the impulse of a rocket system containing a condensable component partially condensed at the nozzle entrance and completely condensed and solidified at the nozzle exit. From this expression, it is apparent that the isentropic expansion must have been evaluated[2] as

$$T_e = T_c\left(\frac{P_e}{P_c}\right)^{R(1-y_{lc})/\bar{C}_p} \exp\left(\frac{y_{gc}\Delta H_v}{\bar{C}_p T_{be}} + \frac{y\Delta H_f}{\bar{C}_p T_f} - \frac{R}{\bar{C}_p}(1 - y_{gc})\ln(1 - y_{gc})\right) \quad [1]$$

where y_{lc} is the mole fraction of condensed component in the combustion chamber; $\bar{C}_p$, an over-all mean heat capacity; y_{gc}, the mole fraction of uncondensed vapor in the chamber; y, the mole fraction of condensable component; and "... T_{be}, the boiling point of the condensable species at P_e ...."[2] The expression is based on what appears to be an unnecessarily difficult and incorrectly evaluated isentropic path. In addition, the use of T_{be} indicates a probable error in concept since at that temperature and a pressure of P_e the condensable component has a vapor pressure of but $y_{gc}P_e/(1 - y_{lc})$ and *is not* at the point of incipient condensation.

The path chosen was "... an isothermal expansion to P_e followed by a constant pressure cooling at P_e, the exhaust pressure. ..."[2] This path may be evaluated as follows:

1. Expansion

$$\Delta S_1 = -(1 - y_{lc})R \ln \frac{P_e}{P_c} \quad [2]$$

2. Cooling to T_{be}

$$\left.\begin{aligned} \Delta S_2 &= (1 - y)\bar{C}_p \ln \frac{T_{be}}{T_c} + y_{lc}\bar{C}_{pl} \ln \frac{T_{be}}{T_c} + y_{gc}\bar{C}_{pg} \ln \frac{T_{be}}{T_c} \\ \Delta S_2 &= \bar{C}_p \ln \frac{T_{be}}{T_c} \end{aligned}\right\} \quad [3]$$

The first three terms of Equation [4] represent the entropy decrease resulting from the separation of the vapor at its partial pressure of $y_{gc}P_e/(1 - y_{lc})$ from the permanently gaseous phase at its partial pressure of $(1 - y)P_e/(1 - y_{lc})$ and the subsequent compression of each phase to a pressure of P_e.

3. Separation and condensation

$$\Delta S_3 = Ry_{gc} \ln y_{gc} + R(1 - y)\ln(1 - y) - R(1 - y_{lc})\ln(1 - y_{lc}) - y_{gc}\frac{\Delta H_v}{T_{be}} \quad [4]$$

4. Cooling to T_f

$$\Delta S_4 = \bar{C}_p \ln \frac{T_f}{T_{be}} \quad [5]$$

5. Fusion

$$\Delta S_5 = -y\frac{\Delta H_f}{T_f} \quad [6]$$

6. Cooling to T_e

$$\Delta S_6 = \bar{C}_p \ln \frac{T_e}{T_f} \quad [7]$$

For an isentropic expansion, the sum of the entropy changes is zero. With rearrangement, the sum becomes

$$0 = -(1 - y_{lc})R \ln \frac{P_e}{P_c} + \bar{C}_p \ln \frac{T_e}{T_c} + Ry_{gc} \ln y_{gc} + R(1 - y)\ln(1 - y) - R(1 - y_{lc})\ln(1 - y_{lc}) - y_{gc}\frac{\Delta H_v}{T_{be}} - y\frac{\Delta H_f}{T_f} \quad [8]$$

Received Aug. 9, 1957.

[1] Senior Research Engineer, Missile Development Division.

[2] Wilde, Kenneth A., "An Approximate Specific Impulse Equation for Condensable Gas Mixtures," Jet Propulsion, vol. 27, June 1957, p. 668.

And upon rearrangement of Equation [8]

$$T_e = T_c \left(\frac{P_e}{P_c}\right)^{R(1-y_{lc})/\bar{\bar{C}}_p} \exp\left(\frac{y_{gc}\Delta H_v}{\bar{\bar{C}}_p T_{be}} + \frac{y\Delta H_f}{\bar{\bar{C}}_p T_f} - \frac{R}{\bar{\bar{C}}_p}(1-y)\ln(1-y) - \frac{R}{\bar{\bar{C}}_p} y_{gc} \ln y_{gc} + \frac{R}{\bar{\bar{C}}_p}(1-y_{lc})\ln(1-y_{lc})\right) \quad [9]$$

A comparison between Equations [1, 9] reveals the absence of several terms in the exponential portion of Equation [1].

Since entropy is a state property, any convenient path may be chosen for its evaluation. It can be shown that the use of partial pressures will allow separate evaluation of expansion paths for the permanently gaseous portion and the condensable portion without consideration of the entropy of mixing. The permanently gaseous portion is expanded from $P_c - p_c$ to P_e and then cooled to T_e. For the condensable portion, condensation is completed at T_c and the liquid is cooled to T_f where it solidifies and is then cooled to T_e. The isentropic equation resulting from a summation of these paths is

$$0 = -(1-y)R \ln\left(\frac{P_e}{P_c - p_c}\right) + (1-y)\bar{C}_p \ln\frac{T_e}{T_c} - y_{gc}\frac{\Delta H_v}{T_c} + y\bar{C}_{pl}\ln\frac{T_f}{T_c} - y\frac{\Delta H_f}{T_f} + y\bar{C}_{ps}\ln\frac{T_e}{T_f} \quad [10]$$

where p is the saturation vapor pressure of the condensable component. Equation [10] can be rearranged

$$T_e = T_c\left(\frac{P_e}{P_c - p_c}\right)^{R(1-y)/\bar{C}_p} \exp\left(\frac{y_{gc}\Delta H_v}{\bar{C}_p T_c} + \frac{y\Delta H_f}{\bar{C}_p T_f}\right) \quad [11]$$

and the impulse expression becomes

$$I_{sp} = \frac{1}{g}\left\{\frac{2}{\bar{M}}\left[\bar{C}_p T_c\left(1 - \left(\frac{P_e}{P_c - p_c}\right)^{R(1-y)/\bar{C}_p} \times \exp\left(\frac{y_{gc}\Delta H_v}{\bar{C}_p T_c} + \frac{y\Delta H_f}{\bar{C}_p T_f}\right)\right) + y_{gc}\Delta H_v + y\Delta H_f\right]\right\}^{1/2} \quad [12]$$

From Wilde's discussion concerning the desirability of vaporization, it appears that an increase in the vaporized fraction of the condensable component is thermodynamically beneficial. However, it can be shown that for systems operating at a constant pressure level and fuel-oxidizer ratio, an increase in y_{gc} is accompanied by an increase in entropy and therefore a decrease in energy available from a given process. Furthermore, it can be shown that for constant fuel-oxidizer ratio and nozzle pressure ratio, increased vaporization would always exert an adverse effect on impulse according to the expression

$$\frac{\partial I_{sp}}{\partial y_{gc}} = \frac{-T_e}{\bar{M}g^2 I_{sp}}\left(\frac{R(1-y)}{1-y_{lc}} + \frac{y_{gc}\Delta H_v^2}{\bar{C}_p T_c^2}\right) \quad [13]$$

Complete condensation of a condensable component in the combustion chamber is then the more desirable situation.

New Patents

George F. McLaughlin, *Contributor*

Aircraft fuel pumping system (2,823,518). J. F. Murray, Macedonia, Ohio, assignor to Thompson Products, Inc.

Two-stage pump with an initial centrifugal stage in series with a positive displacement stage. A by-pass conduit from the main and after-burner controls minimizes fuel temperature rise in the system.

Distance measuring systems with compressed returned pulses (2,823,375). G. D. Camp, Chevy Chase, Md., assignor to Malpar, Inc.

Means for transmitting rectangular pulses of predetermined durations to a remote target and return to a receiver.

Antenna (2,823,381). J. F. P. Martin and L. H. Kellogg, Far Hills, N. J., assignors to the U. S. Army.

Turnstile antenna to be carried by a high velocity missile and for use at high frequency. Four half dipole radiator elements extend outwardly at 90 deg intervals from a center structure.

Moon projector apparatus (2,827,830). G. Vaux and G. L. Stitely, Elkton, Md.

Apparatus for simulating phases of a heavenly body. The image of one edge of a circular aperture is projected through a lens having barrel distortion and variable illumination.

Laminated internal finned air-cooled turbine blade (2,826,106). W. B. Schramm and R. R. Ziemer, North Olmstead, Ohio, assignors to U. S. Navy.

Blade consists of laminated interspaced spacers, channel-shaped primary fins and secondary fins extending beyond the spacers. Flanges of primary fins constitute part of the upper and lower chambers of the blade.

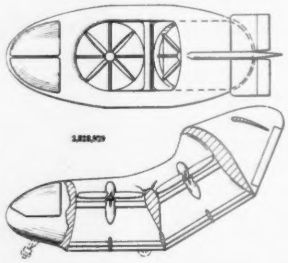

Wingless aircraft (2,828,929). A. M. Lippisch, Cedar Rapids, Iowa, assignor to Collins Radio Co.

Two ducted fans in a body having an upwardly extending rear part. Ducts are at an angle of 30 deg relative to each other, in the shape of an inverted V. Propulsion means are mounted in each duct, and aerodynamic controls mounted on the body control the attitude of the aircraft.

Multiflap variable nozzle (2,828,602). A. W. Gardiner, Indianapolis, Ind., assignor to General Motors Corp.

Overlapping flaps on brackets for rotation about the axis tangent to the duct circumference. Each flap comprises two spaced plates defining a passage for additional cooling air. The outlet of the passage is at the free end of the flaps so that air flow is induced by the gas stream flowing through the variable area nozzle.

Afterburner for turbojet engines (2,828,603). R. G. Laucher, Van Nuys, Calif., assignor to Westinghouse Electric Corp.

Movable means in the casing to vary the exhaust nozzle exit area. A screwjack selectively moves a plug between a position in the exhaust nozzle and a position adjacent to the diffuser cone flameholder step.

Rocket engine thrust control device (2,828,604). J. Hirsch and J. M. Pollard, Ventura, Calif.

Cover of ductile material having uniform holes over its surface, placed over the exhaust nozzle. As exhaust gas pressures increase, the cover is deformed to progressively cover a smaller portion of the nozzle, exposing a greater number of holes, until pressure blows the cover off the nozzle.

Method of generating combustion gases (2,828,605). G. Dobson, London, England, assignor to Power Jets (Research and Development) Ltd.

A small part of a low calorific value gaseous combustible mixture is ignited by the pilot flame, causing it to flow in a stream. Further parts of the mixture are added at progressively downstream points

Editors Note: Patents listed above were selected from the Official Gazette of the U.S. Patent Office. Printed copies of patents may be obtained from the Commissioner of Patents, Washington 25, D. C., at a cost of 25 cents each; design patents, 10 cents.

Kodak reports on:

the things some people want in front of a television camera tube . . . the answers an infrared photoresistor buyer is expected to know

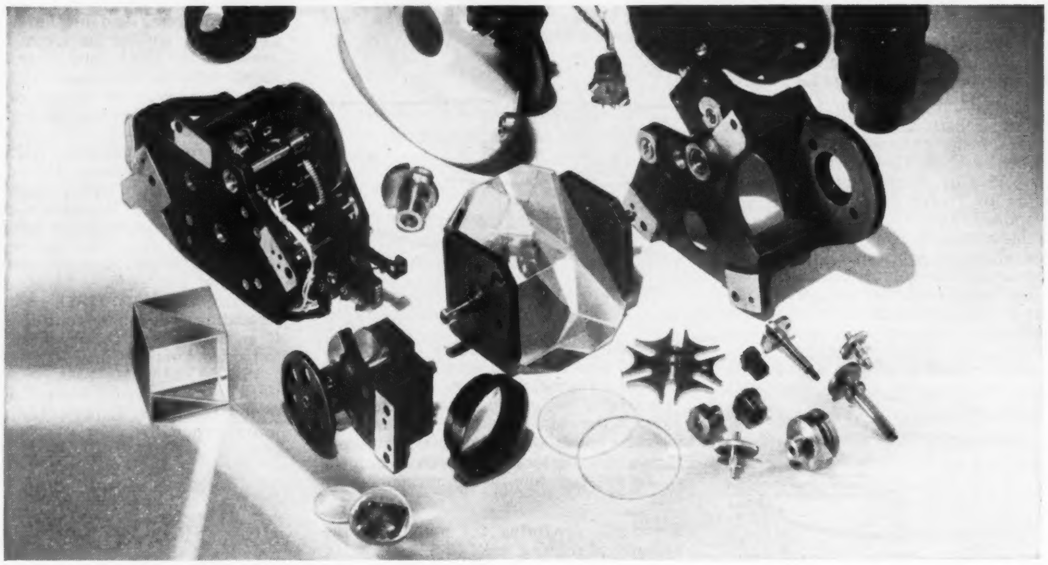

It will be interesting to see if this picture and the paragraph of type you are now reading succeed in their purpose (and it's a long, long shot) of eliciting even a single letter, wire, or phone call from a party seeking a strong and competent organization to take on the development, design, and/or construction of a complex optical-mechanical system for feeding some sort of image into a television camera tube. The quest for such a contact is suggested by the very satisfactory manner in which our work is progressing on two such projects, the first television bombsight and the first airborne television gunsight. In security-dictated disorder, the photograph suggests the kind of components we make and put together for these affairs. Nor are our talents along these lines newly acquired, even if Ed Sullivan* doesn't stress them on Sunday evenings when discussing our more popular mechanical and optical products. The letter, wire, or phone call goes to Eastman Kodak Company, Military and Special Products Division, Rochester 4, N. Y.

*The fact may little signify, but Ed and most of the other figures of live television reach the magic screen through *Kodak Television Ektanon Lenses* on the studio cameras.

Lead selenide in the open

Between the kind of technical news picked up at a meeting where clearances are checked at the door and the kind picked up from reading a technical ad in a magazine, there is a difference in newsiness. At the latter level we must content ourselves with trumpeting the news that chemically deposited lead selenide photoresistors can now be procured with no more than the normal yardage of red tape required in a commercial transaction.

The purchase order will read *Kodak Ektron Detector* (*Lead Selenide*), *Type R2*. The exact size of sensitive area (minimum dimension, 0.25mm) and its configuration (anything from a square to as intricate a multiple array as you can afford) will have been worked out in correspondence with Eastman Kodak Company, Military and Special Products Division, Rochester 4, N. Y. This is the freedom you get with a chemically deposited photoresistor.

Lead selenide, *Type R*, responds well out to 4.5μ at room temperature, with a time constant less than 10 microseconds.* Cooled with dry ice, it goes out to 5μ, but the time constant doubles or triples.

Of course, you don't want lead selenide at all unless you need the long wavelength response and the short time constant. To a 500°K source, for example, chopped at 90 cycles, you can get 35 times more response with lead sulfide, as in the *Kodak Ektron Detector*, *Type N*. Its time constant, though, is characteristically in the range of 500 to 1000 microseconds.

We have two other kinds of lead sulfide depositions besides *Type N*. In respect to 500°K, 90-cycle radiation, they lie between *Type N* and *Type R*. There is *Type O*, with around half the time constant of *Type N* and two-thirds its response. The other one is *Type P*, with a time constant near 100 microseconds and a 500°K response about one-quarter that of *Type N*. You can get beyond 3μ with it at room temperature, and beyond 4μ by cooling it. That was the best we could do for you on long wavelength response till they let us start selling lead selenide.

In the infrared business one doesn't dare quit racing one's engine.

*For the instruction of the young, that's how long it takes response to drop off to 1/e what it was before the radiation was turned off. e is the base of natural logarithms and is worth around 2.72.

This is another advertisement where Eastman Kodak Company probes at random for mutual interests and occasionally a little revenue from those whose work has something to do with science

Kodak
TRADEMARK

at which the preceding part has become burnt. Each added further part is ignited by the heat of the flame from combustion of the preceding part.

Dual engine supports (2,828,607). K. O. Johnson, Camby, Ind., assignor to General Motors Corp.

Units for supporting a pair of gas turbine engines side-by-side with freedom for movement axially and freedom for relative movement radially.

Improved construction of combustion chamber of the cyclone or vortex type (2,828,608). C. J. Cowlin, D. R. Bettison and M. Cox, Farnborough, England, assignors to Power Jets (Research and Development) Ltd.

An outer casing enclosing the combustion chamber, with space for flow of cooling air over the volute chamber. Cool air is discharged from the casing with combustion products from the volute chamber. Mounting and supporting means permit thermal expansion and contraction of the combustion chamber relative to the outer casing.

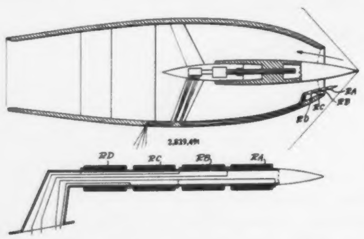

Automatic control means for varying the geometry of the air inlet of a jet engine (2,829,490). A. O. Kresse, Cleveland, Ohio, assignor to Thompson Products, Inc.

Sensing device comprising a strain gage for constantly determining the position of the shock wave set up in an air inlet during operation at Mach 1 velocity. Change in position of the wave, caused by change in average pressure on one of the gage windings, electrically unbalances a bridge circuit and modifies a means for adjusting the shock wave position.

Aircraft design (182,524). F. W. Kux, Northridge, Calif., assignor to Bell Aircraft Corp.

Twin jet airplane with high aspect ratio wing with squared tips, the leading edge swept back about 18 deg. Engine pods project forward under the wing which has a downward dihedral.

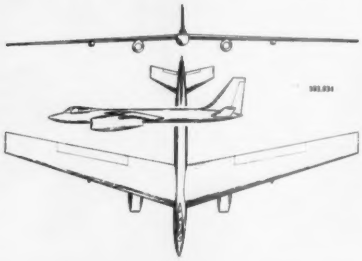

Emergency exhalation valve (2,828,740). Bob A. Kindred, Duarte, Calif., assignor to Sierra Engineering Co.

A release button connected to the vent valve in the closed breathing system of an aircraft pilot's oro-nasal pressure receptacle. The button connects to a compensating pressure line in the oxygen supply line.

Electronic apparatus for stabilizing the attitude of moving craft (2,828,930). R. J. Herbold, Denver, Colo., assignor to Lafayette M. Hughes.

Photosensitive elements in which the electrical output varies in accordance with light activation. When the craft is tilted, a motor moves controls in opposite directions as determined by an unbalanced activation of one element relative to the other caused by variation in the ratio of sky light to earth light.

Cooled turbine blade (2,828,940). P. P. Newcomb, Manchester, Conn., assignor to United Aircraft Corp.

An air passage extending transversely of the rotor disk between the base of the slot and the base surface of the spar root portion. Radial passages in the spar surface extend from the base surface for the flow of air from the passage.

Combustion chambers including suddenly enlarged chamber portions (2,828,609). I. B. Ogilvie, Bristol, England, assignor to Bristol Aero-Engines Ltd.

First and second duct portions enclosing a passage. A ring extends radially from the downstream end of the second duct to form a sudden enlargement of the passage. A third duct extends downstream from the fuel supply chamber, and a flame deflector is spaced downstream part way across the passage.

Blade damping means (2,828,941). J. R. Foley, Manchester, Conn., assignor to United Aircraft Corp.

V-shaped slot in the rotor blade forming a tab. Dimensions of the tab and blade structure are such that the natural frequency of vibration of the tab is equal to that of the blade.

Repeating cycle igniter control (2,829,489). R. E. Meyer, Glastonbury, Conn., assignor to United Aircraft Corp.

Pistons responsive to the fuel supplied to the afterburner for controlling a second piston means to displace additional fuel into the engine.

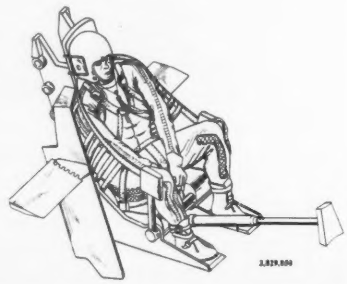

Aircraft ejection seat (2,829,850). I. H. Culver, Burbank, Calif., assignor to Lockheed Aircraft Corp.

Means for modifying airflow patterns to reduce decelerative g loads and airblast on the pilot. An extension rod on the seat carries a skip-flow generator to intercept the oncoming air flow upon ejection from the aircraft.

Technical Literature Digest

M. H. Smith, *Associate Editor,* and **M. H. Fisher,** *Contributor*
The James Forrestal Research Center, Princeton University

Jet and Rocket Propulsion Engines

A New Concept in the Design of Jet Engine Mufflers and Test Cells, by E. J. Richards and D. J. Evans, *J. Roy. Aeron. Soc.*, vol. 61, Sept. 1957, pp. 619–630.

Large Turbojet Engines Will Beat out Small Ones for Large Aircraft, by C. A. Grinyer, *SAE J.* vol. 65, Sept. 1957, pp. 25–26.

Some Effects of Inlet Pressure and Temperature Transients on Turbojet Engines, by D. Gabriel, L. Wallner, R. Lubick, and G. Vasu, *Aeron. Engng. Rev.*, vol. 16, Sept. 1957, pp. 54–59, 68.

Editor's Note: Contributions from E. R. G. Eckert, J. P. Harnett, T. F. Irvine Jr. and P. J. Schneider of the Heat Transfer Laboratory, University of Minnesota, are gratefully acknowledged.

NACA 65-Series Compressor Rotor Performance with Varying Annulus-Area Ratio, Solidity, Blade Angle, and Reynolds Number and Comparison with Cascade Results, by Wallace M. Schulze, John R. Ersin and George C. Ashby Jr., *NACA TN* 4130, Oct. 1957, 62 pp. (supersedes RM L52L17).

The Application of Digital Computers to Jet Engine Design, by D. W. Peterson, *SAE Prepr.* 191, Oct. 1957, 7 pp. 6 figs.

The Dynamic Response Characteristics of a Turbojet Engine Obtained by Frequency Response Testing, by George W. Smith, *SAE Prepr.* 233, Oct. 1957, 3 pp., 7 figs.

Design and Development of the F102 Power Plant Installation, by R. J. Chillo, *SAE Prepr.* 232, Oct. 1957, 7 pp., 15 figs.

Radial Equilibrium in Supersonic Compressors, by Andrew Hammitt and Seymour M. Bogdonoff, *Princeton Univ. Conference, Report* 7, 1957, 10 pp., 6 figs.

Simulator for Use in Development of Jet Engine Control, by Emile S. Sherrard, *Nat. Bur. Standards, Circ.* 584, Sept. 1957, 17 pp.

Missile Auxiliary Power, by Paul C. Ricks, *SAE Prepr.* 213, Oct. 1957, 5 pp.

An Aerodynamic Screen for Jet Engines, by Harold Klein, *Aeron. Engng. Rev.*, vol. 16, no. 11, Nov. 1957, pp. 48–53.

The Turbine Engine Position in 1957, *Intervia*, vol. 12, no. 10, Oct. 1957, pp. 1021–1022.

Investigations of an Experimental Air Cooled Turbine, Part I: General Description of Turbine and Experimental Technique; Part II: Cooling Characteristics of Blades Having a Multiplicity of Small Diameter Coolant Passages, by D. G. Ainley, N. E. Waldren and K. Hughes, *Gt. Brit., Aeron. Res. Council, Rep. & Mem.* 2975 (Formerly *A.R.C. Tech. Rep.* 16957

and 16958; *Nat. Gas Turbine Estab. Rep.* R 153 and R 154), 1957, 64 pp.

Operation of a "Free" Ram Jet in a Supersonic Airstream, *Experiment Inc. CM*-123, by J. W. Mullins, II, Oct. 1945, 10 pp., 6 fig. (Declassified from Confidential by authority of Johns Hopkins University, Applied Physics Lab., letter dated 2/5/57, signed Paul E. Clark.)

Analytical and Experimental Investigation of Thrust Augmentation of Axial and Centrifugal Compressor Turbojet Engines by Injection of Water and Alcohol, by David S. Gabriel, Harry W. Dowman and William L. Jones, *NACA RM* E9K29, Apr. 1950, 43 pp. (Declassified from Confidential by authority of *NACA Res. Abs.* 122, p. 7, 12/3/57.)

Investigation of Altitude Ignition, Acceleration and Steady State Operation with Single Combustor of J47 Turbojet Engine, by William P. Cook and Helmut F. Butze, *NACA RM* E51A25, March 1951, 35 pp. (Declassified from Confidential by authority of *NACA Res. Abs.* 122, p. 7, 12/3/57.)

Analysis of Performance of Four Symmetrical-diagram-type Subsonic Inlet-stage Axial-flow Compressors, by Robert J. Jackson, *NACA RM* E53KO3, Jan. 1954, 72 pp. (Declassified from Confidential by authority of *NACA Res. Abs.* 122, p. 9, 12/3/57.)

The Versatile Orpheus, *Aeroplane*, vol. 93, Nov. 22, 1957, pp. 779–782.

Turbojets for Advanced Missiles? *Aviation Age*, vol. 28, Dec. 1957, pp. 36–37.

Standardized Thrust Analysis Catches Performance Lags in Time, *Aviation Age*, vol. 28, Dec. 1957, pp. 46–52, 54–55.

Chemical Rocket Engines—Principles and Applications, by Robert R. Bradley and John G. Donovan, *Sperry Engng. Rev.*, vol. 10, Sept.–Oct. 1957, p. 2.

Gas Turbine Combustion System Design, by F. D. M. Williams, *IAS Prepr.* 754, Oct. 1957, 30 pp.

Recent Advances in the Aerodynamic Design of Axial Turbomachinery, by W. H. Robbins and H. W. Plohr, *IAS Prepr.* 762, Oct. 1957, 16 pp., 12 fig.

Standby Rocket Engines for Civil Aircraft, by G. E. Rice, *IAS Prepr.* 760, Oct. 1957, 19 pp., 10 fig.

Part Load Characteristics for the Free Piston and Turbine Compound Engine, by A. L. London, *Stanford Univ., Dept. Mech. Engng., Tech. Rep.* FP-5, Nov. 1957, 38 pp.

The Turbine Engine in Salt Atmosphere Operation, by F. Herbert Sharp, *Aeron. Engng. Rev.*, vol. 17, Jan. 1958, pp. 47–49, 56.

Small Turbojets Challenge High-thrust Engines, by William Beller, *American Aviation*, vol. 21, Dec. 30, 1957, pp. 30–31.

Scientists Study Mach 7 Ramjet Theory, by Robert H. Cusman, *Aviation Week*, vol. 68, Jan. 6, 1958, pp. 57–63.

Experimental Investigation of the Rotating Stall in a Single-stage Axial Compressor, by Jacques Valensi, *J. Aeron. Sci.*, vol. 25, Jan. 1958, pp. 1–10.

Seals for Pressures to 10,000 Atmospheres, by W. B. Daniels and A. A. Hruschka, *Rev. Sci. Instrum.*, vol. 28, Dec. 1957, pp. 1058–1059.

Rockets as Research Vehicles. by P. H. Wyckoff, *Shell Aviation News*, no. 233, Nov. 1957, pp. 2–4.

Investigation of Carbon Deposition in an I-16 Jet Propulsion Engine at Static Sea Level Conditions, by Edmund R. Jonash, Henry C. Barnett and Edward G. Stricker, *NACA RM* E6K01, Apr. 1947, 11 pp. (Declassified by authority of *NACA Res. Abs.* 122, p. 1, 12/3/57.)

Theoretical and Experimental Supersonic Flow Studies Related to Turbomachine Design, by E. Beder, *Propulsion Res. Corp.*, Rep. SN48-Pl, July 1957, 28 pp.

Rotating Stall in Single State Axial Flow Compressors, by Theodore J. Falk, *Cornell Univ. Grad. School Aeron. Engng.* (*AFOSR-TN*-56-512; *ASTIA AD* 110-327), Sept. 1956, 39 pp., 24 fig.

Three-Dimensional Effects in Supersonic Compressors, Part A: The Analytical Method and Its Application for Rotating and Fixed Coordinate System, by Roberto Vaglio-Lauren, *Brooklyn Polytech. Inst., Dept. Aeron. Engng. Appl. Mech., PIBAL Rep.* 234, Oct. 1953, 57 pp., 8 fig.

A New Experimental Approach to the Analysis of Compressor Performance; Application of the Bomelburg Spark Method; the Measurement of Directional Velocity Transverses at the Outlet of an Impeller, by Josef Herzog. *Univ. Maryland, Inst. Fluid Dynamics Appl. Math., TN* BN-90 (*AFOSR-TN*-57-3; *ASTIA AD* 115035), Jan. 1957, 9 pp., 14 fig.

The Two-Dimensional Inflow Conditions for a Supersonic Compressor with Curved Blades, by Philip Levine, *Wright Air Devel. Center, Tech. Rep.* 55–387, May 1956, 27 pp.

Low-speed Cascade Investigation of Thin Low-camber NACA 65-series Blade Sections at High Inlet Angles, by James C. Emery, *NACA RM* L57E03, June 1957, 93 pp. (Declassified from Confidential by authority of *NACA Res. Abs.* 121, p. 28, 11/4/57.)

Investigation of the Effect of Velocity Diagram on Inlet Total-pressure Distortions Through Single-stage Subsonic Axial-flow Compressors, by George C. Ashby Jr., *NACA RM* L57A03, Apr. 1957, 21 pp. (Declassified from Confidential by authority of *NACA Res. Abs.* 121, p. 28, 11/4/57.)

Experimental Investigations of an Axial-flow Compressor Inlet State Operating at Transonic Relative Inlet Mach numbers, I: Over-all Performance of Stage with Transonic Rotor and Subsonic Stators up to Rotor Relative Inlet Mach Nymber of 1.1, by Seymour Lieblein, George W. Lewis Jr. and Donald M. Sandercock, *NACA RM* E52A24, March 1952, 21 pp. (Declassified from Confidential by authority of *NACA Res. Abs.* 121, p. 15, 11/4/57.)

Experimental Investigation of Axial-flow Compressor Inlet State Operating at Transonic Relative Inlet Mach Numbers, II: Blade-coordinate Data, by George W. Lewis Jr., *NACA RM* E52C27, June 1952, 9 pp. (Declassified from Confidential by authority of *NACA Res. Abs.* 121, p. 16, 11/4/57.)

Aerodynamics of Jet Propelled Vehicles

An Approximate Method for the Calculation of the Aerodynamic Characteristics of Ogive Cylinders Near Zero Lift, by Felix W. Fenter, *Univ. Texas, Defense Res. Lab.* CF2547, (*DRL*-390), Jan. 1957, 30 pp., 11 fig.

Exit and Re-entry Problems, by G. V. Bull, K. R. Enkenhus and G. H. Tidy, *IAS Prepr.* 759, Oct. 1957, 11 pp., 12 fig.

Trajectory Programming for Maximum Range, by George Leitmann, *J. Franklin Inst.*, vol. 264, Dec. 1957, p. 443.

On Optimum Nose Curves for Missiles in the Superaerodynamic Regime, by H. S. Tan, *J. Aeron. Sci.*, vol. 25, Jan. 1958, pp. 56–57.

On Optimum Nose Shapes for Missiles in the Superaerodynamic Region, by I. D. Chang, *J. Aero. Sci.*, vol. 25, Jan. 1958, pp. 57–58.

Supersonic Flow Around Blunt Bodies, by Hyman Serbin, *J. Aeron. Sci.*, vol. 25, Jan. 1958, pp. 58–59.

Heat Transfer and Fluid Flow

Experimental Verification of Nozzle Admittance Theory in a Simulated Rocket Chamber, by Sotirios Lambiris, *Princeton Univ., Dept. Aeron. Engng., Rep* 401, Sept. 1957, 48 pp., 22 fig. (M.S.E. thesis).

Investigation of a Wide Angle Diffuser with Air Augmentation for Use as a Jet Muffler, by A. J. Campbell, *Univ. Toronto, Inst., Aerophys., TN* 15, Aug. 1957, 11 pp., 9 fig.

The Calculation of the Thermodynamic Properties of Air at High Temperatures, by J. G. Logan Jr., *Cornell Aeron. Lab., Inc., Rep.* AD-1052-A-1 (*AFOSR-TN*-56-344; *ASTIA AD* 95220), May 1956, 68 pp.

Turbulence in Small Air Jets, by L. W. Lassiter, *J. Appl. Mech.*, vol. 24, Sept. 1957, pp. 349–354.

The Vorticity Jump Across a Gasdynamic Discontinuity, by Wallace D. Hayes, *J. Fluid Mech.*, vol. 2, Aug. 1957, pp. 595–600.

The Collision of Two Ionized Streams, by F. D. Kahn, *J. Fluid Mech.*, vol. 2, Aug. 1957, pp. 601–615.

Radial Distribution Function of Fluids, II, by Kazuo Hiroike, *J. Physical Soc. Japan*, vol. 12, Aug. 1957, pp. 864–873.

A Note on the Mixing Process in the Flow Induced by a High Velocity Air Jet, by J. Black, *J. Roy. Aeron. Soc.*, vol. 61, Sept. 1957, pp. 631–633.

An Experimental Study of Accelerated Fluids (The Taylor Problem), by Barron C. Watson, *Harvard Univ., Div. Engng. Appl. Phys., Combustion Aerodynam. Proj., Interim Tech. Rep.* 16, June 1957, 87 pp.

The Influence of Design Pressure Ratio and Divergence Angle on the Thrust of Convergent Divergent Propellant Nozzles, by P. F. Ashwood and D. G. Higgins, *Grt. Brit., Aeron. Res. Council, Current Paper* 325 (formerly *ARC Tech. Rep.* 17833; *Nat. Gas Turbine Estab. Rep.* R168), 1957, 16 pp.

Drop-size Distribution for Crosscurrent Breakup of Liquid Jets in Airstreams, by Robert D. Ingebo and Hampton H. Foster, *NACA TN* 4087, Oct. 1957, 36 pp.

Effect of Fluid-system Parameters on Starting Flow in a Liquid Rocket, by Richard P. Krabs, *NACA TN* 4034, Sept. 1957, 38 pp.

The Principles of Turbulent Heat Transfer, by H. Reichardt, *NACA Tech. Mem.* 1408, Sept. 1957, 45 pp. (translation from *Archiv. für die gesamte Wärmetechnik*, no. 6/7, 1951, pp. 129–142).

Total Normal Emissivity Measurements for Porous Materials Used for Mass Transfer Cooling, by T. F. Irvine Jr., J. P. Hartnett and E. R. G. Eckert, *ASME* Paper 57-F-8, Sept. 1957, 5 pp.

Design Manual of Natural Methods of Cooling Electronic Equipment, by James P. Welsh, *Bur. Ships*, NAVSHIPS 900,192 (*Cornell Aeron. Lab., Rep.* HF-845-D-8), Nov. 1956, 188 pp.

Theories of Gas Transport Properties, by C. F. Curtiss, J. O. Hirschfelder and R. B. Bird, *Univ. Wisconsin, Naval Res. Lab.*, CF-2659, July 1957, 22 pp.

Higher Approximations for the Transport Properties of Binary Gas Mixtures, II: Applications, by Edward A. Mason, *J. Chem. Phys.*, vol. 27, Sept. 1957, pp. 782–790.

Propagation of Strong Shock Waves in Pulsed Longitudinal Magnetic Fields, by Alan C. Kolb, *Physical Rev.*, vol. 107, Aug. 15, 1957, pp. 1197–1198.

The Transient Response of a Two Fluid Counter Flow Heat Exchanger—the Gas Turbine Regenerator, by A. L. London, A. J. Oberg and R. M. Cima, *Stanford Univ., Dept. Mech. Engng., Tech. Rep.* 32, Aug. 1957, 49 pp.

An Experimental Investigation of the Bounded Mixing of Two Compressible Axially Symmetric Jet Streams, by James E. A. John, *Princeton Univ., Dept. Aeron. Engng., Report* 399, 1957, 23 pp. (MSE Thesis).

Investigation of Compressible Flow Mixing Losses Obtained Downstream of a Blade Row, by Warner L. Stewart, *NACA Res. Mem.* E54I20, Dec. 1954, 21 pp. (Declassified from Confidential by authority of *NACA Res. Abstracts* 120, p. 8, 10/3/57.)

Combustion, Fuels and Propellants

Spark Ignition of Flowing Gases, by Clyde C. Swett Jr., *NACA Rep.* 1287, 1956, 18 pp.

Combustion Studies of Astrophysical Significance, II: A Survey of Chemical Kinetics for Premixed Hydrocarbon/Oxygen Flames, by G. V. Marr, *Western Ontario Univ., Dept. Physics., Molecular Excitation Group, Scientific Rep.* 1 (Series 2) (*ASTIA AD* 110208), July 1957, 59 pp.

Detonations in Gaseous Fuming Nitric Acid-Hydrocarbon Mixtures, by D. H. Wayman and R. L. Potter, *Combustion and Flame*, vol. 1, no. 3, Sept. 1957, pp. 321–329.

A Method for Determining Minimum Ignition Energies: Results for a Neopentane-Air Mixture, by I. W. Wolf and V. T. Burkett, *Combustion and Flame*, vol. 1, no. 3, Sept. 1957, pp. 330–338.

Temperature Stability of the Laminar Combustion Wave, by J. F. Wehner and J. B. Rosen, *Combustion and Flame*, vol. 1, no. 3, Sept. 1957, pp. 339–345.

Present Status of Information on Transport Properties Applicable to Combustion Research, by A. A. Westenberg, *Combustion and Flame*, vol. 1, no. 3, Sept. 1957, pp. 346–359.

Measurement of Chapman-Jouguet Pressure for Explosives, by W. E. Deal, *J. Chem. Phys.*, vol. 27, Sept. 1957, pp. 796–800.

Burning of a Liquid Droplet, IV: Combustion Inhibition in a Fuel-Oxidizer System, by Bernard J. Wood, Henry Wise and Willis A. Rosser, *J. Chem. Phys.*, vol. 27, Sept. 1957, pp. 807–808.

Investigation of the Effect of Pressure on Flame Propagation, *Univ. Göttingen, Inst. Physikalische Chemie* (*ASTIA AD* 139206), Apr. 1957, 21 pp.

Preparation and Physical Properties of Some Trialkylboranes, by Louis Rosenblum and Harrison Allen Jr., *NACA Res. Mem.* E55E06, Nov. 1955, 19 pp. (Declassified from Confidential by authority of *NACA Res. Abstracts* 120, p. 8, 10/3/57.)

Study of Liquid-Vapor Equilibrium Between Acetone, Isopropanol, and Water, Part 3, by B. Choffe and L. Asselineau, *Inst. Francais Petrole, Rev. Annales Combustibles Liquids*, vol. 12, no. 5, 1957, pp. 565–575 (in French).

Experimental Study of the Accelerating Influence of Oxygen Traces on the Gas Phase Pyrolysis of Some Saturated Hydrocarbons, by J. Engel, A. Combe, M. Letort and M. Niclause, *Inst. Francais Petrole, Rev. Annales Combustibles Liquides*, vol. 12, no. 5, 1957, pp. 627–638 (in French).

Theory of Detonations, I, by C. F. Curtiss and J. O. Hirschfelder, *Univ. Wisconsin, Naval Res. Lab., Dept. Chem.*, CM-911, Aug. 1957, 46 pp.

Part A, Some Remarks on the Excess Enthalpy of Ozone Decomposition Flames; Part B, Minimum Ignition Energies and Flame Extinction, by F. Williams and S. S. Penner, *Calif. Inst. Tech., Daniel Florence Guggenheim Jet Propulsion Center, Tech. Rep.* 17 (*ASTIA AD* 122213), Feb. 1957, 11 pp.

Design of a Low Pressure Burner System for Laminar Flame Studies, by R. M. Fristrom and S. D. Raezer, *Johns Hopkins Univ., Applied Phys. Lab.*, CM 912, Aug. 1957, 10 pp.

Simulated High Altitude Combustion Research, Quarterly Progress Report No. 3, 1 December 1955 to 29 February 1956, *MIT, Dept. Chem. Engng., Fuels Res. Lab.* (*ASTIA AD* 122868), March 1956, 5 pp.

Analytical and Experimental Investigation of the Fluid Dynamics of Ramjet Combustion Research, *Marquardt Aircraft Co., 3rd Quarterly Progr. Rep.*, 1 July–30 Sept. 1956, *Rep.* PR-138-3 (*ASTIA AD* 122815), Nov. 1956, 18 pp.

Combustion and Flames at High Pressures, by H. G. Wolfard and A. Strasser, *Project Squid, Tech. Rep.* BUM-21-P (*ASTIA AD* 136842), July 1957, 31 pp. (available only on microcard).

The Ignition of Combustible Gases by Flames, by H. G. Wolfard and D. S. Burgess, *Project Squid, Tech. Rep.* BUM-22-P (*ASTIA AD* 138401), Aug. 1957, 17 pp. (available only on microcard).

Spontaneous Ignition Temperature of Fuel Nitric Oxide Mixtures, by H. G. Wolfhard and A. Strasser, *Project Squid, Tech. Rep.* BUM-23-P (*ASTIA AD* 138402), Aug. 1957, 3 pp. (available only on microcard).

Ion Recombination Rates in Methane Air Flames, by I. R. King, *Project Squid, Tech. Rep.* EXP-4-P (*ASTIA AD* 135911), July 1957, 4 pp. (available only on microcard).

On the Dissociation of Ionized Carbon Monoxide, by Willard E. Meador Jr., *Project Squid, Tech. Rep.* EXP-5-P (*ASTIA AD* 136298), July 1957, 16 pp. (available only on microcard).

A Flow Reactor for High Temperature Reaction Kinetics, by L. Crocco, I. Glassman and I. E. Smith, *Princeton Univ., Aeron. Engng. Lab., Rep.* 398 (*AFOSR-TN-57-373; ASTIA AD* 132445), June 1957, 4 pp.

Dynamic Factors Affecting the Combustion of Liquid Spheres, by George A. Agoston, Henry Wise and Willis A. Rosser, *Calif. Inst. Tech., Jet Prop. Lab., Progr. Rep.* 20-291, Nov. 1956, 23 pp.

Design, Development and Reliability Testing of the NN 114 Igniter, *American Potash and Chem. Corp., Natl. Northern Div.*, Aug. 1957, 10 pp.

Calculation of Interior Ballistics by Analog Computer, by August G. Edwards and Arthur I. Rubin, *Picatinny Arsenal, Samuel Feltman Ammunition Lab., Tech. Rep.* 2421, Aug. 1957, 62 pp.

The dry and dustless direct-recording oscillograph that records without the use of powders, liquids, vapors, or other processing . . .

The new 36-Channel Model 1012 VISICORDER OSCILLOGRAPH

is the only direct-recording oscillograph . . .

* that provides a consistently accurate grid line system (amplitude reference coordinates). By recording longitudinal reference lines *simultaneously* with galvanometer traces and timing lines, the reference is always accurate, even if the paper should shift slightly during recording, or is susceptible to subsequent dimensional changes.
* that can be loaded and unloaded *in a matter of seconds,* in daylight, without separate magazines.
* that permits running the record backward, as well as forward, for closer study and analysis.
* that gives you a choice of 5 time lines intervals (.001, 0.01, 0.10, 1.00, 10.0 second) recorded by means of a flash tube, with provision for external synchronization. External signals applied simultaneously to galvanometers and timing system are in exact time relationship on the record.
* that offers complete push-button control of record speeds, without changing gears, in 15 steps from 0.1 to 160 in./sec., with automatic recording intensity control.
* that provides "center galvanometer" performance in all galvanometer positions.
* that utilizes hermetically sealed plug-in galvanometers that do *not* require dummies in unfilled positions, and that are completely interchangeable between various models (700C, 906A-1) because optical arms (11.8") and, consequently, sensitivities are identical.
* that provides loading, operation and control from one surface.

. . . *And these are just a few of its versatile features!* The Model 1012 Visicorder is the most versatile instrument ever devised for converting dynamic data into immediately readable analog records. It has been specifically designed to make full utilization of the direct-recording Visicorder Principle that Honeywell pioneered and introduced with the Model 906 (see back cover). With the 1012, you can take records up to 200 feet in length with a wide selection of record speeds that provide maximum readability of the galvanometer traces even at the highest frequencies. You can record at frequencies from DC to 5000 cycles per second, at sensitivities identical to photographic-type oscillographs, and monitor the information as it goes on the record. The features of the Model 1012 give you conveniences never before possible in analog recording. Paper loading and unloading is quick and foolproof. A complete system of readily accessible controls, with indicator lamps, provides simple, positive control of recording. The 1012 records with or without longitudinal grid lines, as desired. Time lines may be varied through a choice of five ranges or not used at all; provisions for external timing are included. Galvanometer traces may overlap, with deflections as great as 8 inches peak-to-peak, and trace identification occurs on a 45° slope, interrupting galvanometer traces one at a time so that records are easy to read and analyze.

GENERAL FEATURES

FREQUENCIES & SENSITIVITIES
From DC to 5000 cycles per second without peaked amplifiers of any kind. Identical to photographic-type oscillographs.

RECORDING METHODS
Makes full use of the new Visicorder Principle. Records directly on paper which requires no powder magazines, liquids, vapors, or other processing. Daylight loading. Recording is accomplished in full view of the operator. Records are immediately visible and usable.

NUMBER OF CHANNELS
12, 24, or 36 active channels, as desired. Three magnet assemblies, each of which holds up to twelve ⅛" Series M Honeywell galvanometers, plus two reference traces.

RECORDING WIDTH
12" Visicorder paper (11⅝" for active recording; ⅜" margin for record numbering and event marking).

TRACE IDENTIFICATION
45° slope, interrupting galvanometer traces in sequence.

RECORDING SPEEDS
0.1 to 160 in./sec. Five speeds in each of 3 ranges (15 steps) via push-button control. No manual change of gears is required.

TIME LINES
Flash tube system. Choice of 5 intervals (.001, 0.01, 0.10, 1.00, 10.0 second) with each 10th line heavier. May be turned "off" or synchronized with external signals. With optical parallax being held to a minimum and negligible delay in initiating flash tube, timing lines and other data are recorded in exact time relationship.

RECORDING INTENSITY CONTROL
Proper aperture automatically established with record speed selection, or manually controlled as desired.

"NO RECORD" INDICATOR
Red indicator lamp and automatic shut-down of drive system indicates "No Record" if operator fails to turn on all necessary switches, if lamp fails, or if recording paper supply is exhausted. A separate lamp indicates when less than 25 feet of paper remains in supply.

PAPER LOADING
Simply done in a matter of seconds even by untrained personnel. All paper transport and take-up functions are integral. No separate magazines or other units required.

OTHER FEATURES
Automatic record length, adjustable 0-25′ (forward or reverse). Unused paper indicator. Paper knife. Push-button jump speed control. Record numbering system with provision for external actuation. Integral fluorescent light Intensifier. Rack, table, or shock mounting. Provision for remote and/or multiplexed operation.

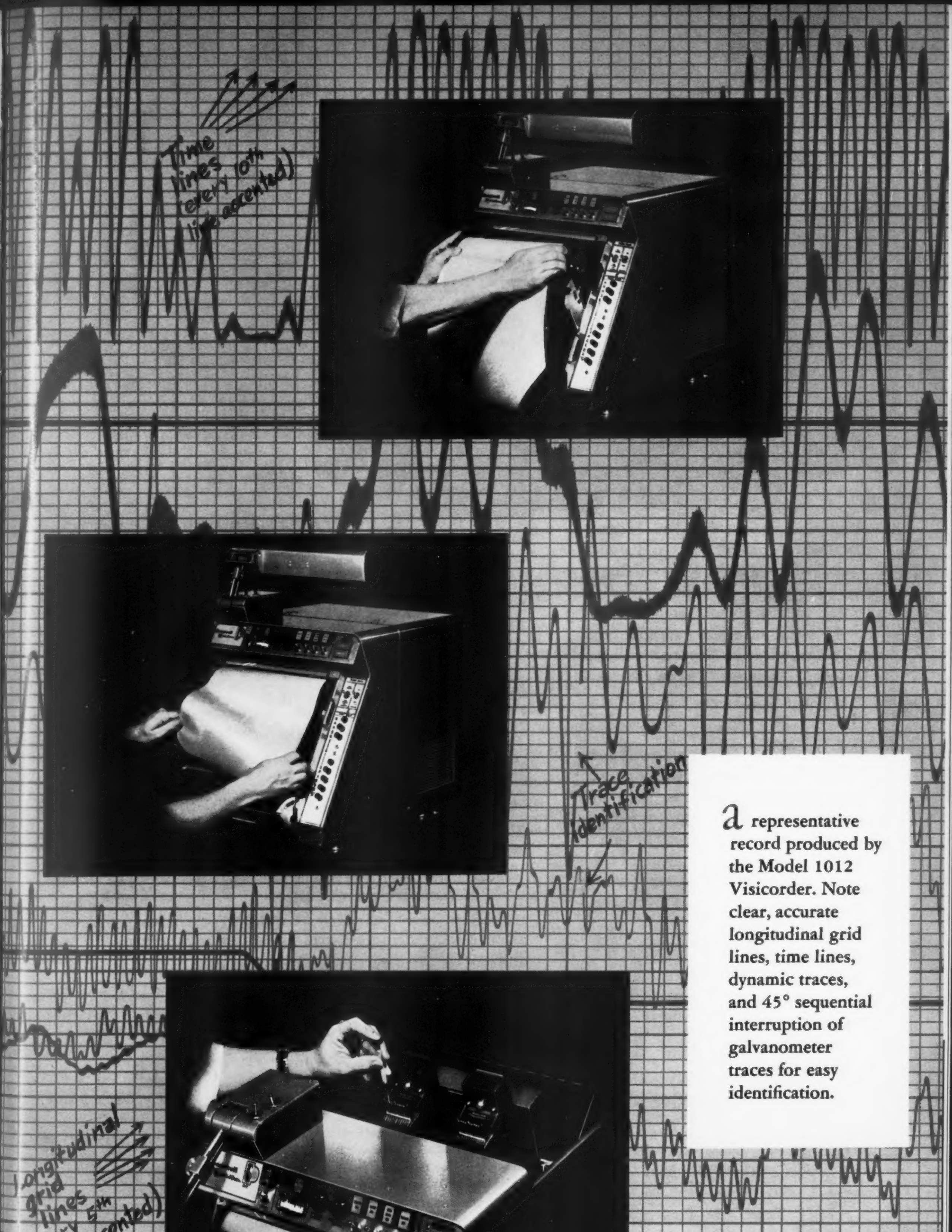

a representative record produced by the Model 1012 Visicorder. Note clear, accurate longitudinal grid lines, time lines, dynamic traces, and 45° sequential interruption of galvanometer traces for easy identification.

Application of Well Stirred Reactor Theory to the Prediction of Combustor Performance, by H. C. Hottel, G. C. Williams and A. H. Bennell, *Project Squid, Tech. Rep.* MIT-15-P (*ASTIA AD* 135111), July 1957, 27 pp. (available only on microcard).

Measurement of Fluorine Concentration in Gas Mixtures with the Acoustic Gas Analyzer, by B. J. Bogardus and R. C. Smith, *Atomic Energy Comm.*, K1279, June 1956, 32 pp.

Combustion Bibliography; Operation of Card Indexing System, by R. M. Friston, *Johns Hopkins Univ., Appl. Phys. Lab.*, TG-211, Oct. 1953, 11 pp.

Analysis of Steady, Finite Amplitude Cellular Flames, by G. H. Markstein, *Preprints of papers, Heat Transfer and Fluid Mech. Inst.*, 1957, pp. 295–320.

Ignition in the Laminar Boundary Layer of a Heated Plate, by Donald A. Dooley, *Preprints of papers, Heat Transfer and Fluid Mech. Inst.*, 1957, pp. 321–342.

Ignition in Transient Flows, by D. Bitondo, M. Thomas and D. Perper, *Preprints of papers, Heat Transfer and Fluid Mech. Inst.*, 1957, pp. 343–358.

The Kinetics of the NO-N_2O_5 Reaction, by I. C. Hisatsune, Bryce Crawford Jr. and R. A. Ogg Jr., *J. Amer. Chem. Soc.*, vol. 79, Sept. 5, 1957, pp. 4648–4652.

Safety Hazards of Handling Liquid Oxygen, by C. S. McCamy, *Indus. Engng. Chem.*, vol. 49, Sept. 1957, Pt. 1, pp. 81A–82A.

Fluorine-Derived Chemicals as Liquid Propellants, by J. F. Gall, *Indust. Engng. Chem.*, vol. 49, Sept. 1957, Pt. 1, "Rockets and the Chemical Industry," pp. 1331–1332.

Applied Research and Product Development for Rocket Propellants, by A. R. Deschere, *Indus. Engng. Chem.*, vol. 49, Sept. 1957, Pt. 1, "Rockets and the Chemical Industry," pp. 1333–1336.

Utilization of High-Energy Fuel Elements, by E. A. Weilmuenster, *Indus. Engng. Chem.*, vol. 49, Sept. 1957, Pt. 1, "Rockets and the Chemical Industry," pp. 1337–1338.

Liquid Rocket Propellants—Is There an Energy Limit? by J. F. Tormey, *Indust. Engng. Chem.*, vol. 49, Sept. 1957, Pt. 1, "Rockets and the Chemical Industry," pp. 1339–1343.

Homogeneous Solid Propellants and the Chemical Industry, by L. G. Bonner, *Indust. Engng. Chem.*, vol. 49, Sept. 1957, Pt. 1, "Rockets and the Chemical Industry," p. 1344.

Chemical Lessons Learned from Nike Ajax Development, by R. B. Canright, *Indust. Engng. Chem.*, vol. 49, Sept. 1957, Pt. 1, "Rockets and the Chemical Industry," pp. 1345–1347.

The Chemical Industry in Missile Systems Planning, by S. A. Johnston and H. R. Lawrence, *Indust. Engng. Chem.*, vol. 49, Sept. 1957, Pt. 1, "Rockets and the Chemical Industry," p. 1348.

Rate of Propagation of Propane-Air Flames Irradiated with a 10,000-Curie Gold Source, by S. W. Churchill, Alexander Weir Jr., R. L. Gealer and R. J. Kelley, *Indust. Engng. Chem.*, vol. 49, Sept. 1957, Pt. 1, "Rockets and the Chemical Industry," pp. 1419–1422.

Emission Spectra of Propane-Air Flames Irradiated with a 1000-Curie Gold Source, by Alexander Weir Jr., S. W. Churchill, L. F. Ornella and M. E. Gluckstein, *Indust. Engng. Chem.*, vol. 49, Sept. 1957, Pt. 1, "Rockets and the Chemical Industry," pp. 1423–1428.

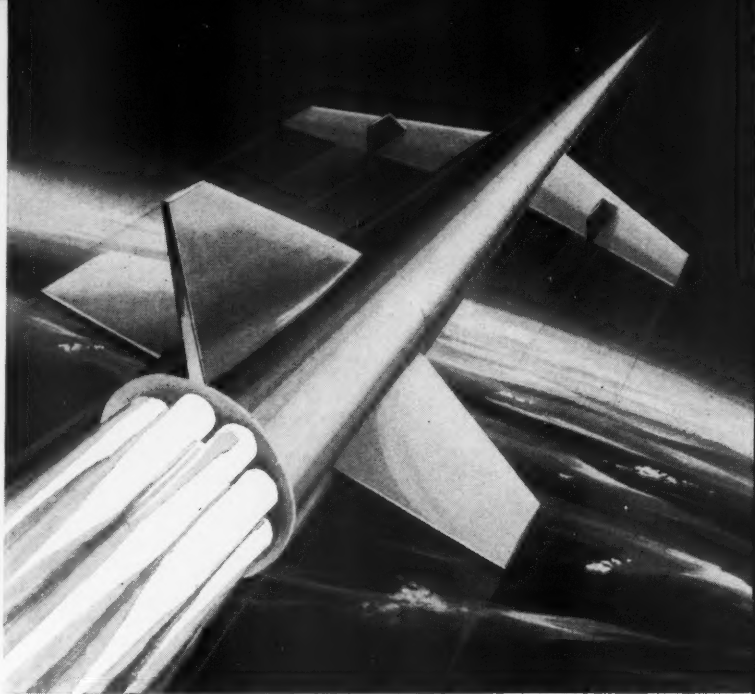

Combustion, by Raymond Friedman and John H. Grover, *Indust. Engng. Chem.*, vol. 49, Sept. 1957, Pt. 2, pp. 1470–1477.

Decomposition of Hydrocarbons, by Charles V. Berger and Herbert R. Appell, *Indust. Engng. Chem.*, vol. 49, Sept. 1957, Pt. 2, pp. 1478–1484.

A Type of Flame-Excited Oscillation in a Tube, by J. J. Bailey, *J. Appl. Mech.*, vol. 24, Sept. 1957, pp. 333–339.

1957 Liquid Propellant Round-up, *Missiles and Rockets*, vol. 2, Sept. 1957, pp. 82–86.

Nonmetallic Material Compatibility with Liquid Fluorine, by Harold G. Price Jr. and Howard W Douglass, *NACA RM* E57G18, Oct. 1957, 7 pp.

Behavior of Inverted Propane-Hydrogen Sulphide Flames at the Blow-off Limits, by P. F. Kurz, *Combustion and Flame*, vol. 1, no. 3, Sept. 1957, pp. 257–263.

Technique to Produce Free Radicals in the Solid State, by Harold A. Papazian, *J. Chem. Phys.*, vol. 27, Sept. 1957, pp. 813–814.

Ion Recombination Rates in Methane-Air Flames, by I. R. King, *J. Chem. Phys.*, vol. 27, Sept. 1957, pp. 817–818.

Effect of Initial Mixture-Temperature on Burning Velocity of Hydrogen-Air Mixtures with Preheating and Simulated Preburning, by Sheldon Heimel, *NACA TN* 4156, Oct. 1957, 23 pp.

Problems Encountered in the Use of Liquid Oxygen, by Paul L. Castron, *SAE Prep.* 238, Oct. 1957, 4 pp.

Mechanism and Kinetics of the Reaction between Fuming Nitric Acid and/or Its Decomposition Products and Gaseous Hydrocarbons, by Francis G. Taylor, Barbara G. Faunce, Nancy K. Asawa and Albert L. Myerson, *Wright Air Dev. Center, Tech. Rep.* 57-138, June 1957, 54 pp. (*ASTIA AD* 118105; *Franklin Inst., Final Tech. Rep.* F-2452).

The Controlled Thermal Decomposition of Cellulose Nitrate, III, by M. L. Wolfrom, Alan Chaney and P. McWain, *Ohio State Univ. Res. Foundation, Tech. Rep.* 675-7, Sept. 1957, 22 pp.

Space Flight

Space Flight: A $2-Billion-a-Year Business by 1962, *Aviation Age*, vol. 28, Dec. 1957, pp. 16–21.

U.S. Space Flight R & D Makes Good Showing at IAF Congress, *Aviation Age*, vol. 28, Dec. 1957, pp. 76–81.

Soviet Space Agency Revealed, *Missiles and Rockets*, vol. 2, Dec. 1957, pp. 42–47.

Nuclear Propulsion

Airborne Nuclear Propulsion System Design Considerations, by Robert B. Ormsby Jr., *Aeron. Engng. Rev.*, vol. 17, Jan. 1958, pp. 20–23.

Transport of Radioactivity by Liquid Sodium in a Stainless Steel Circulation System, by D. Fieno and D. Bogart, *NACA RM* E54K03, March 2, 1955, 17 pp. (Declassified from Confidential by authority of *NACA Res. Abs.* 31, p. 28, 11/4/57.)

A Study of Monte Carlo Methods Applied to a Nuclear Reactor Problem, by Fred Leah, *Calif. Inst. Tech., Jet Propulsion Lab., Mem.* 20-143, May 1957, 20 pp.

Bibliography

(*Continued from page 401*)

ward. A table on page 23 gives details of U. S. vs. Russian satellites.

Hoenig, S. A.

Meteoric Dust Erosion Problem and Its Effect on the Earth Satellite. Aero. Eng. Rev. 16: 37–40 illus. July 1957. A survey of research on the subject indicating that for a satellite whose life is measured in days the effect of erosion is negligible.

Hoffman, B.

General Relativistic Red Shift and the Artificial Satellite. Phys. Rev. 106: 358–359, Apr. 15, 1957. Singer's formula for the general relativistic red-shift of an earth satellite is modified to take account of the diurnal rotation of the earth and the lack of spherical symmetry of its gravitational field. It is shown that the Singer rates of the earth and satellite clocks need slight modifications, but that these modifications tend to cancel each other except at large distances from the earth, so that when one uses a mean radius of the earth in Singer's formula, the formula is adequate for present purposes.

Hoover, G. W.

Sectional Satellites—A Bit-by-Bit Approach to Space Flight. Missiles and Rockets 2: 135–137, illus., Oct. 1957. Proposes development of a series of small satellites, each as a component in a total system.

Humphries, John

Observation of Artificial Satellites. Brit. Interplanetary Soc. J. 15: 347–349, Dec. 1956; 16: 57–58, Jan./Mar. 1957. Report on American Moonwatch program and Minitrack equipment.

Iatsunskii, I. M.

O Vliianii Geofizicheskikh Faktorov na Dvizhenie Sputnika (*Effect of Geophysical Factors upon the Motion of an Artificial Satellite*). Usp. Fiz. Nauk 63(1a): 59–71, Sept. 1957. In Russian. Translation No. R-3054 available at Special Libraries Association Translation Center, Crerar Library, Chicago, Ill. Study of the effect of geophysical factors on the motion of an artificial satellite. Establishment of a problem pertaining to the specification of coefficients included in the mathematical expression of disturbing forces, based on satellite coordinates.

Instrument Society of America Journal

Instrumentation of Sputnik. 4: 572–573, illus., Dec. 1957. This article, based on articles by Vasily Parfenov and E. Blinova, gives brief bits of information concerning the scientific importance of artificial satellites; power from the sun; meteorological measurements; weather forecast via Sputnik; moon missiles.

Interavia

The New Dimension. The Launching of the Soviet Earth Satellites. 12: 1229–1233, illus., Dec. 1957. A diary of the days following the launching of Sputnik I; a comment on its weight and accuracy; details of Sputnik I and II; and comparative data for the Sputniks and Vanguard.

Jastrow, R., and Pearse, C. A.

Atmospheric Drag on the Satellite. J. Geophys. Res. 62: 413–423, Sept. 1957. The drag exerted on the satellite in its orbit arises partly from collisions with neutral air particles and partly from losses associated with the passage of a charged sphere through an ionized medium. It is found that the charged and neutral effects are comparable

The mobility problem in cooling electronic equipment in vans and for missile pre-launching has been answered by new AiResearch Freon air conditioning units. *One-fourth the weight and one-third the size* of conventional equipment, these lightweight, air-transportable units utilize highly efficient AiResearch Freon components (see diagram) originally developed for commercial aircraft applications.

Heat source for the circuit can be either electrical, or exhaust gas from an AiResearch gas turbine. When the gas turbine assembly includes an alternator, it supplies *400 cycle power to run both the refrigeration unit and all electronic gear in the van.*

Easily operated manually or automatically, this compact air conditioning unit provides from 5 to 12 tons cooling capacity and up to 85,000 BTU's per hour heating capacity. It operates on 400 cycles, 208 volts. The unit shown stands 54" high, 52" wide and 27" deep, with a charged weight of only 452 lbs.! Your inquiries are invited.

SPECIFICATIONS
Performance Data:
Typical operation—cooling

Refrigerant	Freon 12
Evaporator tonnage	7.5
Ambient temperature	100F
Condenser air flow	5000 cfm
Condensing temperature	131F
Evaporator air flow	1230 cfm
External distribution ducting pressure drop	2 in H_2O
Evaporating temperature	48F
Electrical power	26KVA

ENGINEERING REPRESENTATIVES: AIRSUPPLY AND AERO ENGINEERING, OFFICES IN MAJOR CITIES

THE GARRETT CORPORATION

AiResearch Manufacturing Divisions

Los Angeles 45, California • Phoenix, Arizona

Systems, Packages and Components for: AIRCRAFT, MISSILE, ELECTRONIC, NUCLEAR AND INDUSTRIAL APPLICATIONS

under the atmospheric conditions expected at an orbital altitude of 300 miles.

JET PROPULSION

Operation Moonwatch. 27: 208–209, Feb. 1957. Plans for optical tracking of the artificial satellite.

Kallmann, H. K., and Kellogg, W. W.
Use of an Artificial Satellite in Upper Air Research. Am. Meteorol. Soc. Bull. 38: 17–19, Jan. 1957. Discussion of the types of data to be collected by satellites and their scientific applications.

Kane, J. T.
Operation: Moonwatch. Natural Hist. 66: 126–129, illus., Mar. 1957. America's amateur astronomers are building "optical fences" for charting the behavior of the first space satellites.

Kaplan, Joseph
How Man-Made Satellites Can Affect Our Lives. Natl. Geog. Mag. 112: 791–810, illus., Dec. 1957. Explains how satellites can teach us about the most fundamental problems of science which will enable us to improve many things we already possess and to achieve things that we now only dream about.

Kazantsev, A.
Nablyodeniya za Radiosignalami s Iskusstvennogo Sputnika Zemli i iks Nauchnoe Znachenie (Observation of Radio Signals from the Artificial Earth Satellite and Their Scientific Significance). Radio (Moscow) 6: 17–19, June 1957. In Russian. Translation No. R-2387 available at Special Libraries Association Translation Center, Crerar Library, Chicago, Ill. See also Wireless World 63: 574–578, Dec. 1957 for summary.

"A U.S.S.R. satellite launched during the IGY will be equipped with two 1-W transmitters operating at 20 and 40 Mc/s respectively, alternating transmitting pulse signals of 0.05–0.7 sec duration from above the F layer." (Electronic and Radio Engr. Abs. and Ref. 34: 3861, Dec. 1957.)

Kemp, N. H., and Riddell, F. R.
Heat Transfer to Satellite Vehicles Reentering the Atmosphere. JET PROPULSION 27: 132–137, 147, illus., Feb. 1957. Computations of use in determining conditions under which a satellite may be expected to survive. For addendum see Detra, R. W.

Ketchum, H. B.
The Orbit Lifetimes of the U. S. Artificial Satellites. In American Astronautical Society. Proceedings, 3rd Annual Meeting, Dec. 6–7, 1956, pp. 31–41, New York, The Society, 1957. Presents a method of calculating the probable orbit lifetimes of the satellites in so far as present knowledge of the upper atmosphere will allow. Also in J. Space Flight 7: 1–5, Oct. 1955.

King-Hele, D. G.
The Satellite Paradox. Brit. Interplan. Soc. J. 16: 111–112, Apr./June 1957. Comment on article by C. A. Cross with the same title (see item under Cross) and a suggestion that the explanation be re-worded so as to emphasize that the blunt statement "air resistance speeds up a satellite" is not true.

Klemperer, W. B.
Satellite Librations. Astronautica Acta 3: 16–27, Nov. 1957. The paper deals with the computations of the frequency of oscillations about the equilibrium altitude which are called librations and which can be computed from the shape and the orbital period of the satellite. Mathematical details are given in two appendices: I. Integration of equation of dumbbell oscillations, and II. Plane libration of a prolate spheroid.

Koelle, H. H.
Sputnik and Vanguard: A Comparison. ASTRONAUTICS 2: 32–33, 80, illus., Dec. 1957. An educated guess as to what the first Soviet launching vehicle was like, along with an analysis of the different approaches used by Russia and this country in constructing their orbital carriers.

Kooy, J. M. J.
On the Application of the Method of Variation of Elliptic Orbit Elements in Case of a Satellite Vehicle. Astronautica Acta 3: 180–214, 1957. An outline is given of the determination of the six elliptical orbit elements of the instantaneous Kepler motion of an artificial earth satellite and of the application of the method of variation of orbit elements, if the influences of the oblateness of the earth and the atmospheric drag, as well as the solar and lunar disturbing force are taken into account, more specially in connection with the purpose to use the satellite as a celestial tool for geophysic research.

Krause, E. H.
Telemetering for Interplanetary Flight. Instr. Soc. Am. J. 4: 478–480, Oct. 1957. The article is primarily concerned with telemetering details. Mention is made of the use of long distance telemetry in the Vanguard satellite, and problems which may arise as space flight develops are outlined.

Lang, Daniel
Earth Satellite No. I. New Yorker 33: 106–121, May 11, 1957. Scientific facts about Project Vanguard are interpreted for the general reader.

Lawden, D. F.
The Simulation of Gravity. Brit. Interplan. Soc. J. 16: 134–140, illus., July/Sept. 1957. The artificial gravitational field produced by rotating a spaceship or artificial satellite about its axis is compared and contrasted with normal gravity at the Earth's surface.

Ley, Willy
Rockets, Missiles and Space Travel. Rev. and enl. ed., 528 pp., illus., New York, Viking Press, 1957. A book devoted to the past, present and future of rockets. Especially valuable for its historical material.

Long, E. J.
Tracking the Satellite. Nature Mag. 50: 154–155, 162, illus., Mar. 1957. The role of amateur watchers in the satellite observation program.

MacDonald, N. D.
Computation for an Earth Satellite. Computers and Automation 6: 6–9, 23, illus., Feb. 1957. Illustrated description of the Navy-IBM high speed electronic computer facility for predicting the satellite's orbit.

Mandel'shtam, S. L., and Efremov, A. I.
Issledovaniia Korotkovolnovogo Ul'trafioletovogo Izlucheniia Solntsa (Investigation of Short Wave Ultraviolet Solar Radiation). Usp. Fiz. Nauk. 63(1b): 163–180, Sept. 1957. In Russian. Discusses use of artificial earth satellites for discovering and studying shortwave ultraviolet radiations.

Matthews, Whitney
Earth Satellite Instrumentation. Elec. Eng. 76: 562–567, July 1957. Design requirements of a unique telemetering encoder system are examined in the light of the limitations imposed by the over-all satellite program.

Telemetering in Earth Satellites. Elec. Eng. 76: 976–981, illus., Nov. 1957. A new instrumentation technique combining square hysteresis loop magnetic cores with switching transistors is discussed in the description of the magnetic telemetry encoding system.

Mengel, J. T.
Ear to the Sky. ASTRONAUTICS 2: 28–30, 48, illus., Oct. 1957. A report of the Minitrack system, how it works, and how it will be used to prove the earth satellite has been placed in orbit.

Minitrack Details: Satellite Tracking Based on Phase Comparison. Aviat. Age 27: 98–105, Mar. 1957.

Minitrack System Design Criteria. Elec. Eng. 76: 666–672, Aug. 1957. Examination of the operating principles of the radio phase-comparison angle-tracking system, and discussion of the appropriate design with reference to the severe weight and size limitations and altitude limits of the Vanguard satellite.

Radio System Will Track Earth Satellite. Soc. Automotive Engrs. J. 65: 30–33, Apr. 1957.

Midwest Engineer

Last Place on Earth. 10: 8–9, Aug. 1957. A look at the launching platform—the last place on earth where the satellite Vanguard and its launching vehicle will be.

Mikhailov, A. A.
O Nabliudenii Iskusstvennogo Sputnika (On the Observation of the Artificial Satellite). Astron. Zhurn. SSSR 34: 313, 1957. In Russian. Relates to tracking of a satellite. Translation No. R-2679 available at Special Libraries Association Translation Center, Crerar Library, Chicago, Ill.

Military Electronics

Electronics Will Play Key Role in Earth-Satellite Observations. 2: 26–27, June 1957.

Mirtov, B. A., and Istomin, V. G.
Issledovanie Ionnogo Sostavz Ionizirovannykh Sloev Atmosfery (Investigation of the Ion Composition of the Ionized Layers of the Atmosphere). Usp. Fiz. Nauk. 63(1b): 227–238, Sept. 1957. In Russian. Use of artificial satellite for study of the spectrum of ions in the ionosphere.

Missiles and Rockets

U. S. Army's Jupiter-C Becomes Satellite Carrier. 2: 57–59, Dec. 1957. Includes illustration of Jupiter C alongside Jupiter satellite launcher (Jupiter plus three Sergeants, second stage; one Sergeant, final stage).

Vanguard Instrumentation. 2: 66–69, Jan. 1957. Photographic illustrations with pertinent commentary pertaining to the instrumentation carried by the IGY satellite.

Møller, C.
On the Possibility of Terrestrial Tests of the General Theory of Relativity. Nuovo Cimento 6: Suppl. 1: 381–398, 1957. Appendix B, Satellite problems. Considers the application of artificial satellites to testing of the general theory of relativity. The idea which suggests itself, according to the writer, is an attempt at using atomic clocks to verify the relativistic formula for the rate of clocks placed at different potentials in the gravitational field.

Mullard Radio Astronomy Observatory Staff
Radio Observations of the Russian Earth Satellite. Nature 180: 879–883, illus., Nov. 2, 1957. Observational methods; derivation of an approximate orbit; variation of the intensity of the received signal; investigation of the ionosphere.

Nature

End of the Rocket of the First Artificial Earth Satellite. 180: 1392, Dec. 21, 1957. Brief report of last instrumental observation.

Radar Observations of the First Russian Earth Satellite and Carrier Rocket by Staff of the Jodrell Bank Experimental Station, University of Manchester. 180: 941–942, illus., Nov. 9, 1957. Fig. 1 is a typical example of the echo from the rocket. Fig. 2 gives typical values of detection ranges, signal noise ratios and effective scattering cross sections.

Radio Observations of the Russian Earth Satellite. 180: 879–883, Nov. 2, 1957. Satellite vehicle tracking in Great Britain.

The Second Artificial Earth Satellite. 180: 931, Nov. 9, 1957. A review of the launching of Sputnik II.

Newell, H. E., Jr.
Some Preparations for the International Geophysical Year Earth Satellite Program. Am. Geophys. Union. Trans. 38: 450–456, Aug. 1957. Background; experiments

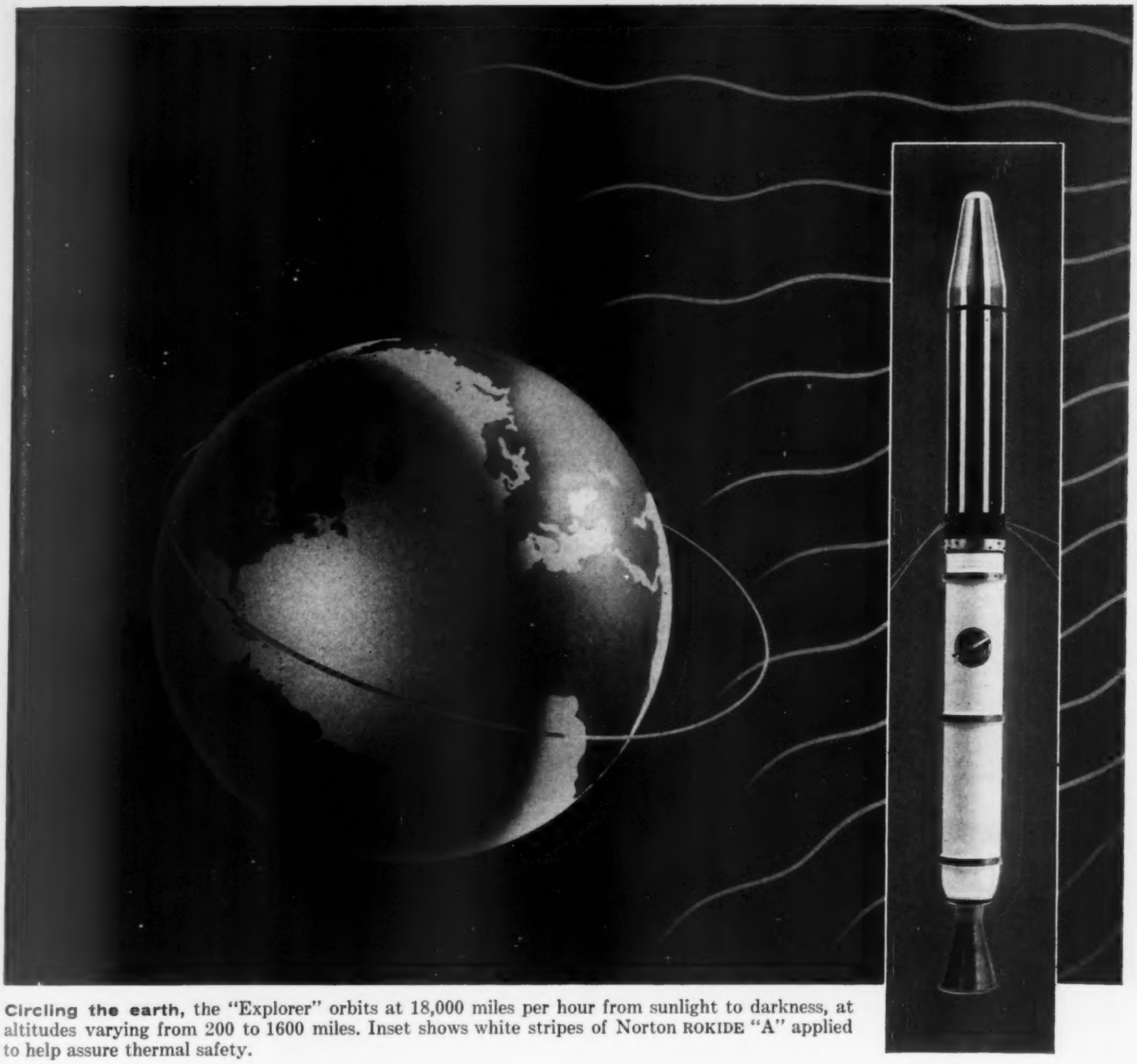

Circling the earth, the "Explorer" orbits at 18,000 miles per hour from sunlight to darkness, at altitudes varying from 200 to 1600 miles. Inset shows white stripes of Norton ROKIDE "A" applied to help assure thermal safety.

selected by TPESP for performance; progress to date.

Nonweiler, T. R.
Skin Heating During Re-entry of Satellite Vehicles to the Atmosphere. Brit. Interplan. Soc. J. 16: 10–21, Jan.-Mar. 1957. Shows that particular attention to the flight plan and over-all design can greatly simplify the problems of kinetic heating.

O'Keefe, J. A.
An Application of Jacobi's Integral to the Motion of an Earth Satellite. Astron. J. 62: 265–266, Oct. 1957. It is shown that the speed N of the satellite referred to the surface of the earth can be related to the geopotential V by a modification of the Jacobi integral, so that $N^2 = 2V +$ const. This equation neglects the very small luni-solar perturbations, but includes the effects of the anomalies of terrestrial gravitation, which are more important. It is useful because it relates quantities easily measurable from the surface of the earth, and because it governs the possible gravitational changes of the orbit over rather long times.

Geodesy Comes of Age with Vanguard. By Providing a Fresh Approach to Classical Geodetic Problems, It Will Bring Greater Advances in the Next 18 Months Than in Past 50 Years. Astronautics 2: 71–73, 92, illus., Aug. 1957. Tracking the satellite from observation stations throughout the world will provide geologists with a three-dimensional approach to the problem of large-area surveys, and a new method of measuring intercontinental distance.

Perturbations of a Close Satellite by the Equatorial Ellipticity of the Earth. Astron. J. 62: 183–185, Aug. 1957. If the earth is triaxial, there will be a semi-diurnal motion of the node of a close satellite. The author finds an amplitude of 65″ for the motion, as seen from the surface of the earth, assuming Jeffreys' value of the coefficient of $P2^2 \cos 2\lambda$.

Okhotsimskii, D. E., and Eneev, T. M.
Nekotorye Variatsionnye Zadachi, Sviazannye Zapuskom Iskusstvennogo Sputnika Zemli (Certain Variational Problems Connected with Launching of an Artificial Earth Satellite). Usp. Fiz. Nauk. 63(1a): 5–32, Sept. 1957. In Russian. Deals with problems of time variation of the thrust direction of rocket motors involved in the placing of a satellite in a predetermined orbit with minimum fuel consumption. Discusses optimum modes of fuel consumption to achieve minimum initial weight. Considers both single and multistage rockets.

Okhotsimskii, D. E., Eneev, T. M., and Taratynova, G. P.
O Predelenie Vremeni Sushchestvovaniia Iskusstvennogo Sputnika Zemli i Issledovanie Vekovykh Vozmushchenii Ego Orbity (Determination of the Lifetime of an Artificial Earth Satellite and Investigation of the Secular Perturbations of Its Orbit). Usp. Fiz. Nauk. 63(1a): 33–50, Sept. 1957. In Russian. For the general case of an elliptic orbit, a rapid and accurate method of computing lifetime of satellite. Translation No. R-3053 available at Special Libraries Association Translation Center, Crerar Library, Chicago, Ill.

Ordway, F. I.
Project Vanguard—Earth Satellite Vehicle Program. Characteristics, Testing, Guidance, Control and Tracking. Astronautica Acta 3: 67–86, 1957.

Packard, M. E.
Miniaturizing Magnetometers. Mil. Electron. 3: 22–24, illus., Nov. 1957. Modern techniques enable equipment for measuring the earth's magnetic field to be made light enough to be carried as the payload of satellite vehicles.

Peterson, A. M.
Radio and Radar Tracking of the Russian Earth Satellite. Inst. Radio Engrs. Proc. 45: 1553–1555, illus., Nov. 1957. Reports observations from Stanford Research Institute.

Petroleum Refiner
Satellite Will Blast Off with Kerosene. 36: 335–336, illus., May 1957. Fuel for Vanguard's first stage rocket is "direct but improved descendant of the oil that burned in grandfather's buggy lamp." Also in Oil and Gas J. 55: 124, May 27, 1957.

Phalen, F. W.
Telemetered Data Checks Vanguard Flight. Electron. Indus and Tele-Tech. 16: 40–41, July 1957. Discussion of test instrumentation, data channels and transducers to measure and record fuel temperature, fuel pressures and Vanguard skin temperature.

Poloskov, S. M., and Nazarova, T. N.
Issledovanie Tverdoi Sostavliaiushchei Mezhplanetnogo Veshchestva s Pomoshch'iu Raket i Iskusstvennykh Sputnikov Zemli (Investigation of the Solid Components of Interplanetary Space by Means of Rockets and Artificial Satellites). Usp. Fiz. Nauk, 63 (1b): 253–265, Sept. 1957. In Russian. Discussion of the two most important problems which should be investigated: determination of the flow of meteor particles and study of their spectra.

Porter, R. W.
Role of the Earth Satellite in Four Important IGY Experiments. Aero. Eng. Rev. 16: 89–93, May 1957. Tasks are: Measurement of the solar ultraviolet radiation at 1216 A; measurement of the earth's magnetic field; cosmic ray analysis; and determination of the terrestrial energy balance.

Prew, H. E.
Space Exploration—The New Challenge to the Electronics Industry. In American Astronautical Society Proceedings, 3rd Annual Meeting, New York, Dec. 6–7, 1956, pp. 17–29, diags., New York, The Society, 1957. The challenge is to control remotely a space research vehicle. The paper discusses initial

requirements, namely, hyper-range guidance and data links, operating with command control loops.

Also in J. Astronautics 4: 9–11, diags., Spring 1957, and Inst. Radio. Engrs. Trans. Prof. Group. Mil. Electron. 1:43–48, diags., Dec. 1957.

Prosser, William

Three-Stage Rocket Will Launch Satellites. Flight 491: 12–15, illus., Dec. 1957. Details of operation of the Vanguard rocket.

Radio (Moscow)

Iskusstvennye Sputniki ZanuskaemievUSA. (Artificial Satellites to Be Launched in USA) 7: 24–25, July 1957. In Russian. Translation No. R-2440 available at Special Libraries Association Translation Pool, Crerar Library, Chicago, Ill.

Nabliodenie za Signalami Iskusstvenniu Sputnikov Zemli (The Observation of Signals from Artificial Earth Satellites). 7: 17–25, July 1957. In Russian. Basic transmitter data of the U. S. and U.S.S.R. satellites are summarized. The following papers outline methods and describe the equipment for use by amateurs in locating the satellites and a further paper deals with the proposed U.S.A. satellite: U.S.W. Receiver, by O. Rzhiga and A. Shakhovskoi, pp. 17–20; Radiolocation Unit, by V. Dubrovin, pp. 21–23.

Nabliodenie za Signalami Iskusstvenniu Sputnikov Zemli (Observations of Signals from Artificial Satellites). 8: 17–20, Aug. 1957. In Russian. The following papers are included: Method of Observation, by O. Rzhiga and A. Shakhovskoi, pp. 17–19; Work Done with the Direction-Finding Equipment, by V. Dubrovin, pp. 19–20. Methods are outlined for the observation and recording of signals from a satellite and for determining the instant of its passage overhead. A brief description is given of receiving equipment and reference is made to its experimental use with an airborne transmitter, illustrating the change in the received signal when the aircraft passes overhead.

Raketentech. u. Raumfahrtforsch.

Entwichlungsstand der Vanguard-Rakete (State of Development of the Vanguard Rocket). Pp. 79–81, Oct. 1957. In German. Presentation of charts and discussion on the Vanguard rocket.

Richter, H. L., Jr.

Microlock. A Tracking Receiver for Satellite Communications. QST 41: 20–24, illus., Dec. 1957. This article describes a technique recently applied to communications. The receiver described has been built by the San Gabriel Valley (California) Radio Club for use in tracking the earth satellite and for receiving telemetering from the satellite. Using a phase lock-loop system with very narrow bandwidth, the receiver has been designed for reception of signals approaching or below the noise threshold of conventional receivers.

Roberson, R. E.

Orbital Behavior of Earth Satellites. I. Frank. Inst. J. 264: 181–201, Sept. 1957. Reviews some of the more recent contributions toward an analytical and integrated treatment of the orbit of an earth satellite with the requirements of satellite engineering rather than classical astronomy primarily in mind.

Orbital Behavior of Earth Satellites. II. Frank. Inst. J. 264: 269–285, Oct. 1957. Presentation of a method (a) to deduce the orbit geometry in the field of an oblate spheroid, as if no other external forces act; (b) to calculate a rotating reference frame with respect to which the orbit is periodic; (c) to relate the elements of the orbit to the kinematic and geometric initial conditions which exist when the orbit is established; and (d) to develop the time behavior of the basic dependent variables which describe the

orbit. The principal limitation of the analysis is its restriction to first order effects in the oblateness parameter.

Rochelle, R. W.
Earth Satellite Telemetry Coding System. Elec. Eng. 76: 1062–1065, illus., Dec. 1957. The different bandwidth requirements for the various inputs from the transducers in the Vanguard satellite led to a system which is a combination of time-sharing and frequency-sharing telemetry. To illustrate, a simple three-channel system is first described. This is then extended to cover the 48-channel system.

Rosenstock, H. B.
The Effect of the Earth's Magnetic Field on the Spin of the Satellite. Astronautica Acta 3: 215–221, 1957. It is expected that the earth satellite will spin about its axis several times per second at launching time. This is desired to make certain experiments feasible, as well as for aerodynamic stability. It has long been known that conductors rotating in a magnetic field will slow down; the purpose of this report is to review the results existing on this subject and to apply them to the case of the satellite moving in the geomagnetic field.

Russell, O. J.
Satellite Observations for Amateurs. Wireless World 63: 579–581, illus., Dec. 1957. Use of frequencies of 20 to 40 Mc/s in the Russian satellites opened up the possibility of large-scale amateur observations with gear already at hand in most amateur stations.

Schmidt, C. M., and Hanawalt, A. J.
Skin Temperatures of a Satellite. JET PROPULSION 27: 1079–1083, Oct. 1957. Analysis of temperatures that exist on a particular satellite configuration and study of various pertinent parameters in order to determine their relative importance.

Schmidt, I.
Berechnungen zur Sichtbarkeit von Erdtrabanten (Calculations on the Visibility of Earth Satellites). Weltraumfahrt 8: 104–107, Dec. 1957. In German.

Schmidt, Ingeborg
Visibility of Artificial Satellites of the Planet Earth. J. Aviat. Med. 28: 435–446, Oct. 1957. Paper given at 28th Annual Meeting of Aero Medical Association, Denver, Colo., May 8, 1957. Calculation of spaces of potential visibility in eight oblique meridians.

Scott, J. M. C.
Estimating the Life of a Satellite. Nature 180: 1467–1468, Dec. 28, 1957. Suggests that one can forecast rather simply how long one of the new satellites will continue in an orbit, provided only that one has good information about the period and some knowledge of the eccentricity.

Science
Rocket and Satellite Conference. 126: 933, Nov. 1, 1957. Summary of international conference on rocket and earth satellite programs for the IGY held in Washington Sept. 30–Oct. 5, 1957.

Singer, S. F.
Meteorological Measurements from a Minimum Satellite Vehicle. Am. Geophys. Union. Trans. 38: 469–482, Aug. 1957. Discusses some problems connected with the satellite itself, its orbit and its orientation, and its instrumentation; then takes up some of the applications to important meteorological problems.

Singer, S. F., and Wentworth, R. C.
A Method for the Determination of the Vertical Ozone Distribution from a Satellite. J. Geophys. Res. 62: 299–308, June 1957. Application of an artificial earth satellite to synoptic measurements of ozone concentration which can be used as an indicator of the motion of air masses, particularly in the stratosphere.

Singer, S. F.
Minimum Earth Satellite as "Storm Patrols." Sci. Mon. 84: 95–98, Aug. 1957. Description of the use of a photocell for obtaining meteorological data from a satellite vehicle.
Space Vehicles as Tools for Research in Relativity. In American Astronautical Society Proceedings, 3rd Annual Meeting, Dec. 6–7, 1956, pp. 121–125, New York, The Society, 1957. Special attention is given to a presentation of the application of close orbit earth satellites, with the aid of atomic clocks, to perform an experimental test of relativity. Also in J. Astronautics 4: 49–51, Autumn 1957.

Sky and Telescope
Artificial Satellite No. 1. 17: 11, Nov. 1957. Details, known at the time of writing, of the first Russian artificial satellite. Includes photograph of the screen of an oscilloscope, fed by a short-wave receiver, showing 20.005-megacycle pulses from the satellite during the night of Oct. 5, 1957.
The First Man-Made Satellites. 17:-56–60, illus., Dec. 1957. A review of activity after launching of the Russian satellites.

Sletten, C. J., Holt, F. S., and Others
A New Satellite Tracking Antenna. In Institute of Radio Engineers 1957 IRE Wescon Convention Record. Part I. Sessions Sponsored by IRE Professional Groups at the Western Electronic Show and Convention, San Francisco, Calif., Aug. 2–23, 1957, pp. 244–261, illus., New York, The Insitute, 1957. Describes system for 108 Mcps operation using 22 new type radiating elements electromagnetically coupled to a balanced two-wire line.

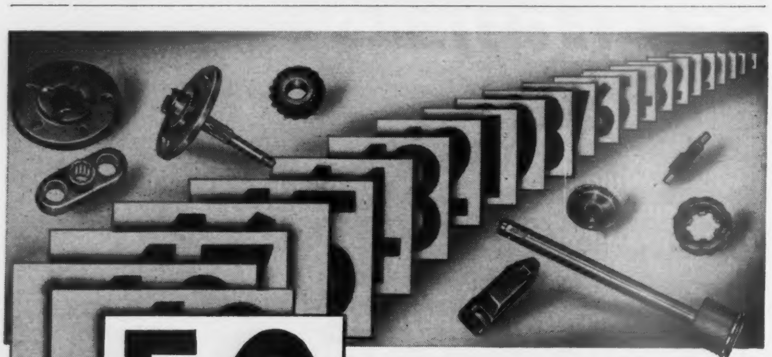

Smith, E. T. B.
Solid Propellant Rocket Motors. Brit. Interplan. Soc. J. 16: 198–211, diags., Oct.-Dec. 1957. A description is given of the basic features and methods of design. Among the uses is that for the third stage of the Vanguard satellite project. It is suggested that solid propellant rockets are worth considering for vehicle propulsion.

Southern Research Institute
The Age of Space. Proceedings of a Nontechnical Conference on Missiles, Rockets and Space Travel and Their Impact on Our Times, May 16, 1957. 43 pp., illus., Birmingham, Ala., The Institute, 1957. Papers include: A trip to Mars, by Ernst Stuhlinger, pp. 6–14; Beyond the sky with rocket power, by D. A. Kimball, pp. 15–18; Metals for space travel, by F. L. LaQue, pp. 19–24; The earth satellite program, by J. P. Hagen, pp. 30–38.

Spaceflight
Building the Earth Satellite Vehicle. 1: 164–168, illus., Oct. 1957. A series of twelve photographs showing various stages and processes of the actual satellite vehicle to be launched during the Vanguard Project.

Spitz, A. N.
Project Moonwatch-Visual Tracking of IGY Satellites. In American Astronautical Society Proceedings, 3rd Annual Meeting, Dec. 6–7, 1956, pp. 169–177, New York, The Society, 1957. The visual tracking program for Project Vanguard is outlined. A general description of the amateur visual tracking program, Project Moonwatch, and the coordination of this world-wide effort under the sponsorship of the Smithsonian Astrophysical Observatory is presented.

Stanford Research Institute, Applied Research Center, Palo Alto, Calif.
Effects of Satellite Spin on Ground-Received Signal, by J. T. Bolljahn. 22 pp., Aug. 1957. (Tech. Rpt. 6.)

Steier, H. P.
Vanguard Satellite Tracking Camera Developed. Missiles and Rockets 2: 64–65, Jan. 1957. Structural and operational details of the camera, including diagrammatic illustrations of the camera and of a satellite tracking camera station.

Sterne, T. E.
Celestial Mechanics of Artificial Satellites. Sky and Telescope 17: 66–68, illus., Dec. 1957. Motion in an elliptical orbit; the orbit in space; perturbations of a satellite.

Stine, G. H.
Earth Satellites and the Race for Space Superiority. 190 pp., diags., New York, Ace Books, 1957. The author, who is a rocket engineer at White Sands Proving Ground, tells what artificial man-made satellites are, describes how they are made and what kind of rocket ships can be used to reach the new satellites. Chapter III, Vanguard.

Stohl, J.
Artificial Satellites of the Earth Should Confirm the Theory of Relativity. Nasa Veda 4: 60–63, Feb. 1957. In Czech. Not examined.

Strong, James
Project Vanguard. Aeroplane 92: 919–932, June 28, 1957. An IGY program, Vanguard vehicle, earth satellite design, ascent into space, tracking the satellite, and research in space are discussed.

Subotowicz, M.
Satellites for Checking Einstein's Relativity Theory. Missiles and Rockets 2:57–59, Feb. 1957. Discusses the artificial satellite of the earth and the possibility of new experimental verification of the general theory of relativity.

Summerfield, Martin
Problems of Launching an Earth Satellite. Astronautics 2: 18–21, 34–37, 86–88, illus., 1957.

Sutton, G. P.
Ein Vergleich Moeglicher Antriebs-Systeme fuer Raumfahrzeuge (A Comparison of Possible Propulsion Systems for Space Flight). Raketen-tech. & Raumfahrforsch. pp. 73–75, Oct. 1957. In German. Discussion of the actual propulsion systems for space vehicles including liquid power plants, nuclear propulsion, free radical (atomic gases), heating through solar energy, and electrical discharge and Lorin propulsion.

Swetnick, M. J.
Meteoric Abrasion Studies Proposed for Vanguard. In American Astronautical Society Proceedings, 3rd Annual Meeting, Dec. 6–7, 1956, pp. 59–64, New York, The Society, 1957. Discussion of two Vanguard methods, approved for inclusion in the satellite program, for studying meteoric abrasion of satellite skins. Also in J. Astronautics 4: 69–71, Winter 1957.

Taratynova, G. P.
O Dvizhenii Iskusstvennogo Sputnika v Netsentral'nom Pole Tiagoteniia Zemli pri Nalichii Soprotivleniia Atmosfery (The Motion of an Artificial Earth Satellite in the Eccentric Gravitational Field of the Earth When Atmospheric Resistance Is Taken into Account). Usp. Fiz. Nauk. 63 (1a): 51–58, Sept. 1957. In Russian. The atmosphere is assumed to revolve together with the earth Translation No. R-3057 available at Special Libraries Association Translation Center, Crerar Library, Chicago, Ill

Time
Data from the Sputniks. 70: 57, Dec. 30. 1957. Indicates revisions in standard theories of the earth and its atmosphere as a result of information obtained from the Russian Sputniks.

Thiruvenkatachar, V. R.
An Artificial Satellite for the Earth. J. Sci. and Indus. Res. 15A: 61–63, Feb. 1957. Discusses some of the prominent general scientific questions raised by the earth satellite project.

Thompson, G. V. E.
Artificial Satellites. Aeronautics 35: 42–43, Jan. 1957. Reviews of papers on artificial satellites presented at the Rome Congress of the International Astronautics Federation, 1956.

Tousey, R.
Optical Problems of the Satellite. Opt. Soc. Am. J. 47: 261–267, Apr. 1957. Some of the optical problems connected with an artificial satellite are: Visibility, the photographic determination of the precise orbit, and the temperature that the satellite will reach through radiation exchange. These matters are discussed with particular reference to the plans for the satellites to be launched by the United States during the International Geophysical Year. One of the first experiments to be flown will be the monitoring of the Lyman-alpha line radiation of hydrogen emitted by the sun and the measurements of intensity variations associated with solar flares.

Vakhnin, V.
Iskusstvennie Sputniki Zemli (Artificial Earth Satellites). Radio (Moscow) 6: 14–17, June 1957. In Russian. Includes information for radio amateurs taking part in the IGY program. General data regarding the orbit of the U.S.S.R. satellite are given, its functions are outlined and the problem of signal reception from it is discussed. Translation No. R-2361 is available from Special Libraries Association Translation Center, Crerar Library, Chicago, Ill.
See also condensation in QST 41: 22–24, 188, Nov. 1957, and Wireless World 63: 574–578, Dec. 1957.

Vavilov, V. S., Malovetskaya, V. M., and Others
Kremnievi Solnechni Batari Kak Istochniki Elektricheskogo Nitaniya Iskusstvennikh Sput-

nikov Zemli (Silicon Solar Batteries as Sources of Electrical Energy for Charging the Artificial Satellites). Usp. Fiz. Nauk. 63 (1a): 123–129, illus., Sept. 1957. In Russian. Discusses silicon solar batteries as sources of electric power for telemetering and research instruments in artificial earth satellites.

Vernov, S. N., Ginzburg, V. L., and Others

Issledovanie Sostava Pervichnogo Kosmicheskogo Izlucheniia (Investigation of the Composition of Primary Cosmic Radiation). Usp. Fiz. Nauk, (63 1a): 131–144, Sept. 1957. In Russian. Use of artificial earth satellites for investigating the nuclear components of cosmic radiation.

Vernov, S. N., Logachev, Y. I., and Others

Issledovania Variatsii Kosmicheskogo Izlucheniia (Investigation of Variations of Cosmic Radiation). Usp. Fiz. Nauk. 63 (1b): 149–162, Sept. 1957. In Russian. Discusses the problem of using the artificial earth satellite for studying the variations of cosmic radiation.

Welding and Metal Fabrication

Fabricating Earth Satellites. 25: 433, 441, illus., Nov. 1957. Details of U. S. satellite fabrication.

Wexler, Harry

The Satellite and Meteorology. In American Astronautical Society Proceedings, 3rd Annual Meeting, Dec. 6–7, 1956, pp. 5–15, New York, The Society, 1957. The earth satellite will introduce a revolutionary chapter in meteorological science—not only by improving global weather observing forecasting, but by providing a better understanding of the atmosphere and its ways. Also in J. Astronautics 4: 1–5, 8, illus, Spring 1957.

Whipple, F. L., and Hynek, J. A.

Observations of Satellite I. Sci. Am. 197: 37–43, illus., Dec. 1957. An account of how the first satellite's orbit was determined, and how our knowledge of this orbit can be applied.

Wireless World

Artificial Satellites of the Earth. 63: 574–578, illus., Dec. 1957. Quotes from two Russian articles appearing in Radio (USSR) for June 1957 (see Kazantsev and Vakhnin); also comments on observations made in England on the first Russian satellite.

1958

Adams, M. C., and Probstein, R. F.

On the Validity of Continuum Theory for Satellite and Hypersonic Flight Problems at High Altitudes. JET PROPULSION 28: 86–89, illus., Feb. 1958. Results of the study are applied to the re-entry problem and it is concluded that a continuum analysis, with no slip at the body surface, is valid for the flight conditions where heating is important.

Allward, Maurice

The Space Age Is Here. Spaceflight 1: 196–197, illus., Jan. 1958. A summary of remarks by various persons forecasting space flight and a summary of press reports regarding the Russian Sputniks.

ASTRONAUTICS

Make-Ready for Satellite Launching. 3: 28–30, illus., Feb. 1958. A step-by-step picture story of Vanguard TV-3 from the time it arrived in Cape Canaveral until the moment it was fired, suggests the magnitude of the job.

A National Space Flight Program. 3: 21–28, Jan. 1958. A report by the Space Flight Technical Committee of the AMERICAN ROCKET SOCIETY.

Aviation Week

Army Launches Satellite, Bids for Space: Vanguard Fails. 68: 28–32, illus., Feb. 10, 1958.

Radio Technique Tracked Sputnik During Final Disintegration Period. 68: 37, Jan. 27, 1958. Technique developed to count meteor trails tracked Sputnik I, according to scientists of Ohio State University's Radio Observatory.

"From the time that its 20 and 40 mc transmitters failed, Sputnik I was tracked by detection signals transmitted on 20 mc by WWV, National Bureau of Standards station near Washington (Ohio), that were reflected from the ionization column generated as the satellite sped through the relatively thin upper atmosphere."

Chemical and Engineering News

Putting It Together. 36: 24–25, illus., Feb. 10, 1958. Picture story of Explorer.

Chemical Week

Fuel Push Gets Satellite Off Ground. Roaring Skyward with First U. S. Earth Satellite Is Army's Jupiter C Missile. 82: 30–31, illus., Feb. 8, 1958. Concerns the relative merit of solid and liquid fuels.

Cox, Donald, and Stoike, Michael

Spacepower. 260 pp., illus., Philadelphia, Winston, 1958. Discusses in detail Sputnik's and Mutnik's impact on the world; why go into space; where we are at present; the social impact of satellites; spacepower; the international control of outer space; a philosophy of space power; organization of the U. N. space force; and importance of the moon as a stepping stone to space.

Croome, Angela, Compiler

The International Geophysical Year Month by Month. Discovery 19: 29–31, illus., Jan. 1958. British observations of Sputnik I and II; mechanical features of Sputnik II.

Current History

Sputnik I and II; Texts of Soviet Announcements October 4 and November 3, 1957. 34: 48–50, Jan. 1958.

Dempewolff, R. F. *Forecast: A Sky Full of Satellites.* Pop. Mech. 109: 138–141, 262, 264, illus., Jan. 1958. Describes some of the projects underway.

Electronics

Vanguard Gear in Explorer. Army's Globe-Circling Satellite Carries Navy Circuits. 31: 8, Feb. 14, 1958. Explorer I is investigating three areas: cosmic rays; density and size of micrometeorites; and temperatures both inside and outside the satellite's shell. Vanguard I is primarily concerned with ultraviolet radiation.

Franklin Institute Journal

Satellites Followed with Transparent Earth-Sky Globe. 265: 82, Jan. 1958. Establishing the orbit of a satellite on the earth-sky globe is done in three simple steps with equipment available from a commercial source. Details are given as well as price.

Friedman, Herbert

Soviet Satellite Instrumentation. ASTRONAUTICS 3: 32–33, 82, illus., Feb. 1958. Comparison of Russian and U. S. techniques reveals different approaches to the problem of measuring solar X-ray and ultraviolet radiation.

Gatland, K. W.

Russia's Second Satellite. Spaceflight 1: 204–205, Jan. 1958. An appraisal of the techniques necessary to establish half a ton of research equipment in orbital motion.

IGY Bulletin

Ionospheric Studies Using Earth Satellites. 7: 11–16, Jan. 1958. Refers to conference held Nov. 5, 1957 at the Central Radio Propagation Laboratories of the National Bureau of Standards, Boulder, Colo., which brought together groups that had spontaneously initiated ionospheric experiments utilizing radio transmissions from satellites

launched by the U.S.S.R. A table lists observations of signal strength, Doppler data, interferometric and other phase-difference data, and direction finding and radar data.

Lovell, A. C. B.
Radio Astronomy and the Jodrell Bank Radio Telescope. Radio and TV News 59: 35–38, 166, Jan. 1958. Details of the powerful new tool that has been making headlines tracking the Soviet satellite. It is the great steerable radio telescope built at Jodrell Bank in Cheshire, England.

Mallan, Lloyd
Space Satellites. 144 pp., illus., Greenwich, Conn., Fawcett Publications, 1958. Gives, in nontechnical language, many details about Project Vanguard, its beginning, launching and tracking plans, the computing center and Operation Moonwatch. Interprets for home owners the meaning of earth satellites as far as taxes, food prices, travel, business profits, etc., are concerned.

Marshack, Alexander
The World in Space. The Story of the I.G.Y. 176 pp., illus., New York, Nelson, 1958. Includes discussion of rockets and satellites.

Massey, H. S. W., and Boyd, R. L. F.
Scientific Observations of the Artificial Earth Satellites and Their Analysis. Nature 181: 78–80, Jan. 11, 1958. Summary of discussion meeting called by the Royal Society on Nov. 29, 1957 to discuss the wide range of techniques employed.

Matthews, Whitney, Rochelle, R. W., House, C. B., Van Allen, R. L., Schaeffer, D. H., and Schaffert, J. C.
Cyclops Cores Simplify Earth-Satellite Circuits. Electron. (Eng. ed) 31: 56–63, illus., Feb. 28, 1958. A discussion in four parts of satellite electronics which serves as an introduction to the so-called Lyman-alpha environmental satellite of Vanguard with emphasis on the telemeter encoder, memory and meteor counter.

Matthews, Whitney, and Ludwig, G. H.
Scientific Telemetry for USNC-IGY. QST 42: 41–45, 160, 162, 164, illus., Jan. 1958. How amateur recordings can aid in the satellite program.

Mengel, J. T., and Herget, Paul
Tracking Satellites by Radio. Sci. Am. 198: 23–29, illus., Jan. 1958. The fastest, most reliable way to detect an artificial satellite and initially to determine its orbit is by radio. A far-flung system called Minitrack has been established for this purpose.

Missiles and Rockets

Ohio State Records Death of Sputnik I. 3: 158, 160, Feb. 1958. The radio telescope at Ohio State University, using a new system of radio reflection, recorded the final flight of Russia's first satellite.

Radar Antenna Awaits First U. S. Satellite. 3: 153, illus., Jan. 1958. A general news item about the five parabolic radio telemetry antennas, weighing 35 tons each, featuring an aluminum reflector measuring 60 ft in diam, to be used for tracking. Location, design and manufacturer are mentioned.

Neckel, Heinz
A Photographic Observation of the Satellite 1957 Beta Leaving the Earth's Shadow. Nature 181: 257–258, illus., Jan. 25, 1958. Photograph taken at the Warner and Swasey Observatory of the Case Institute of Technology, Cleveland, Ohio, on December 15 is used to derive the distance of the satellite from the earth's surface.

Paiewonsky, B. H.
Transfer Between Vehicles in Circular Orbits. Jet Propulsion 28: 121–123, figs., Feb. 1958. A simple method is developed for calculating the angular relationship required between vehicles desiring to use Hohmann orbits for orbital transfer.

Roberson, R. E.
Effect of Air Drag on Elliptic Satellite Orbits. Jet Propulsion 28: 90–96, figs., Feb. 1958. Variation of parameters and the Krylov-Bogoliuboff approximation method are used to find simple approximate expressions for the decay of eccentricity with radius, the decay of radius with true anomaly and the growth of true anomaly with time. The special case of spiral orbits and the effect of asphericity and rotation of the earth's atmospheric shell are discussed.

Gravitational Torque on a Satellite Vehicle. Frank. Inst. J. 265: 13–22, Jan. 1958. Purpose of the paper is to derive the torque components along the principal axes of inertia of the satellite.

Schaefer, D. H.
Magnetic Core Event Counter for Earth Satellite Memory. Elec. Eng. 77: 52–56, illus., Jan. 1958. Description of the counter circuitry being developed to record micrometeorite bombardment of artificial earth satellites.

Sky and Telescope

Amateur Astronomers. Some Satellite Observing Statistics. 17: 182, Feb. 1958. A summary of reports from the Astronomical Society of Western Australia and a number of places in the United States.

Spaceflight

The First Days of Sputnik I. 1: 198–202, illus., Jan. 1958. Includes the following reports: Visual observations of the first Russian satellite rocket, by V. C. Reddish (Royal Observatory, Edinburgh); Observations of Sputnik I made at the Mullard Radio Astronomy Observatory, Cambridge, by Martin Ryle; First observations from Jodrell Bank, by a Member of the Research Team; Radio observations of the satellite, by H. V. Griffiths (BBC Measurement and Receiving Station, Tatsfield, Surrey); Observations by the B.A.A. and the R.S.G.B., by John Heywood; The Russian "Moonwatch" program.

Stehling, K. R.
Aspects of Vanguard Propulsion. Astronautics 3: 44–47, 68, illus., Jan. 1958. Previously established techniques as well as new approaches have been used to find the answers to major technical problems, many encountered in the past, but never at one time or of such a degree of complexity.

Warren, C. S., Rumble, W. G., and Helbig, W. A. *Transistorized Memory Monitors Earth Satellite.* Electron. 31: 66–70, illus., Jan. 17, 1958. Telemetered data from the U. S. earth satellite will be decoded by transistor-operated magnetic-core memory. Circuits required to numerically translate input information and present modified output information use alloy-junction transistors as current drivers, gated-impulse amplifiers, voltage amplifiers, high-speed switches and flip-flops. Memory storage capacity is 64,000 bits arranged as 256 characters of 25 bits each.

Woodbury, D. O.
Around the World in 90 Minutes: The Fabulous True Story of the Man-Made Moons, Including Sputnik. 248 pp., illus., New York, Harcourt, 1958. A comprehensive, lively explanation of the space age, of scientific difficulties in launching rockets and satellites; what science expects to accomplish and what significance these satellites and space travel have for the future of the world.

Acknowledgment

The compiler wishes to acknowledge the valuable contributions of Mrs. Kathryne Kozak in checking, assembling and editing many of the references and in typing the completed bibliography.

Missiles/Rockets—and Steel

Lukens Steel Company, with the world's largest capacity for producing spun and pressed "head" shapes, is forming nose cone blanks for the Air Force's Thor and Atlas, as well as other vital rocket and missile parts.

In the past, the men who carried the major burden in developing weapons systems had little need to know about the techniques for forming steel plate and other heavy materials. But now such problems are a vital part of our missile age, and steel companies having the necessary facilities and know-how are playing an important role in missile weapon systems development.

That is why, for example, the nose cone blanks for the Air Force's Atlas and Thor ballistic missiles are being formed by Lukens Steel Company on one of the most unusual facilities in the steel industry—a mammoth four-post hydraulic press capable of exerting a force of up to 4 million pounds. Lukens is performing this work for General Electric Company's Missile and Ordnance Systems Department, prime contractor for the ballistic nose cone.

Over Seventy-Five Years of Experience

Lukens produces its own steel and possesses the world's largest capacity for spinning and pressing the dome shapes known to the steel industry as "heads." In 1880, Lukens pioneered a machine which produced steel heads by means of a spinning or flanging operation—similar in working principle to a potter's wheel. Since that time, this process has undergone constant refinement. Today, supplemented by a line of presses for volume production items, Lukens facilities offer the widest range of types, sizes and qualities of head shapes available anywhere. The versatile flanging machines can spin heads from 12 inches to 21 feet in diameter and from 3/16 inch to 6½ inches in thickness. Huge hydraulic presses, like the one used for the Air Force program, have turned out the largest heads pressed —hemispheres nearly 7 inches thick. These same machines can press ultra-high strength steel in sheet gages to the order of 180,000 psi tensile material.

The metals used in head production range from the various steels and clad steels rolled on Lukens own mills to such materials as aluminum, copper, nickel, stainless steel, Monel, Inconel, titanium and Hastelloy.

For Missile Production and Handling

As the long-time leader in producing heads, Lukens has served many fields of industry—the most recent being the nation's missile producers. The areas connected with missile production and handling in which head shapes are playing a growing role are often areas in which Lukens heads have been employed in similar manner for many years. The storage of fuels and oxidants at test and launching sites requires tanks with heads at each end. Formed from corrosion-resistant Lukens clad steels, heads have long been supplied to the chemical industry for precisely such application. Solid rocket engine casings utilize dome ends which must withstand enormous pressures. Both the petroleum and chemical industries use steel heads for vessels in which liquids are contained under high pressures. To meet the demands of absolute safety, Lukens has spent years working with the latest high-strength steels and perfecting the required precision. This skill and knowledge is immediately available to missile engineers to fulfill their own design requirements.

On this mammoth hydraulic press capable of exerting up to 4 million pounds pressure, Lukens Steel Company has formed nose cone blanks for the Air Force's Atlas and Thor ballistic missiles.

Nose cones, fuel tanks, and rocket casings are, of course, only a few of the literally hundreds of uses to which heads can be put. In using them as examples our point has simply been this: wherever a metal dome shape can be utilized in the missile industry, experienced craftsmen can provide it —swiftly, accurately, with a quality achieved through long experience.

Send for More Information

Lukens specialized knowledge of head uses, sizes, types and qualities is immediately available. For assistance with specification or production problems, write to Manager, Marketing Service, Lukens Steel Company, 153 Lukens Building, Coatesville, Pennsylvania.

LUKENS ®

Index to Advertisers